QUANTIFYING GROUNDWATER INTERACTION WITH STREAMS AND THERMAL REGIME IMPLICATIONS

By

YAN ZHOU

Bachelor of Engineering in Hydraulics and Hydropower
Northwest Agricultural and Forestry University
Yangling, Shaanxi, P.R.China
2009-2013

Submitted to the Faculty of the
Graduate College of the
Oklahoma State University
in partial fulfillment of
the requirements for
the Degree of
DOCTOR OF PHILOSOPHY
December, 2017

QUANTIFYING GROUNDWATER INTERACTION

WITH STREAMS AND THERMAL

REGIME IMPLICATIONS

Dissertation Approved:

Dr. Garey Fox

Dissertation Adviser

Dr. Daniel Storm

Dr. Shannon Brewer

Dr. Chris Zou

ACKNOWLEDGEMENTS

This work would not have been possible without the guidance of my committee members, help from friends, and support from my family.

I would like to express my deepest gratitude to my adviser, Dr. Garey Fox, for his valuable guidance in research, patience in correcting my writing, insights to my questions, and the excellent research atmosphere he provided to our research group. I appreciate Dr. Shannon Brewer for her advices, support on field works, and especially introducing me to the research of fishery and ecology. I would like to thank Dr. Daniel Storm for the statistical knowledge he passed on to me within and beyond class. I would also like to thank Dr. Chris Zou for his valuable career advices and merging my knowledge gap between hydrology and ecology.

I am grateful to all of those whom I had the pleasure to work with during my study. Many thanks to Justin Alexander, Dr. Ron Miller, Adrian Saenz, Dr. Robert Mollenhauer and Dr. Lucie Guertault who helped me repeatedly on field works and writing. Special thanks to members of Fox's group, Abigail Parnell, Dr. Anish Khanal, Dr. Erin Porter, Dr. Holly Enlow, Kate Klavon, Mikayla Wanger, Rebecca Purvis and Whitney Lisenbee, for their help both personally and professionally. I'd also like to thank other friends I had the pleasure to make, Alex McLemore, Brad Rogers, John McMaine, Michelle Melone and Nelly Ruiz, to name a few. It would have been much tougher without them.

I am forever indebted to my family whose love, guidance and encouragement are with me all the time through good times and bad.

Name: YAN ZHOU

Date of Degree: DECEMBER, 2017

Title of Study: QUANTIFYING GROUNDWATER INTERACTION WITH STREAMS AND THERMAL REGIME IMPLICATIONS

Major Field: BIOSYSTEMS ENGINEERING

Abstract: Groundwater interaction plays an essential role in aquatic ecosystems and is involved in a range of water quantity and quality issues. However, quantifying stream-groundwater interactions has been difficult and labor intensive due to the complex nature of the hydrological connectivity. Therefore, there remains considerable need for advancements that can help understand and quantify groundwater interaction with lower cost, better flexibility and convenience. The objectives of this study were to (i) understand the transient storage mechanisms due to surface exchange and hyporheic flow by applying a stream transient storage zone model to soil pipe systems; (ii) develop the thermal equilibrium method to estimate the time-averaged point groundwater flux using monitored stream water temperature at a single point and existing atmospheric and hydrological data and (iii) evaluate the effects of reservoir operations in the Kiamichi River as related to stream fish thermal tolerances during summer baseflow conditions with an emphasis of groundwater interactions. Tracer data from a pulse input were collected in four different soil pipes after a fluorescein dye was injected upstream of each soil pipe network. The transient storage zone model OTIS-P was successfully applied to estimate solute transport parameters. The result suggested larger transient storage potential compared to stream systems reported in previous research. In the second part, a thermal equilibrium method was developed to quantify point groundwater flux in streams, and was evaluated by comparing with measurements from seepage runs. Statistics evaluated by FITEVAL indicated result from two methods agreed with each other, and the thermal equilibrium method was proven to be a suitable technique for quantifying point groundwater flux. In the third part, the WASP stream temperature model was calibrated and validated for four summers with an emphasis of groundwater interactions. Downstream water temperature was predicted using the validated model for 15 hypothetical release scenarios and evaluated based on critical thermal maximum of three fish guilds. Results indicated the current release operation was insufficient to provide a suitable downstream thermal regime for most of the fishes tested. Increasing release magnitude and/or releasing from hypolimnetic layers could improve the downstream thermal habitat for these fishes.

TABLE OF CONTENTS

Chapter Page

LIST OF TABLES

Table Page

LIST OF FIGURES

Figure Page

CHAPTER I

GENERAL INTRODUCTION

The interaction of surface water with groundwater, as a key component of the hydrological cycle, plays an essential role in aquatic and riparian ecosystems and are involved in a range of water quantity and quality issues. Streams with high groundwater interactions are often characterized by high biological and microbial diversity and activity due to elevated solute transport and nutrient exchange across the streambed interface (Laursen and Seitzinger, 2005; Schmidt et al., 2007). Groundwater flux can also limit benthic invertebrate exposure to low oxygen and contaminants (Malard and Hervant, 1999), provide thermal refugia as well as microbial food supply for anadromous fish (e.g., salmon), both for resting and spawning (Kurylyk et al., 2013). As a result, understanding the interaction between streams and aquifers has received an increasing amount of research interests due to its crucial importance in sustainable watershed management (Kalbus et al., 2006).

Surface water and groundwater interacts in two ways. First, when water table is at a higher elevation than the surface of the stream, groundwater may flow upward and contribute the surface water (known as groundwater discharge) and vice versa (known as groundwater recharge). In

humid regions, most streams receive groundwater contributions throughout the year due to high groundwater elevation and as a result named perennial streams. In semi-arid regions with higher seasonal hydrology variation, for some streams groundwater contributions are only available during certain seasons when water table is higher than the elevation of stream surface. Those streams only flow in certain seasons of the year and are known as intermittent streams. The rest of the streams never receive hydraulic support from groundwater and thus only flow in response to precipitation, known as ephemeral streams. The portion of the stream flow that is attributable to surface-groundwater interaction, known as baseflow or low flow, can serve as an indicator to describe the level of surface-groundwater interactions.

The potential of surface-groundwater interactions is dependent on many watershed physical characteristics including watershed geology, topography, soil and vegetation type. Watershed geology is a primary control factor on surface-groundwater interactions (Farvolden, 1963; Freeze, 1972; Smakhtin, 2001; Tague and Grant, 2004; Neff et al., 2005; Bloomfield et al., 2009). Stream channels composed of permeable, soluble, or highly fractured bedrock allow significant volumes of groundwater storage within the bedrock where recharge from surface water network may be readily available. In addition to bedrock type, geologic structure is also of great importance in some regions (Delinom, 2009), and boundaries between geologic units have been shown to be important zones of groundwater-surface water interaction (Konrad, 2006; Arnott et al., 2009). Watershed geology also has indirect effect on hydrology due to its influence on drainage network structure. Easily eroded bedrock lends itself more readily to channel formation and pedogenesis, both affecting storage capacities and rates of water transmission (Farvolden, 1963; Mwakalila et al., 2002). Surface topography is a key control factor on surface-groundwater interactions (Vivoni et al., 2007) and its influence is most pronounced in relatively high relief settings (Tetzlaff et al., 2009). Topographic gradients control the rate at which water moves downslope within soil matrix, thereby determining whether stormwater is flushed to the channel network or retained in the soil post-event. Subsurface

topography, in addition to surface topology, also has strong influence on water storage and throughflow pathways, and thus influences the potential of surface-groundwater interactions. Throughflow processes require a confining layer through which water cannot easily infiltrate, thereby initiating lateral subsurface flow (Hutchinson and Moore, 2000). Soil characteristics play a significant role in determining the rate of moisture loss due to surface or subsurface topographic gradients (Dodd and Lauenroth, 1997; Yeakley et al., 1998). However its effect on water storage and baseflow is likely to be correlated with surface and/or subsurface topography (Price, 2011). Low gradients are usually combined with finer particle size and thicker soils to encourage soil moisture retention. Conversely, steep upper slopes are likely characterized by coarser, less developed, and thinner soils, thereby more rapidly transmitting water (Price, 2011). Furthermore, soil hydrology is strongly affected by spatial variability of soil moisture, which may be predominantly controlled by surface and/or subsurface topography (Woods et al., 1997). The influence of vegetation on baseflow is twofold. On the one hand, greater vegetation cover will introduce greater interception and evapotranspiration rates which lead to decrease in water availability (Harr et al., 1982; Keppeler and Ziemer, 1990; Hicks et al., 1991; Smith, 1991). However, permanent canopy cover is associated with high infiltration and recharge of basin subsurface storage, which has a positive effect on baseflows due to improved infiltration, increased soil organic matter, and increase in surface permeability (Gregory et al., 2006; Zimmermann et al., 2006; Ohnuki et al., 2008; Price et al., 2010).

Quantifying surface-groundwater interactions is usually difficult and labor intensive due to the complex nature of hydrological connectivity. Over the last few decades, many approaches have been developed to quantify surface-groundwater flux from various theoretical background as reviewed by Kalbus et al. (2006), Brodie et al. (2007) and Turner (2009). These methods can be categorized into four main groups: Darcian methods, streamflow methods, tracer methods and water budget methods (Table 1).

Darcian methods estimate surface-groundwater flux similarly to the method used to investigate water table movement in terrestrial aquifers. The surface-groundwater flux is calculated as the product of hydraulic gradient and conductivity based on Darcy's Law:

$$q = -K\frac{dh}{dl} \quad (1)$$

where q is Darcy flux [L/T], K is hydraulic conductivity [L/T], h is hydraulic head [L] and l is distance [L]. The vertical hydraulic gradient in the streambed can be estimated by piezometers driven into the streambed: the hydraulic gradient is calculated based on the depth of the screen of the piezometer and elevation difference between the stream surface and the water surface in the piezometer (Freeze and Cherry, 1979). Hydraulic conductivity can be estimated by grain size analysis, permeameter tests, slug and bail tests or pumping tests as reviewed by Kalbus et al. (2006). The Darcian methods give point surface-groundwater flux estimation, and data analysis is straightforward and easy to apply. However, the time and material cost for proper placement and maintenance of piezometers is high and does not lend itself to broad area surveys. Installation of piezometer can artificially induce preferential flow.

Streamflow methods include a variety of approaches such as direct measurement using seepage meter, incremental streamflow methods (e.g. seepage runs) and hydrograph separation. The seepage meter method allows direct point measurement of surface-groundwater flux without measuring the permeability of bottom sediments by calculating the rate of volume change in a collection bag and the area of the collecting bucket pushed into the streambed (Zamora, 2008). The seepage run method for estimating groundwater flux involves measuring streamflow at multiple transects along the river, and the surface-groundwater flux is assumed to be the flow rate difference between transects (Rosenberry and LaBaugh, 2008). The method is easy to apply and inexpensive; however, accuracy of the method depends on the relative magnitude of groundwater flux and significance of evaporation and bank-storage, which can be difficult to estimate (Rosenberry and LaBaugh, 2008). The hydrograph

separation method separates a stream hydrograph into different components (e.g. direct runoff, interflow, baseflow) based on various assumptions. For instance, the recession-curve displacement method is based on the assumption that the streamflow-recession curve is displaced upward during periods of groundwater recharge while stream base-flow analysis filters surface runoff (high frequency signals) from baseflow (low frequency signals) analogous to the filtering of high frequency signals based on the recursive digital filter technique described by Nathan and McMahon (1990).

Water budget methods include groundwater and watershed modeling. Groundwater modeling estimates groundwater recharge by calibrating of the groundwater model to "known" values of aquifer transmissivity, hydraulic head, and discharge (base flow). Recharge for various temporal and spatial scales can be estimated; however, the accuracy of the estimates is dependent upon the availability and quality of the data for transmissivity, head, and discharge. The most widely used models include MODFLOW, ParFlow and HydroGeoSphere. Similarly, watershed models simulate surface transport hydrologic processes within a watershed based on an assumed balance between water sources and sinks. After calibrating the model against streamflow records from a gaging station, groundwater recharge can be estimated as the residual of prediction minus actual discharge. Watershed modeling software includes SWAT, HSPF and HEC-HMS. More recent efforts have combined watershed and groundwater models to achieve an overall water balance between the two systems, which are in actuality interdependent and inseparable.

Tracer methods estimate groundwater flux based on mass balance of environmental or introduced tracers including chloride, chlorofluorocarbons, tritium and temperature. Environmental tracers such as isotopes (e.g. tritium) and geochemical tracers (e.g. chlorofluorocarbons) can be used in hydrograph separation that provides information on the origin of streamflow components. Introduced tracers are usually used in dilution gauging method or transient storage (Zhou et al., 2015) approaches to quantify surface-groundwater interaction by mixing and dilution of the tracer.

Temperature methods use heat as an environmental tracer, with the analysis based on the heat transfer (i.e., energy balance) analogous to the mass balance of common chemical tracers. But unlike chemical tracers, heat comes from a variety of natural source such as the sun, ambient air and atmosphere through process of radiation, conduction latent heat transfer, etc. Thermal methods have emerged as a versatile class of geophysical tools for monitoring focused recharge in arid and semiarid settings (Blasch et al., 2007). The admission and redistribution of heat from natural processes such as insolation, infiltration, and geothermal activity can be used to quantify subsurface flow regimes (Blasch et al., 2007). By monitoring the temperature of stream water and saturated bed sediment at multiple depths, the vertical propagation of heat can be simulated based on the coupled relationship between heat and water, and has been used to investigate infiltration and percolation on the land surface (Suzuki, 1960), to indicate gaining and losing reaches of stream channels (Lapham, 1989; Silliman and Booth, 1993; Constantz, 1998), and to locate areas of inflow to lakes (Lee, 1985). Recently researchers also successfully quantified groundwater flux using remotely sensed thermographic profiles and in situ temperature histories (Loheide and Gorelick, 2006). However, I have not uncovered research that has used temperature as an indicator of heat transfer to quantify the groundwater flux from a thermal equilibrium perspective.

The objectives of this study were to (i) quantify the transient storage mechanisms due to surface exchange and hyporheic flow by applying a stream transient storage zone model to soil pipe systems; (ii) develop a thermal equilibrium method to estimate the time-averaged point groundwater flux using a point monitored stream water temperature profile and readily available meteorological and hydrological data and (iii) evaluate the effects of different reservoir operations in the Kiamichi River as related to stream fish thermal tolerances during summer-baseflow conditions with the consideration of groundwater interactions.

Table 1. Comparison of common methods for estimating groundwater discharge/recharge (adapted from USGS https://water.usgs.gov/ogw/gwrp/methods/compare/).

Category	Method	Spatial Scale	Temporal Scale	Typical Quantity Estimated	Ease of Use	Data Needs	Relative Cost	Reference
Water Budget	Groundwater Modeling	Local / Regional	Month to Years	Recharge	Moderate	High	High	Sophocleous and Perkins (2000)
	Watershed Models	Watershed /Regional	Days to Years	Recharge	Moderate	High	High	Sophocleous and Perkins (2000)
Darcian Method	Piezometers	Point	Instantaneous	Potential Recharge	Moderate	Low	High	Stofleth et al. (2008)
Streamflow Methods	Seepage Meters	Point	Event to Months	Potential Recharge	Moderate	Low	Low	Taniguchi and Fukuo (1993)
	Stream Base-Flow Analysis	Watershed	Years	Net Recharge	Easy	Low	Low	Arnold et al. (1995)
	Incremental Streamflow Method (Seepage Run)	Local	Instantaneous	Potential Recharge	Easy	Low	Low	Rosenberry and LaBaugh (2008)
	Recession-Curve Displacement Method	Watershed	Event to Years	Net Recharge	Moderate	Low	Low	Rutledge (1998)
Tracer Methods	Chloride	Point	Years	Recharge	Easy	Moderate	Moderate	Eriksson and Khunakasem (1969)
	Chlorofluorocarbons	Local	Month to Years	Recharge	Difficult	Moderate	High	Cook and Solomon (1997)
	Temperature	Point	Days to Years	Recharge	Moderate	Moderate	High	Constantz (2008)
	Tritium	Point	Month to Years	Recharge	Moderate	Moderate	High	Allison and Hughes (1975)

CHAPTER II

APPLICATION OF A TRANSIENT ZONE STORAGE MODEL TO SOIL PIPEFLOW TRACER INJECTION EXPERIMENTS

Introduction

Soil pipes are discrete preferential flow paths that are generally parallel to the land slope (Uchida et al., 1999; Weiler and McDonnell, 2007; Sharma et al., 2010). Soil pipe flow is an important component of subsurface flow that dominates many soil erosion phenomena, including embankment failures (Foster et al., 2000; Fox et al., 2007; Midgley et al., 2013), landslides (Uchida et al., 2001) and gully erosion (Wilson, 2011). However, little research has been performed to quantify and characterize soil pipes in terms of their *in situ* flow and transport characteristics throughout a soil pipe network (Wilson et al., 2013) and work in the USA is particularly limited (Jones, 2010).

To characterize the flow and transport properties of soil pipes, two potential approaches can be employed. A common approach is to treat the soil pipe as a stream system. In the companion paper, Wilson et al. (2015) described tracer injections into four individual soil pipe networks in two catchments of Goodwin Creek Experimental Watershed, Mississippi. They verified that these soil pipes were continuous for over 200 m and described the soil pipes as being sinuous like

stream channels with flow velocities in the range of streams. Flow and solute transport through a stream system, i.e., the soil pipe idealized as an underground river channel, is commonly modeled with a transient storage approach. In the transient storage zone approach, the flow domain is divided into two regions: the main flow zone and the transient storage zone. The main flow zone is the center channel where solutes travel by advection. Transient storage refers to temporary detainment of solutes. For stream and river systems, the transient storage zone usually includes surface storage in eddies and back-water pools, and mass transfer with the hyporheic zone as discussed by Johnson et al. (2014) (Figure 1). Correspondingly, the transient storage zone for a soil pipe is due to storage in side pools of partially filled soil pipes and/or mass transfer into the porous walls of soil pipes, especially full-filled pipes (Figure 2). The transient storage can dramatically increase the travel time of solutes and cause a tail-effect on breakthrough curves (Stofleth et al., 2008; Johnson et al., 2014).

Assuming no lateral inflow or outflow between the pipe and the soil matrix (solute exchange only) and no decay of the solute, the following governing equations are used by a transient storage zone model and are based on one-dimensional advection-dispersion for the main flow area and transient storage represented by a first-order storage process:

$$\frac{\partial C}{\partial t} = -\frac{Q}{A}\frac{\partial C}{\partial x} + D\frac{\partial^2 C}{\partial x^2} + \alpha_s\left(C_S - C\right) \tag{2}$$

$$\frac{dC_S}{dt} = \alpha_s \frac{A}{A_S}\left(C - C_S\right) \tag{3}$$

where A is the main channel cross-sectional area (L^2), A_s is the storage zone cross-sectional area (L^2), C is the main channel solute concentration ($M\ L^{-3}$), C_s is the storage zone solute concentration ($M\ L^{-3}$), D is the dispersion coefficient in the main channel ($L^2\ T^{-1}$), Q is the flow

rate in the main channel ($L^3\ T^{-1}$), and α_s is the storage zone exchange coefficient (T^{-1}) (Runkel, 1998).

OTIS (One-Dimensional Transport with Inflow and Storage) is a model used to characterize the fate and transport of water-borne solutes in stream and river systems that simultaneously solves equations (2) and (3) given the appropriate parameters of the model (Runkel, 1998). In this research, OTIS will be used inversely (known as OTIS-P) to estimate main channel and transient storage zone parameters based on data collected from soil pipe tracer tests of Wilson et al. (2015). Typically for a conservative tracer and constant flow rate the A, D, A_s, and α_s are inversely estimated from tracer breakthrough curves (Stofleth et al., 2008). OTIS-P uses a nonlinear-regression method in fitting the advection–dispersion equations (equations 2 and 3) to observed data by minimizing the squared error between observed and modeled concentrations.

A second approach is to conceptualize the soil pipe as porous media with solute flow and transport described by the convective dispersive equation (CDE), e. g. the dual porosity CDE formulation (Brusseau et al., 1991; Brusseau, 1998; Wilson et al., 1998). Similar to OTIS, exchange between the two regions or domains is modeled as a first-order process. One model commonly applied for porous media solute transport is CXTFIT (Parker and Van Genuchten, 1984; Toride et al., 1995), which solves various boundary value, initial value, and production value problems (Toride et al., 1995; Fox et al., 2011). The model uses a nonlinear least-squares parameter optimization method to derive solute transport parameters for various model formulations. Since the governing differential equations for the transient storage zone model (OTIS) and porous media CDE are essentially equivalent, this study will focus on the application of the stream flow and transport model to soil pipes.

The objective of this research was to assess whether a transient storage zone model typically applied for tracer tests in streams or river channels can be applied to soil pipes for the purpose of

quantifying their flow and transport characteristics. The transient storage zone model was applied to data from four independent tracer studies on different soil pipe networks within the main and back catchment of the Goodwin Creek Experimental Watershed. A second objective was to assess consistency in flow and transport parameters for individual continuous soil pipes in the same watershed. Only the transient storage zone model was utilized in this research because of the equivalency between the governing differential equations for the transient storage zone and porous media transport models.

Materials and Methodology

Tracer Test Data

Fluorescein dye was released into four different soil pipe networks identified in the Goodwin Creek Experimental Watershed (GCEW) in northern Mississippi (Wilson et al., 2015). Goodwin Creek drains a fourth-order, 21 km^2 northwest Mississippi watershed located along the bluffline of the Mississippi River Valley. The parent material for soils in Goodwin Creek consists mainly of a thin (<2 m) loess cap over coastal plain sediment (Fox et al., 2007). Wilson et al. (2015) described surveys in 2013 and 2014 of soil pipe collapse features and their association to soil properties and past land use history in a subwatershed of GCEW. The subwatershed consisted of three catchments with only two of these (Main and Back) exhibiting pipe collapse features. The Main (6.5 ha) catchment consist of three upper branches (West, Middle, and East) that exhibit 100 soil pipe collapses. The most common feature is flute holes, i.e. small circular openings at the soil surface connected to the soil pipe. The West Branch consist of a soil pipe at its upper extreme that flows into a large (36 m long) gully window formed by tunnel collapse that extends into the lower swale landscape position where numerous soil pipes divert the flow back into the subsurface. The Middle and East branches consist primarily of continuous soil pipes with numerous flute holes and small gully windows. These three individual soil pipe networks converge at the lower swale position where a berm forces surface flows to flow measurement

instruments. The Back Catchment (1.4 ha) consist of 40 pipe collapses features which are evenly divided among flute holes, sinkholes and gully windows. The soil pipe creating these collapse features in the Back Catchment is larger and more actively eroding than the soil pipes in the Main Catchment.

Individual tracer tests were conducted in each of the three branches to the Main Catchment (West, Middle, and East) and the Back Catchment (Figures 3 and 4). Fluorescein dye was injected in the upstream end and sampling stations were established at various locations, either the flute holes or gully inlets, downstream of the injection point (Figure 3). Releases occurred on different flow events and dates: April 19, 2013 for the Middle pipe, May 3, 2013 for the East pipe, May 22, 2013 for West Pipe and May 29, 2014 for Back Catchment. The fluorescein dye samples were analyzed with a Trilogy laboratory fluorometer (Turner Designs, Inc., Sunnyvale, CA, minimum detection limit of 0.01 mg/L). Fluorescein dye concentrations were normalized in the form of a relative concentration (C/C_o) versus time where C is the sample concentration and C_0 is the average concentration of the injected pulse. Flow data were not available other than measurements at selected locations of the water levels (Wilson et al., 2015). The breakthrough time was determined by the first temporal moment ($t_{c,x}$) of the BTCs for each sample location. Sampling locations, peak values, and breakthrough times are shown in Table 2. The breakthrough time at the upstream (x_1) and downstream ends (x_2) of each soil pipe reach were used to calculate the reach flow velocity (u):

$$t_{c,x} = \hat{E}[t] = \frac{\sum_{j=1}^{n_x}\left[\Delta t_j c_x(t_j) \times t_j\right]}{\sum_{j=1}^{n_x}\left[\Delta t_j c_x(t_j)\right]} \tag{4}$$

$$u = \frac{x_2 - x_1}{t_{c,x_2} - t_{c,x_1}} \tag{5}$$

OTIS-P Setup and Analysis

OTIS-P requires reach-specific parameters for each of the four soil pipes. These variables include (i) the number of segments in each reach, held constant at 100 segments in each simulation, (ii) the reach length which was specific to the linear distance between the measurement locations for each pipe, and (iii) estimated D, A, A_s, and α_s. OTIS-P also requires input parameters for the tracer, such as decay and sorption parameters. This research assumed negligible decay and sorption. Note that the actual soil pipe flow path may be longer, due to toruousity, than the linear distance between sample locations reported in Table 2. The boundary condition was simulated in OTIS-P as a continuous concentration profile, using the first measurement location for each pipe as the upstream boundary.

OTIS-P required a flow file that included the flow rate (Q = 0.002 m^3/s) at the upstream boundary, the lateral inflow and outflow rates (assumed negligible in these simulations), the lateral inflow solute concentration (assumed negligible) and the main channel flow area (A, calculated from flow rate and velocity estimated using first temporal moment). Parameters were inversely estimated using OTIS-P in a series of simulations. Final parameter estimates from the previous OTIS-P run were used as initial estimates for the next run. OTIS-P runs were repeated until the final parameter values did not change between successive simulations.

Hydraulic Metrics

Several investigators have proposed metrics from the parameters estimated by OTIS-P that may be used for comparison of different flow systems, primarily for contrasting different stream systems where the transient storage model has been applied (Runkel, 2002):

- The Damköhler number (D_a) is the ratio of the characteristic reaction rate to the characteristic mass transfer rate by advection:

$$D_a = \alpha_s \left(1 + \frac{A}{A_s}\right) \frac{L}{u} \tag{6}$$

- The average distance a molecule travels downstream within the main channel prior to entering the storage zone is referred to as L_s (Mulholland et al., 1994):

$$L_s = \frac{u}{\alpha_s} \tag{7}$$

- The T_{str} is the main channel residence time or the average time a molecule remains in the main channel before passing the storage zone (Thackston and Schnelle, 1970):

$$T_{str} = \frac{1}{\alpha_s} \tag{8}$$

- The T_{sto} is the storage zone residence time (Thackston and Schnelle, 1970) or the average time a molecule remains into the storage zone after traveling a distance of L_s:

$$T_{sto} = \frac{A_S}{\alpha_s A} \tag{9}$$

- Storage exchange flux, q_s, is the average flux through the storage zone per unit flow path length (Harvey and Bencala, 1993):

$$q_s = \alpha_s A \tag{10}$$

- The hydrological retention factor R_h, represents solute retention as storage zone residence time per meter of stream reach travelled by stream water in the surface; i.e. soil pipe channel, before entering the storage zone (Morrice et al., 1997):

$$R_h = \frac{A_S}{Q} \tag{11}$$

- Because none of the metrics presented above describe the overall effect of these three parameters on downstream transport, and may lead to interpretational conflictions, a new metric was proposed by Runkel (1998):

$$F_{med} = \left(1 - e^{-\frac{L\alpha_s}{u}}\right)\frac{A_S}{A + A_S} \tag{12}$$

The F_{med} is the fraction of median travel time due to storage. Streams with higher transient storage zone effects have a higher F_{med} whereas lower storage influenced streams will have a lower F_{med}. For the purpose of comparing values of F_{med} from different sites and experiments, Runkel (2002) suggests that a reach length L = 200 m be used in equation (12). All values reported herein are for F_{med200}.

Model Performance Metrics

First, the success of OTIS-P parameter estimation was based on obtaining either (i) parameter convergence or (2) residual sum of square convergence (Runkel, 1998) within each reach of the four soil pipes. Two other types of convergence were possible: singular convergence which means that the model contains too many parameters and false convergence which means that convergence criteria are too small for the accuracy of the model (Runkel, 1998). The performance of OTIS-P in estimating the observed breakthrough curves was also quantitatively assessed based on several statistical metrics. The sum of squared errors (SSE) and mean squared error (MSE) are measures of the discrepancy between the observed data and model predictions:

$$SSE = \sum_{i=1}^{n}\left(y_i - x_i\right)^2 \tag{13}$$

$$MSE = \frac{1}{n}\sum_{i=1}^{n}\left(y_i - x_i\right)^2 \tag{14}$$

where x_i and y_i are the i^{th} observed and predicted values, respectively. A smaller SSE *and* MSE indicate a closer fit of the model to the data. The Nash–Sutcliffe model efficiency coefficient (NSE) is used to assess the predictive power of hydrological models (Nash and Sutcliffe, 1970):

$$NSE = 1 - \frac{\sum_{t=1}^{T}\left(Q_o^t - Q_m^t\right)^2}{\sum_{t=1}^{T}\left(Q_o^t - \overline{Q_o}\right)^2} \tag{15}$$

The subscript "o" refers to observed value, and "m" is modeled value. NSE ranges from $-\infty$ to 1 where 1 indicates perfect match. The normalized objective function (NOF) is the ratio of standard deviation of differences (STDD) to the overall mean (X_a) of the observed parameter (Fox et al., 2004):

$$NOF = \frac{STDD}{X_a} = \frac{\sqrt{\frac{\sum_{i=1}^{n}\left(x_i - y_i\right)^2}{x_i}}}{X_a} \tag{16}$$

where x_i and y_i are the i^{th} observed and predicted values respectively. Smaller NOF values indicate a closer fit and an NOF less than 1 satisfies the site-specific criteria.

Results and Discussion

Flow and Transport Characteristics

The tracer breakthrough curves for the three soil pipe networks in the Main Catchment exhibited the expected pattern of decreased peak concentrations and greater spreading with extended tailing downstream of the injection points (Figure 5). The East pipe varied from this expected behavior with a peak concentration higher in the third sampling location as compared to the second sampling locations, and the peaks were typically much larger at the downstream sampling

locations than observed for the West and Middle branches (Figure 5). Potential reasons for this discrepancy include connectivity with a larger network of soil pipes that contribute flow to the West and Middle soil pipes thereby diluting the tracer concentration with distance downslope, i.e., similar to a spring in a stream system. Nieber and Sidle (2010) demonstrated the transient effect of soil wetness on the connectivity of soil pipes within a pipe network. Given that these tracer studies were conducted during natural storm events using *in situ* soil pipes, the assumption of no water exchange (solute only) between the soil pipe and matrix is not strictly valid which will be addressed in future research. It appears that either the solute storage was considerably less in the East soil pipe or the connectivity with the network or inflow from the network of soil pipes was greater for the West and Middle soil pipes. With these constraints, it was much more difficult for OTIS-P to fit the concentration breakthrough curves for the East soil pipe.

Soil pipe reach flow velocity was estimated to be approximately 0.02 m/s (range between 0.02 and 0.03 m/s) using the first temporal moment analysis of the concentration breakthrough curves (Table 3). The reach-specific velocities were used to establish an appropriate *Q/A* in the OTIS-P input files. Based on the convergence criteria, OTIS-P was successful in simulating the observed breakthrough curves in eleven of the twelve reaches; only the middle reach of the East pipe resulted in a false convergence (Table 4). Goodness of fit parameters NSE and NOF confirmed the difficulty in modeling the East pipe compared to the other two pipes (Table 5).

Inversely estimated output parameters obtained from OTIS-P for the four soil pipes were consistent, especially for *A* (Table 4). The *A* ranged between 0.03 and 0.33 m^2, which was consistent with observations in the field of typical pipe diameters 0.2 to 0.6 m. The larger *A* predicted for the Middle Branch (Reach 3) was most likely heavily influenced by larger surface openings in the pipe network. Estimated velocities when considering transient storage ranged between 0.01 and 0.08 m/s. Velocities on this order of magnitude suggest corresponding shear stresses that exceeded the soil's critical shear stress. Erosion of the pipe material can result in

pipe expansion to the point of collapse of the upper material promoting additional capture of runoff from the surface and further promoting gully development. This collapsed material could also create additional sinuosity or subject the adjacent soil matrix to concentrated flow resulting in the formation of new soil pipes. Therefore, it was expected that the velocity and transient storage metrics were functions of time as the gully network continued to develop.

Another possible mechanism for the breakthrough curve response was dilution from other pipes feeding into the main network of the West, Middle, and East soil pipes. In fact, OTIS does account for lateral recharge into and out of specific modeled reaches. Once again the difficulty was attempting to determine the magnitude of lateral inflow without flow measurements throughout the soil pipe network system. Future research investigating such pipe networks should measure flow rates through the pipes. When neglecting transient storage and only considering dilution, it was possible to match the timing and magnitude of the peak concentration with adjusted velocity and dispersion coefficients. This results in symmetrical breakthrough curves with the lateral spread influenced specifically by the estimated dispersion coefficient. However, the shapes of the simulated breakthrough curves could not mimic the tailing effect observed in the field-measured breakthrough curves (Figure 5). The tailing-effect in the observed breakthrough curve indicated that transient storage occurred in the system and assumed to be of greater importance than potential dilution from soil pipes.

Transient Storage Metrics

Stofleth et al. (2008) performed OTIS simulations for Goodwin Creek and compiled stream characteristics from 136 databases with 111 of them were streams with beds coarser than sand. Even though OTIS was applied in this study to a unique flow situation, i.e. soil pipes, compared to typical applications of OTIS-P, it was interesting to compare metrics (Table 6) for the different flow scenarios from Stofleth et al. (2008). The relationship between α_s and u and the relationship between A_s and A mimicked what has been reported in streams (Figure 6). Relative to A, the A_s

values were typically larger for the soil pipe flow condition compared with stream data reported by Stofleth et al. (2008). This difference is mainly attributable to soil pipe configuration i.e., higher wetted perimeter to flow area, as compared to a stream or river channel. Compared to previous studies in stream and river systems, velocities in these soil pipes were typically lower whereas α_s was in upper range of what was observed when applying the transient storage zone model to stream systems (Figure 6). The soil pipes had a large A_s, leading to large F_{med200} and R_h values (Figure 6). Theoretically it was also expected that transient storage has a larger influence on a soil pipe than stream and river systems due to its lower flow velocity and greater soil-fluid contact.

Summary and Conclusions

A transient storage model adequately simulated four soil pipe tracer injection tests. Transient storage in soil pipes acts to reduce the peak concentrations downstream of the source, delay the breakthrough curve, and enhance the tailing effect. Considerable variability was observed in the transport parameters when comparing different soil pipes in the same catchment and even within different reaches of the same soil pipes, especially in terms of the transient storage area and first-order exchange coefficient. This was most likely due to pipe irregularities throughout the pipe network. Dimensionless transport metrics of the transient storage model were calculated for the soil pipes with the observed ranges mimicking those reported for river and stream systems. Velocities in the soil pipes were generally lower, whereas the storage zone area and exchange coefficients were typically in the upper range of values reported for streams due to the higher wetted perimeter to flow area i.e., soil-fluid contact, and lower flow velocities.

Large variability was observed in the inversely estimated A_s and α_s, which suggests differences in potential sinuosity of the different pipe networks or even locations within the pipe network of significant pooling of water before continuing through the network. While these tracer injection

tests provide evidence of the soil pipe flow and transport characteristics, a considerable need still exists for methodologies to map soil pipes, their sinuosity, network connectivity, and flow characteristics. Longer term studies at the site will continue to monitor pipe geomorphology and hydrometrics to document the development of the pipe network and develop a database of the hydrodynamics. Additional tracer studies should also be conducted to quantify changes in flow/transport characteristics, presence of transient storage over time, and dilution from other soil pipe and macropore networks feeding the main soil pipe channel as a function of soil wetness or soil pipe hydrograph.

Table 2. Summary of the measurement locations (distance from injection point, x, and distance between measurement locations, d), relative observed peak concentrations measured (C/C_0), and time to peak concentration for each location.

Soil Pipe	Point	x (m)	d (m)	Peak (C/C_0)	Peak time (min)
West Branch	Injection	0			
	W1	1.4	1.4	1.3488	6.3
	W2	21.2	19.8	0.4424	21.0
	W3	50.3	29.1	0.1603	50.0
	W4	94.1	43.8	0.0504	100.0
	W5	146.2	52.1	0.0125	181.0
	Outlet*	190.8	44.6	0.0015	332.0
East Branch	Injection	0			
	E1**	3.1	3.1	2.0163**	4.0
	E2	14.9	11.8	0.6939	5.0
	E3	21.6	6.7	0.8059	10.0
	E4	48.6	27.0	0.4864	17.5
	E5	68.9	20.3	0.0474	25.0
	Outlet	136.7	67.8	0.0079	45.0
Middle Branch	Injection	0			
	M1**	1.8	1.8	2.2156**	0.5**
	M2	21.1	19.3	0.2588	12.0
	M3	41.2	20.1	0.0696	24.0
	PM4	90.5	49.2	0.0064	152.0
	M5	138.2	47.8	0.0006	241.0
	Outlet	182.8	44.6	0.0001	347.0
Back Catchment	Injection	0			
	B0	3.3	3.3	1.0000	0.3
	B1	6.1	2.8	0.5041	0.7
	B2	10.7	4.6	0.1186	2.0
	B3	17.9	7.2	0.0752	3.3
	B4	25.7	7.8	0.0729	5.0
	B5	38.7	13.0	0.0523	6.0
	B6	57.6	18.9	0.0562	11.0
	B7	78.6	21.0	0.0289	17.3

* Did not reach peak before sampling stopped.

**Unstable concentration fluctuation.

Table 3. Reach interval, distance, and calculated reach flow velocity from the first temporal moments of the breakthrough curves. E, M, W and B represent the sampling points for east, middle, west branch of the main catchment and back catchment, respectively.

Soil Pipe	Reach	Reach Interval	Distance (m)	Velocity (m/s)
West Branch	1	W1 to W2	19.8	0.027
	2	W2 to W3	29.1	0.011
	3	W3 to W4	43.8	0.012
East Branch	1	E1 to E2	11.8	0.063
	2	E2 to E3	6.7	0.020
	3	E3 to E4	27.0	0.065
Middle Branch	1	M1 to M2	19.3	0.030
	2	M2 to M3	20.1	0.021
	3	M3 to M4	49.2	0.005
Back Catchment	1	B0 to B1	2.8	0.100
	2	B1 to B2	4.6	0.059
	3	B2 to B3	7.2	0.077
	4	B3 to B4	7.8	0.075

Table 4. OTIS-P predicted soil pipe storage and transport parameters including dispersion coefficient (D), storage area (A_s), cross-section area (A) and storage rate (α_s) for each of the four soil pipes.

Soil Pipe	Reach	Reach Length x (m)	Dispersion Coefficient D (m^2/s)	Cross-section Area A (m^2)	Storage Area A_s (m^2)	Storage Rate α_s (s^{-1})	A_s/A	Velocity, $u=Q/A$ (m/s)
West Branch	1 [b]	19.8	0.03	0.07	0.01	0.0037	0.19	0.030
	2 [a]	29.1	0.01	0.11	0.08	0.0012	0.80	0.019
	3 [a]	43.8	0.01	0.13	0.55	0.0004	4.14	0.015
East Branch	1 [a]	11.8	0.02	0.03	19.68	0.0015	787.20	0.080
	2 [c]	6.7	0.01	0.08	0.02	0.0037	0.24	0.027
	3 [a]	27.0	0.03	0.04	0.75	0.0006	19.13	0.051
Middle Branch	1 [a], [b]	19.3	0.03	0.07	2.87	0.0017	38.97	0.027
	2 [b]	20.1	0.01	0.07	0.59	0.0013	8.41	0.029
	3 [a]	49.2	0.01	0.33	4.00	0.0001	12.22	0.006
Back Catchment	1 [a]	2.8	0.02	0.07	1.71	0.0063	24.78	0.145
	2 [a]	4.6	0.02	0.16	0.56	0.0059	3.57	0.063
	3 [a]	7.2	0.05	0.13	3.76	0.0005	29.88	0.080
	4 [a]	7.8	0.03	0.13	0.25	0.0001	1.89	0.076

[a] Parameter convergence

[b] Residual sum of squares convergence

[c] False convergence

Table 5. Statistical parameters for the four soil pipes illustrating the goodness of fit between the observed and predicted dimensionless concentrations (C/C_o).

Soil Pipe	Reach	n	SSE	MSE	NSE	NOF
West Branch	1	27	0.019	7.1E-04	0.974	0.175
	2	26	0.006	2.4E-04	0.910	0.404
	3	23	0.001	2.4E-05	0.895	0.331
East Branch	1	23	0.272	1.2E-02	0.799	0.779
	2	6	0.077	1.3E-02	0.849	0.719
	3	6	0.009	1.5E-03	0.751	0.581
Middle Branch	1	35	0.016	4.7E-04	0.909	0.419
	2	42	0.004	8.7E-05	0.815	0.592
	3	18	0.000	9.8E-07	0.783	0.304
Back Catchment	1	22	0.009	4.0E-04	0.972	0.391
	2	13	0.000	7.2E-06	0.995	0.117
	3	14	0.000	6.6E-06	0.990	0.132
	4	11	0.000	4.5E-05	0.901	0.511

Table 6. Hydraulic metrics for the four soil pipes for comparison between soil pipe and stream systems.

Soil Pipe	Reach	Damkohler Number, D_A	R_h (m^{-1})	F_{med200}	q_s
West Branch	1	15.16	6.46	16.17	2.48E-04
	2	4.10	42.44	44.45	1.25E-04
	3	1.37	273.00	80.01	5.04E-05
East Branch	1	0.22	9840.00	97.40	3.70E-05
	2	4.84	9.00	19.35	2.80E-04
	3	0.34	373.00	86.43	2.40E-05
Middle Branch	1	1.27	1433.06	97.50	1.28E-04
	2	1.00	294.50	89.37	8.89E-05
	3	0.64	1997.50	84.05	2.40E-05
Back Catchment	1	0.33	56.46	78.12	9.33E-04
	2	0.03	375.68	67.75	6.02E-05
	3	0.01	24.70	10.88	9.10E-06
	4	0.01	24.70	10.88	9.10E-06

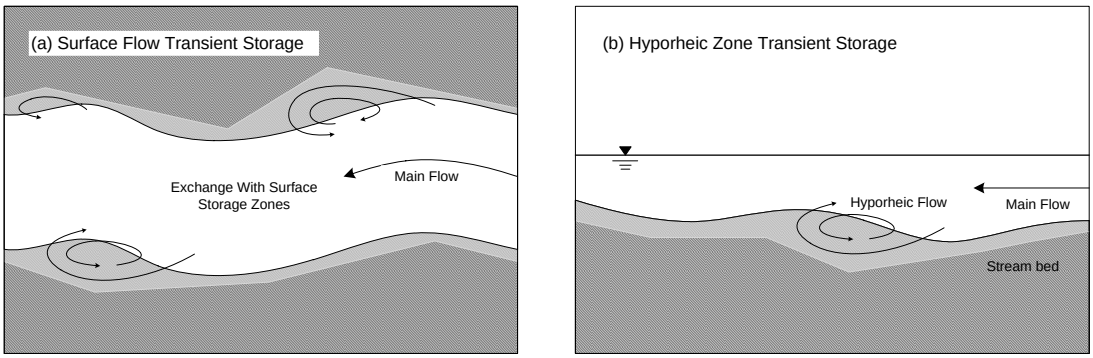

Figure 1. Transient storage in a stream or river system, including (a) surface transient storage with eddies and dead water pools (gray) and (b) transient storage in hyporheic zone (gray).

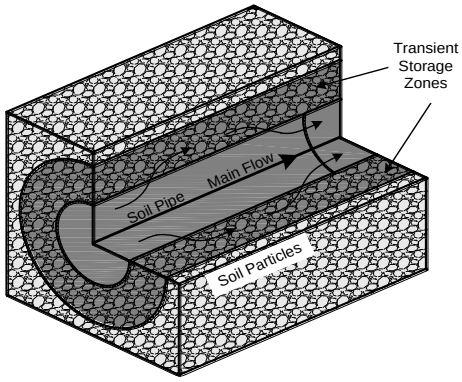

Figure 2. Transient storage zones in full flow soil pipe where the shaded area around the soil pipe is A_s and the soil pipe cross sectional area, A.

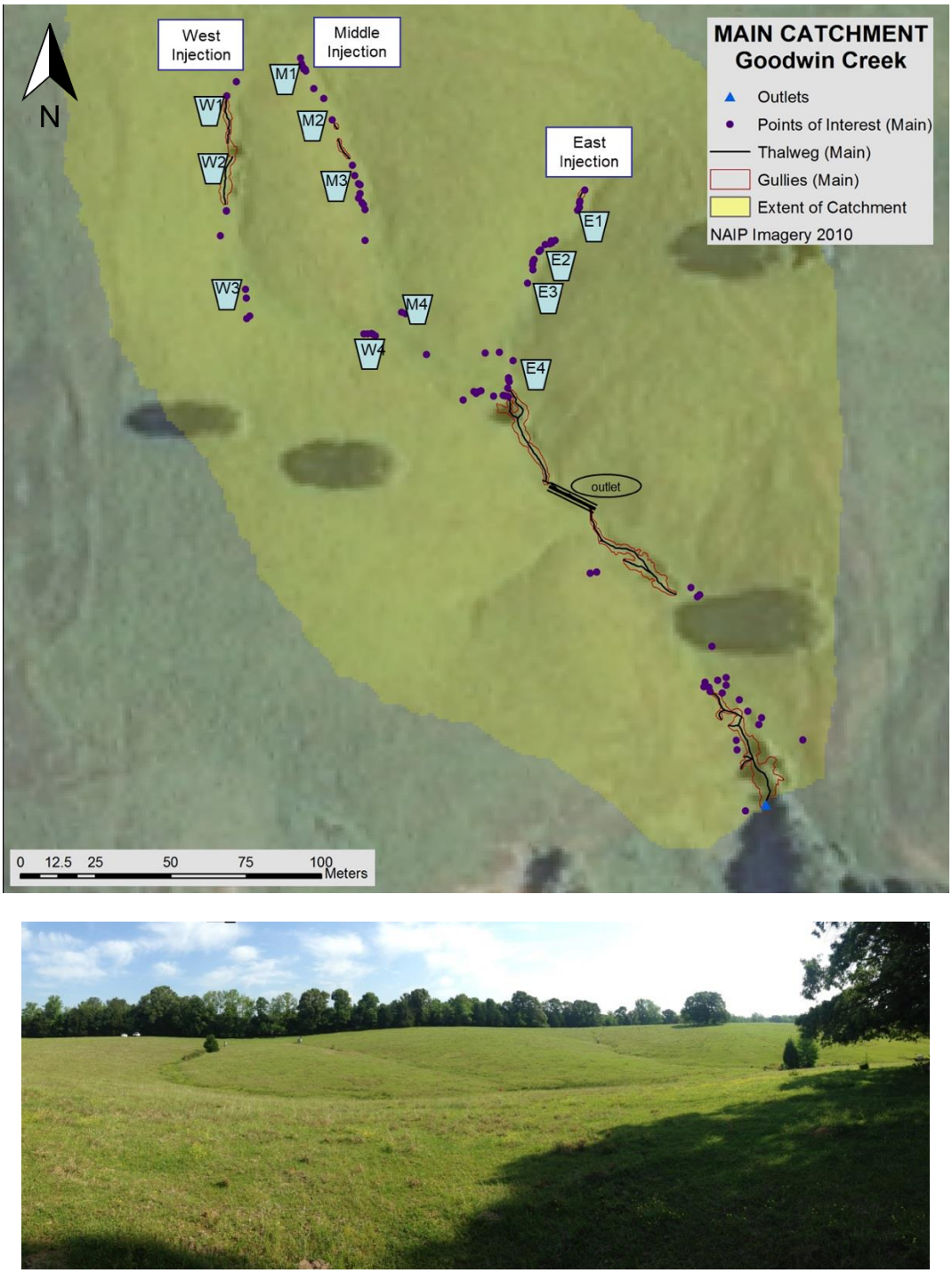

Figure 3. Goodwin Creek main catchment map (top) and picture (bottom) showing the three soil pipe networks (W = West, M = Middle, and E = East). Fluorescein dye was injected at the upper end of the pipe network and flow in the pipe network was sampled at a number of down gradient locations. Picture by Mikayla Wanger (Oklahoma State University).

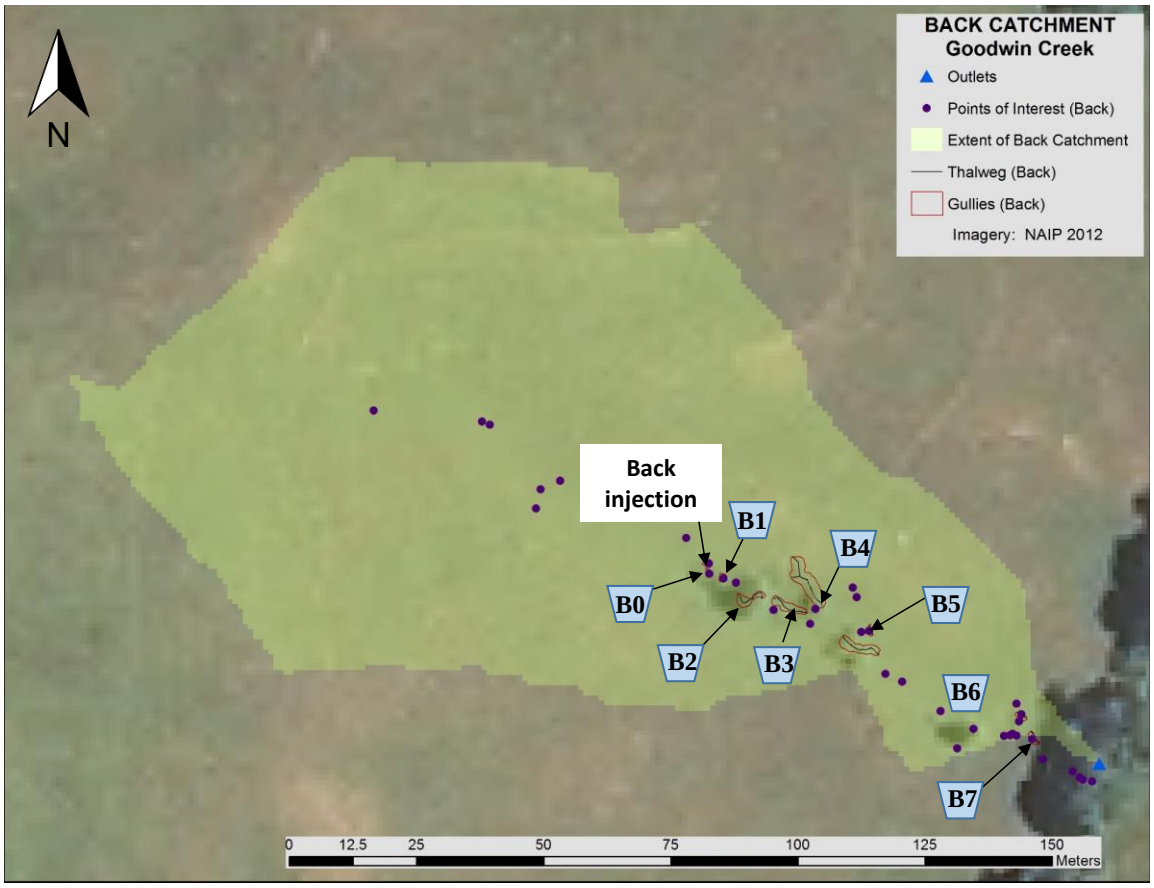

Figure 4. Dye tracer sampling locations in the Back Catchment that were used for modeling pipe flow.

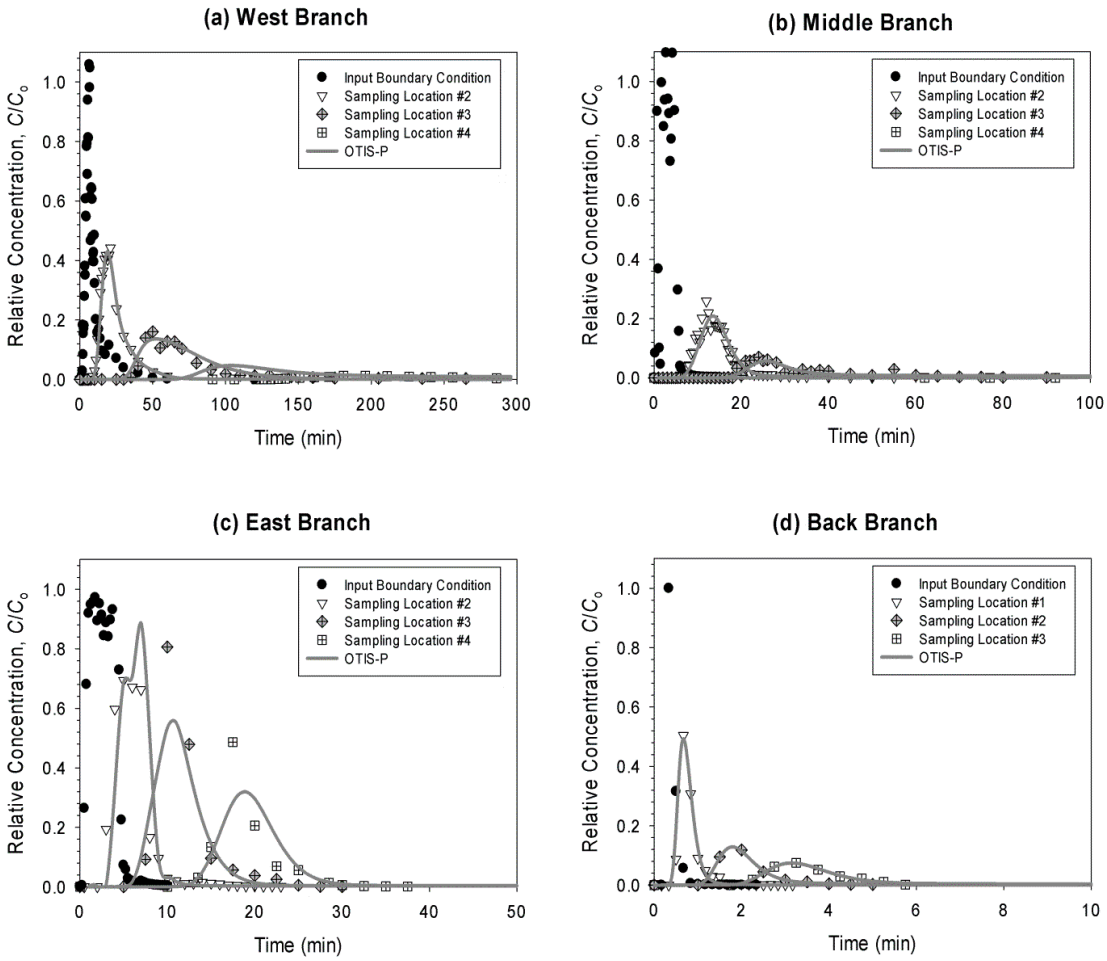

Figure 5. Breakthrough curve and simulated tracer concentrations by OTIS-P for the (a) West pipe branch, (b) Middle pipe branch, (c) East pipe branch and (d) Back catchment branch.

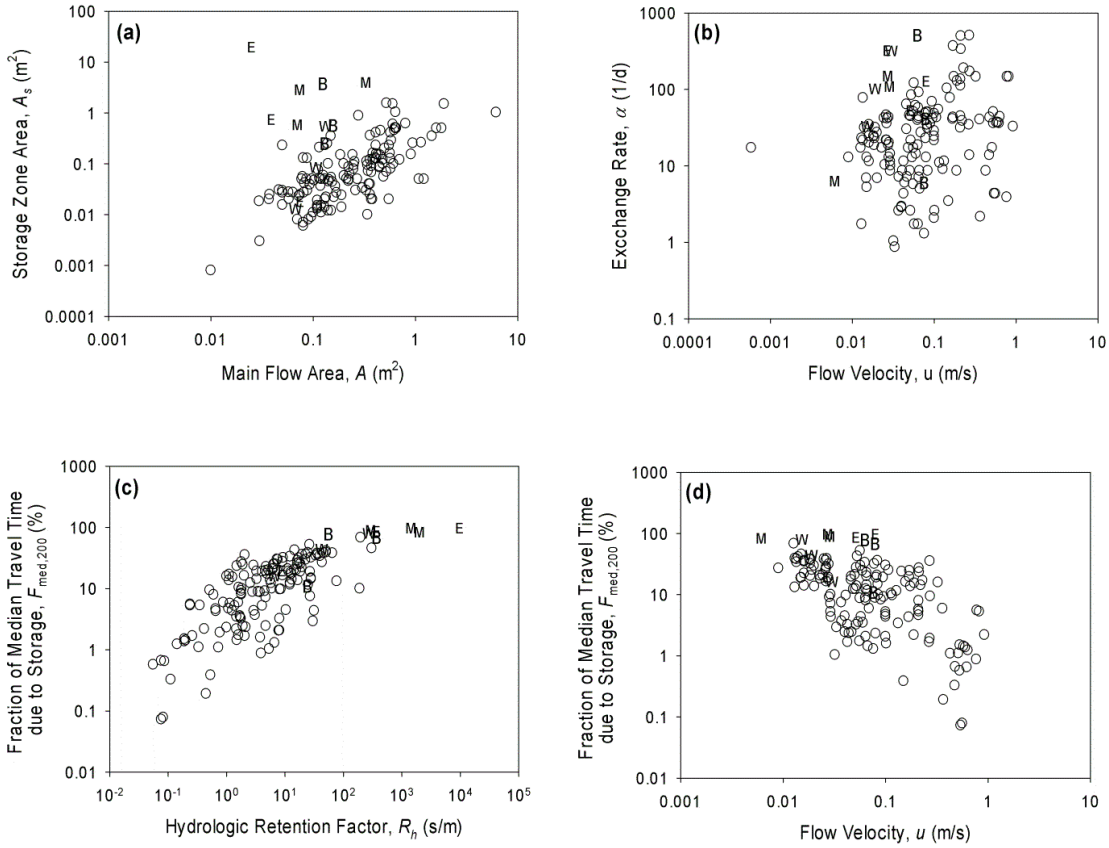

Figure 6. Comparison of parameters derived from the soil pipe tracer tests (E, M, W and B symbols represent the data points for east, middle, west branch of the main catchment and back catchment, respectively) and data from tracer tests in streams: (a) A-A_s, (b) u-α, (c) R_h-F_{med} and (d) u-F_{med}. Stream data (circles) are from Stofleth et al. (2008).

CHAPTER III

GROUNDWATER FLUX ESTIMATION IN STREAMS: A THERMAL EQUILIBRIUM APPROACH

Introduction

The interaction of stream water with groundwater influences water quality and quantity and plays an essential role in aquatic ecosystems. Streams with high groundwater interactions are often characterized by high biological and microbial diversity and activity due to elevated solute transport and nutrient exchange across the streambed interface (Laursen and Seitzinger, 2005; Schmidt et al., 2007). Groundwater flux can also limit benthic invertebrate exposure to low oxygen and contaminants (Malard and Hervant, 1999), provide thermal refugia and microbial food supply for fish (e.g., salmon) (Kurylyk et al., 2013). The importance of groundwater to stream biota has led to increased efforts to quantify the effects on both stream temperatures (Constantz, 1998) and energy sources (Barlocher and Murdoch, 1989). However, the complex nature of stream-groundwater hydrological connectivity can make quantifying those interactions difficult and labor intensive.

Over the past few decades, many approaches have been developed to quantify surface water-groundwater interactions that can be generally categorized into Darcian, streamflow, water

budget and tracer methods (Table 1). Extensive reviews of these approaches have been provided by Kalbus et al. (2006), Brodie et al. (2007), and Turner (2009) but are briefly overviewed below. Darcian methods calculate point surface-groundwater flux as the product of measured hydraulic gradient and conductivity based on Darcy's Law in a manner similar to that used to investigate water movement in porous media (Freeze and Cherry, 1979). Water budget methods use groundwater and watershed models, separately or in combination, to estimate groundwater and surface water interactions as the unknown residual of the water budget by calibrating the model against streamflow records and estimated physical parameters of the aquifer. Streamflow methods include a variety of approaches such as hydrograph separation, direct measurement using seepage meters and seepage runs. The hydrograph separation methods, such as recession-curve displacement and stream base-flow analysis, use various assumptions to separate a stream hydrograph into the different runoff, interflow, and baseflow components (Scanlon et al., 2002). The seepage meter method allows direct point measurement of surface and groundwater flux by calculating the rate of volume change of a collection bag over the area of the collecting bucket pushed into the streambed (Zamora, 2008). The seepage run method for estimating groundwater flux involves measuring streamflow at multiple transects along the river. After eliminating contributions from tributaries, the surface-groundwater flux is assumed to be the flow rate difference between transects (Rosenberry and LaBaugh, 2008). Tracer methods estimate groundwater flux based on the mass balance of tracers. Introduced tracers, commonly chloride or dyes, are usually used in either dilution gauging or transient storage approaches (Zhou et al., 2015) while environmental tracers such as tritium and chlorofluorocarbons are used in hydrograph separation to provide information on groundwater flux. The limitations of these conventional methods are the high time and material cost for proper installation and maintenance (e.g., Darcian method with piezometer and seepage meter) (Berry et al., 2011), and the difficulty in parameter estimation (e.g., water budget methods) (Scanlon et al., 2002). Due to the ease of

monitoring stream temperatures, thermal methods overcome some of these limitations and have gained increasing popularity in recent decades (Webb et al., 2008).

Thermal methods use heat as an environmental tracer, with the analysis based on the heat transfer (i.e., energy balance) analogous to the mass balance of common chemical tracers. Thermal methods emerged as a versatile class of geophysical tools for monitoring focused recharge in arid and semiarid settings, but did not come into common use until the 1960s (Blasch et al., 2007) after analytical solutions to the coupled heat and water transport equations were established by Suzuki (1960), Stallman (1965), and Bredehoeft and Papaopulos (1965). The vertical thermal gradient method uses coupled heat and water transport through both advection and conduction to quantify vertical water movement across the streambed (Anderson, 2005). By monitoring the temperature of stream water and saturated bed sediment at multiple depths, the vertical propagation of heat can be simulated based on the coupled relationship between heat and water. These properties have been used to investigate infiltration and percolation on the land surface (Suzuki, 1960), to indicate gaining and losing reaches of stream channels (Lapham, 1989; Silliman and Booth, 1993; Constantz, 1998), and to locate areas of inflow to lakes (Lee, 1985). Instead of simulating the coupled transport of water and heat across the interface between groundwater and surface water, the emerging stream thermal modeling approach, first introduced by Becker et al. (2004), uses a process-based model (Loheide and Gorelick, 2006) to simulate heat budget of stream water using known hydrological and atmospheric variables, and quantify heat introduced by groundwater flux as the residual of the known stream water heat budget.

Despite these advances in thermal methods, there are still areas that could be improved. The vertical thermal gradient method provides a convenient alternative for quantifying groundwater flux at point scales, but the cost of material and time is significant if the scale is to be expanded using multiple measurements. Stream thermal modeling methods estimate groundwater flux at a larger scale with relatively lower cost, but it loses the sensitivity of point estimations. Thus, there

is still a need for accurate, convenient, and economical means of quantifying point groundwater flux that can be expanded to cover a predetermined area, e.g., reach scale. This research proposes a thermal equilibrium method based on current stream thermal modeling method that uses water temperature, existing atmospheric and hydrological data to simulate heat budget of stream and quantify groundwater interactions. The proposed approach significantly reduces the need and cost of data collection while maintaining the sensitivity and independence of a point measurement.

Therefore, objectives of this study were to establish and evaluate a thermal equilibrium method (hereafter TEM) for quantifying groundwater interactions by (i) identifying the heat transfer mechanisms that regulate stream water temperature with consideration of groundwater interactions; (ii) developing the TEM to estimate the time-averaged groundwater flux to a stream using monitored stream water temperature data at a single point and existing atmospheric and hydrological data, and (iii) validating the performance of the TEM by comparison with estimates from seepage runs.

Materials and Methods

Thermal Equilibrium Method

The TEM was developed based on the assumed thermal equilibrium of all heat transfer processes in the stream including both atmospheric heat transfer and groundwater interactions. Equilibrium water temperature calculated based on atmospheric condition (atmospheric equilibrium water temperature, hereafter T_{AE}) has traditionally been used as an approximation to stream water temperature (hereafter T_S) (Smith, 1981). Recent research pointed out that the T_{AE} calculated on a weekly or broader temporal scale were linearly related, but not equal to T_S (Bogan et al., 2003). The difference between T_{AE} and T_S are attributed to external water inputs, primarily groundwater interactions for 80% of the 596 sites in the eastern and central USA (Bogan et al., 2003; Bogan et al., 2004; Webb et al., 2008). In the current study I assumed that by including groundwater

interactions a more comprehensive equilibrium water temperature (hereafter T_E) could be calculated to appropriately represent T_S on a weekly or broader temporal scale. In another words, I assumed streams were at thermal equilibrium with the combination of atmospheric conditions and groundwater interactions. A stream water temperature model was applied to simulate the atmospheric heat transfer processes (i.e., heat conduction, shortwave solar radiation, longwave atmospheric radiation, etc.) based on the upstream boundary of monitored T_S, atmospheric and hydrological conditions of the monitored point. The monitored stream point was represented by an expanded continuous model domain (Figure 7), allowing the model to stabilize and predict T_{AE} at the downstream boundary. Based on the thermal equilibrium assumption, the difference between T_S (upstream boundary) and predicted T_{AE} (downstream boundary) was attributed to groundwater flux. Therefore, if the predicted T_{AE} of the downstream boundary conditions differed from the upstream T_S, a groundwater flux could be applied to the domain and calibrated until the difference between the two boundaries was minimized ($T_E = T_S$). The magnitude of the flux required for thermal equilibrium would provide an estimate of the unknown groundwater flux at the monitoring point according to the assumption.

The Water Quality Analysis Simulation Program (WASP) was employed in this study to simulate stream heat transfer with an output temporal resolution of 1 hr. WASP, developed by the U.S. Environmental Protection Agency (EPA) (Wool et al., 2006), is a dynamic compartment-modeling program for pollutant transport in aquatic systems. The time-varying processes of advection, dispersion, point and diffuse mass loading and boundary exchange are represented in the basic program. In the WASP temperature module, heat transfer is computed based on the following one-dimensional advection-diffusion equation:

$$\frac{\partial T_s}{\partial t} = -\frac{\partial}{\partial x}(V_x T_s) + \frac{\partial}{\partial x}\left(D_x \frac{\partial T_s}{\partial t}\right) + \frac{H_n A_s}{\rho_w C_p V} + S \quad (17)$$

where T_s is the stream water temperature (°C), V_x is the advective velocity (m/s), D_x is the diffusion coefficient (m^2/s), V is the segment volume (m^3), A_s is the segment surface area (m^2), ρ_w is the density of water (997 kg/m^3), C_p is the specific heat of water (4179 J/kg °C), H_n is the net surface heat flux (W/m^2), S is the loading rate include boundary, direct and diffuse loading (°C /s). The net surface heat flux includes the effects of a number of processes computed as (Cole and Buchak, 1995):

$$H_n = H_s + H_a + H_e + H_c - (H_{sr} + H_{ar} + H_{br}) \quad (18)$$

where H_n is the net heat flux across the water surface (W/m^2), H_s is the incident short wave solar radiation (W/m^2), H_a is the incident long wave atmospheric radiation (W/m^2), H_{sr} is the reflected short wave solar radiation (W/m^2), H_{ar} is the reflected long wave radiation (W/m^2), H_{br} is the back radiation from the water surface (W/m^2), H_e is the evaporative heat loss (W/m^2), and H_c is the heat conduction (W/m^2).

In this study, a one-dimensional conceptual domain with a length of 2 km was constructed in WASP and divided into twenty 100 m-long segments (Figure 8). A monitored T_S time series was input as the upstream boundary and the initial temperature for each segment was set to the T_S at the first time step. The geometry and flow rate in the main channel of the model were assumed to be uniform and described by parameters acquired from transect measurements at the monitored point (see seepage runs below). An atmospheric time series was obtained from the nearest Mesonet station and input into the WASP model to compute heat transfer at each time step. Two model parameters were acquired from the thermal modeling research on Kiamichi River reported in Chapter IV: minimum depth (0.85 m), and light extinction coefficient (3.3 m^{-1}). The effect of canopy cover was considered negligible because the studied reaches were located on unshaded areas of high order streams. Thermal interaction of groundwater flux was represented by a uniform flow input across the twenty segments and incorporated in the model via hydrological

connections (Figure 8). The magnitude of the groundwater flux to each segment was then calibrated until the sum of squared error (SSE) was minimized between the predicted T_E at the downstream boundary and T_S at the upstream boundary. When the temperature at the two boundaries matched, the net heat transfer across the conceptual domain was zero and all the heat transfer processes were equilibrated. The estimated flow represented the optimal groundwater flux required for the T_S to equilibrate as indicated in the thermal equilibrium assumption. In this study, the groundwater temperature time series was estimated from air temperature with 1.5-month time lag as recommended by Pluhowski (1970) (Figure 9). The length and number of segments constructed in the model did not physically represent the monitored point, but served only as a model domain that allows the model to stabilize. The length of the model domain was likely only to influence the overall sensitivity to groundwater flux.

Study Areas

To validate the TEM by comparison with seepage runs, five sampling reaches were chosen on the Kiamichi River (Figure 10). The Kiamichi River watershed in southeast Oklahoma has an area of about 4800 km^2, with elevation ranging 270 to 810 m (Pyron et al., 1998). The sedimentary rocks of the area have been deformed into tightly folding anticlines and synclines forming steep east-west trending ridges separated by a broad and flat bottomed stream valley (Sanford II and Boyd, 2012). The area was expected to have substantial groundwater storage potential as well as permeability to allow groundwater interactions.

Nine additional sampling reaches were located on different streams in the Springfield Plateau in the Ozark Highland ecoregion of Missouri, Arkansas and Oklahoma (Figure 10). The Springfield Plateau comprises the southwest portion of the Ozark Plateau with an area of approximately 26,700 km^2 including parts of west-central and southwest Missouri, northeast Oklahoma, southeast Kansas and northern Arkansas (Adamski et al., 1995). Elevations range 300 to 520 m with mostly gentle topographic relief except for Eureka Springs Escarpment that separates the

Springfield and Salem Plateaus. Most streams in Springfield Plateau drain radially from the plateau center (Adamski et al., 1995; Nigh and Schroeder, 2002). The limestone bedrock in the region is intermittently soluble, producing regionally-abundant sinkholes, springs, and caves (Nigh and Schroeder, 2002). The Springfield Plateau overlies the Ozark Plateau aquifer system, which extends throughout southern Missouri, eastern Oklahoma, southeast Kansas and a large area of northwest Arkansas (Miller and Appel, 1997). Extending sites to the Ozark Highlands allowed us to test the TEM on streams with higher groundwater contributions due to the predominant karst topography.

Seepage Runs

Seepage runs were performed at each site to validate the TEM. Reaches were chosen from candidate streams without flow contributions from tributary streams or major springs as identified by Vineyard and Feder (1974). Once identified, each reach was divided into three to five transects separated by 200 to 500 m. Discharge at each transect was measured with a RiverSurveyor M9 Acoustic Doppler Current Profiler (SonTek, San Diego, CA; hereafter ADCP). The enhanced density of transects per reach was established to achieve a smaller spatial scale which more closely matched the model setup used in the TEM while maintaining accurate groundwater flux estimation in consideration of instrument accuracy (error $\leq \pm 0.015$ m^3/s). At each reach, the ADCP-measured discharge at each transect was normalized for any flow changes detected at pertinent USGS gauges records during the sampling period to remove any temporal variation. The normalized transect discharges were then regressed against the separation distance (upstream to downstream) with the slope of the regression representing the flux between surface water and groundwater for the specific reach (Rosenberry and LaBaugh, 2008). Each seepage run included a flow and transect measurement at each logger site that were used to describe the channel geometry and hydrology in the model. According to T_S measured instantaneously by ADCP, the

T_S difference among transects within each seepage run was < 2 ºC, with this temperature variation likely due to diurnal temperature variations.

Stream Temperature and Atmospheric Time Series

Temperature loggers (HOBO Water Temp Pro v2) were placed in the thalweg of a deeper section at each of the selected reaches, avoiding locations where T_S would vary substantially. Hourly averaged T_S readings were recorded over a 15-d period in September 2016 on the Kiamichi River and June and December 2016 in the Ozark streams. Those time periods covered an extended low-flow period without any significant precipitation event. In the shallow Ozark streams the loggers were placed in a depth between 0.3 and 1 m, and 1.0 to 1.5 m in the deeper Kiamichi River.

A time series of air temperature, wind speed, solar radiation, and relative humidity was obtained for each site from the nearest Oklahoma Mesonet site (OCS, 2016). The Oklahoma Mesonet includes 121 stations distributed throughout Oklahoma, with the largest separation distance from a stream site being approximately 35 km for the Kiamichi River and approximately 40 km for the Ozark streams. The Mesonet stations are automated and collect data at 5-min increments, and reported an hourly average corresponding to the T_S time series.

Statistical Evaluation

To validate the TEM, the FITEVAL software was used to evaluate the fit between groundwater fluxes measured from seepage runs and predicted by the TEM. FITEVAL is a software tool that uses procedures presented by Ritter and Muñoz-Carpena (2013) to incorporate both data and model uncertainty into standardized model evaluation. FITEVAL conducts model evaluations using a combination of graphical illustrations, absolute value error statistics (root mean square error, RMSE), and normalized goodness-of-fit statistics (Nash–Sutcliffe Efficiency coefficient, NSE). Bias corrected confidence intervals are calculated based on approximated probability distributions derived from bootstrapping, followed by hypothesis test results of the indicators,

helping to reduce subjectivity in the interpretation of the model performance (Ritter and Muñoz-Carpena, 2013).

Results and Discussion

TEM versus Seepage Runs

Model validation suggested that TEM was a suitable technique for estimating groundwater flux into streams. The groundwater flux into the streams measured via seepage runs ranged from 0.01 to 1.09 m/d and from 0.00 to 0.95 m/d with the TEM (Table 7). The estimated groundwater flux at the Ozark sites was generally higher than at the Kiamichi sites as expected. The resulting RMSE and NSE for the TEM fit to the seepage run data from FITEVAL were 0.08 m/d and 0.93, respectively, indicated a very good fit. Linear regression analysis showed a uniform variance across the range of estimates with an R^2 of 0.94 (Figure 11). However, the TEM tended to underpredict the seepage run flux estimates by -5.7% (Figure 11). The seepage run represents a spatially integrated flux estimate over a small temporal scale (~2 hr), whereas the TEM represented a temporally integrated flux estimate of a small spatial scale. These two estimates were similar suggesting that the groundwater flux into these streams may not vary widely over the approximately 1.5 km of stream length or the 15-d time period used in this study. Future research could examine the prediction from TEM further by comparison against estimate from other methods at different time of the year and with temporal scale that aligns better with TEM.

The expanded domain length was the only hypothetical model parameter not represented by measurements; therefore, it was important to examine that parameter and its influence on the groundwater flux results. The model domain in the TEM was a 2 km conceptual stream reach composed of twenty segments of 100 m each. To test the effect of model domain length, groundwater flux for Spavinaw Creek in northwest Arkansas were estimates with TEM using alternate total domain lengths of 0.2 and 20 km, each with twenty equal-length segments. The

results indicated that the magnitude of the estimated groundwater fluxes (indicated by the minimum of SSE between the upstream and downstream boundaries) were identical for the 0.2 and 2 km domains, but larger for the 20 km domain. This is likely due to the accumulation of groundwater flux over an extensive simulation distance that significantly changed the heat capacity of the stream. For example, at Spavinaw Creek the average flow rate was 2 m^3/s, and the total estimated groundwater flux accumulation over a 2-km model domain was 0.1 m^3/s; a difference that is unlikely to change the heat capacity of the stream significantly. In contrast, the total groundwater flux accumulation over a 20 km model domain was 1.0 m^3/s with the same rate of groundwater flux, an increase that greatly affected the stream heat capacity.

Since the design of the model domain also affects runtime, some test runs with different domain dimensions may be helpful to balance accuracy and processing time. The temperature module of WASP applied the given thermal and stream parameters sequentially to each segment using a variable internal time-step to reach satisfactory convergence. For the test simulations mentioned above, the run time of the 0.2 km model domain extended to over an hour, whereas the 2-km domain took only 7 to 10 minutes. This was likely due to the extra iterations required for time-dependent thermal processes to converge in the reduced length of the smaller domain.

Where is TEM applicable?

Due to the one-dimensional nature of the temperature model used in TEM, the method was most appropriate for shallow, well-mixed streams that were unlikely to exhibit stratified zones of temperature and/or flow.

A temperature signature of groundwater, meaning the temperature difference between T_{AE} and T_E caused by groundwater flux, was required for the TEM to predict effectively. Streams with low flow and no groundwater flux tend to equilibrate at a high temperature during warm weather conditions ($T_E = T_{AE}$). In contrast, streams with groundwater flux cooler than stream water

equilibrate at a lower temperature during warm weather conditions ($T_E < T_{AE}$), causing a temperature signature that could be used to quantify groundwater flux through TEM. However, groundwater recharge (i.e., losing streams) would not result in a similar temperature signature, and thus could not be quantified by the TEM. Similarly, when T_S approximate groundwater temperatures during certain times of the year (Figure 9) (Briggs et al., 2016; Kurylyk et al., 2016), the temperature signature of the groundwater flux was difficult to detect. Therefore, the TEM is most effective where the temperature signature of groundwater flux is strong, i.e., gaining reaches and seasons when groundwater temperatures deviate from T_S. Nevertheless, the change in heat capacity caused by the loss or addition of stream water volume will lead to an altered T_S temporal variance. Future research with higher data precision may be able to identify the altered T_S variance and use it to quantify groundwater interactions similarly to TEM.

To improve the robustness of the thermal equilibrium assumption, it is important to consider the location of the T_S monitoring point and the sampling duration. When groundwater flux changes gradually, stream water remains at thermal equilibrium and therefore $T_S = T_E$ (Figure 12). In contrast, upwelling where there would be an abrupt changing in groundwater flux can cause loss of thermal equilibrium that recovers over a short distance ($T_S \neq T_E$). Groundwater flux estimates made at any point at thermal equilibrium represented the true magnitude of groundwater flux into the stream at that point. Estimates made at points where thermal equilibrium is recovering yielded an inaccurate groundwater flux because the T_S did not meet the primary assumption of the TEM. Similar thermal unequilibrium may also be introduced by other external heat sources that are not considered in the TEM, e.g., heat discharge from power plant. Although an investigator is unlikely to have prior knowledge of the spatial distribution of groundwater interactions in a particular stream, it would be advantageous to wade the reach in advance to avoid placing temperature loggers at locations with drastically varying temperatures. Moreover, based on

previous research, I suggest that at least one week of T_S time series should be collected for the thermal equilibrium assumption to be solid. (Bogan et al., 2003).

Conclusions

The TEM proposed in this research has several advantages to researchers interested in characterizing groundwater-surface water interactions as long as the primary assumptions of the approach are met. The primary advantage of this approach is resource savings (i.e., reduced field time) if suitable atmospheric and hydrological data are readily available. With this approach, only T_S is needed at a single point to monitor groundwater flux. This can also potentially add significant value to T_S data typically collected in stream biology studies (Hawkins et al., 1997). T_S data are also readily available at a number of USGS gage locations. Although a minimum of one week of T_S data is recommended to sufficiently satisfy the thermal equilibrium assumption (Bogan et al., 2003), the TEM can be used to estimate groundwater flux at any temporal scale larger than one week (i.e., monthly, seasonally or yearly). Similarly, the proposed method has the potential to economically quantify spatial differences in groundwater fluxes at multiple stream points or to create a flux estimate for a large area if applied in an array. The main limitation of the TEM is that it requires a detectable and equilibrated temperature signature of groundwater flux. Another weakness of the method, and one that it shares with other model approaches, is that the precision of groundwater flux is heavily dependent on the availability and quality of the input data. Finally, the approach performs best in well-mixed shallow streams because those conditions most closely match the one-dimensional model structure.

Table 7. Comparison of groundwater flux estimated by seepage run and thermal equilibrium methods for each sample site. Stream water and air temperature during the simulation period were averaged and reported as T_{water} and T_{air}, respectively. Upstream and downstream end of the seepage runs were specified by latitude and longitude (degree).

Site Name		Seepage Run (m/day)	Thermal Equilibrium Method (m/day)	T_{water} (°C)	T_{air} (°C)	Upstream End		Downstream End	
						Latitude	Longitude	Latitude	Longitude
Kiamichi River	NDN	0.11	0.08	24.46	19.20	34.659678	-95.030711	34.657772	-95.041503
	Robins	0.14	0.10	22.20	19.20	34.636061	-95.124994	34.626975	-95.126658
	JFC up	0.08	0.11	22.37	19.20	34.598642	-95.328103	34.597622	-95.336014
	JFC down	0.01	0.12	22.35	19.20	34.595883	-95.336756	34.589489	-95.339547
	Payne	0.01	0.08	22.78	19.20	34.425519	-95.576539	34.418956	-95.572731
Ozark Highland Ecoregion	Spavinaw	0.38	0.46	9.82	3.34	36.324472	-94.706311	36.321369	-94.714228
	Honey	0.74	0.65	10.41	8.08	36.540053	-94.703567	36.542764	-94.711072
	Caney	0.35	0.32	9.31	5.72	35.792650	-94.847528	35.788583	-94.849856
	Buffalo	0.61	0.63	10.68	2.90	36.639628	-94.627314	36.635578	-94.630281
	Saline	0.66	0.54	10.64	2.90	36.289614	-95.084697	36.284992	-95.091744
	Caney	0.15	0.05	9.47	3.44	35.792650	-94.847528	35.788583	-94.849856
	Greenleaf	0.09	0.00	7.08	3.44	35.752292	-95.047200	35.740981	-95.059083
	Spavinaw	0.56	0.61	20.96	24.44	36.349467	-94.566567	36.333483	-94.638617
	Spavinaw	1.09	0.95	21.22	24.44	36.329650	-94.646817	36.327100	-94.668467

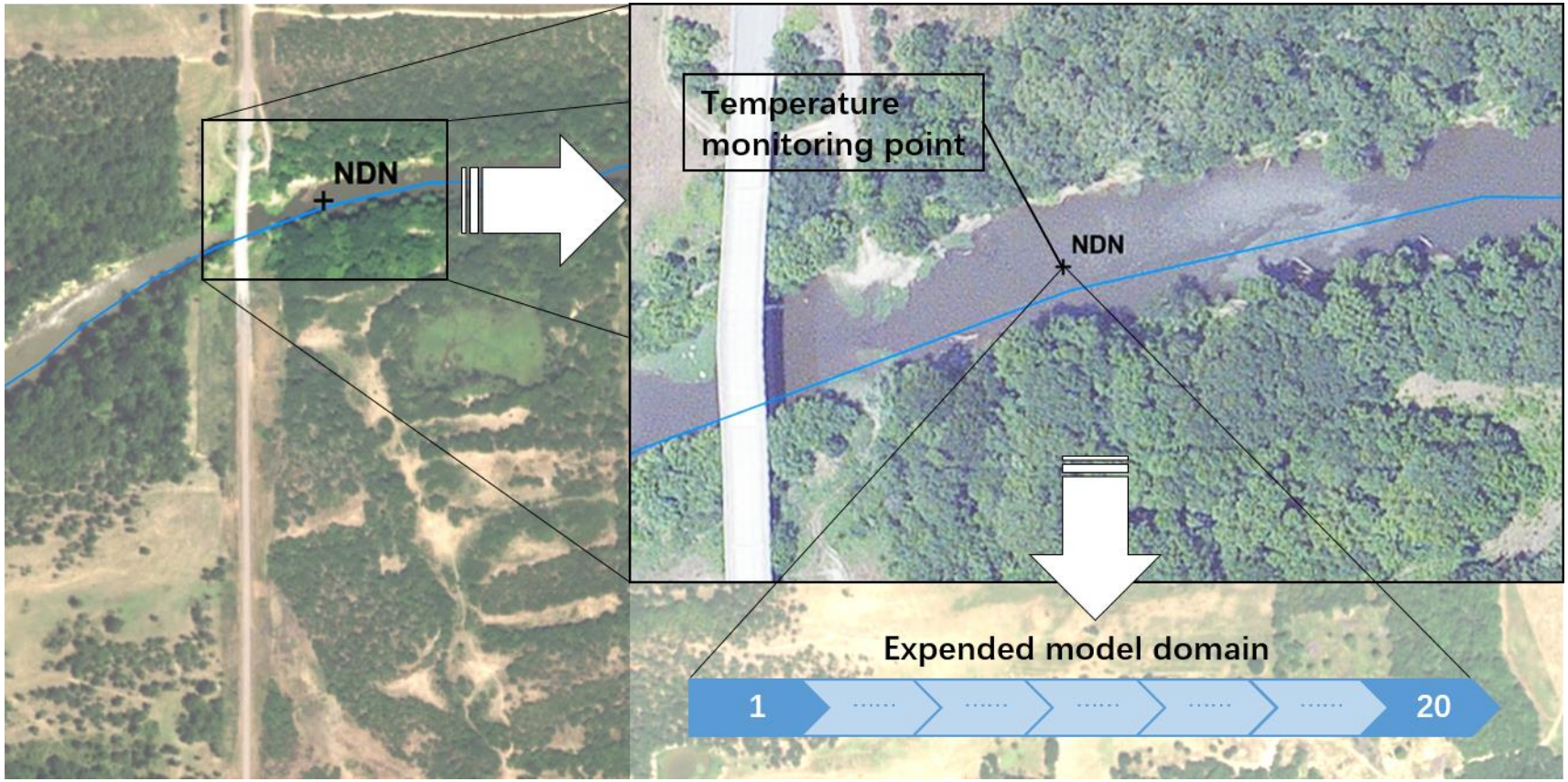

Figure 7. Diagram of thermal equilibrium method (TEM) and assumptions. The TEM assumes stream water temperatures are at thermal equilibrium with the combination of atmospheric conditions and groundwater interactions at the monitoring point. The monitoring point was expanded to a hypothetical model domain to investigate the thermal equilibrium reached at the monitoring point and consequently solve for the unknown groundwater flux.

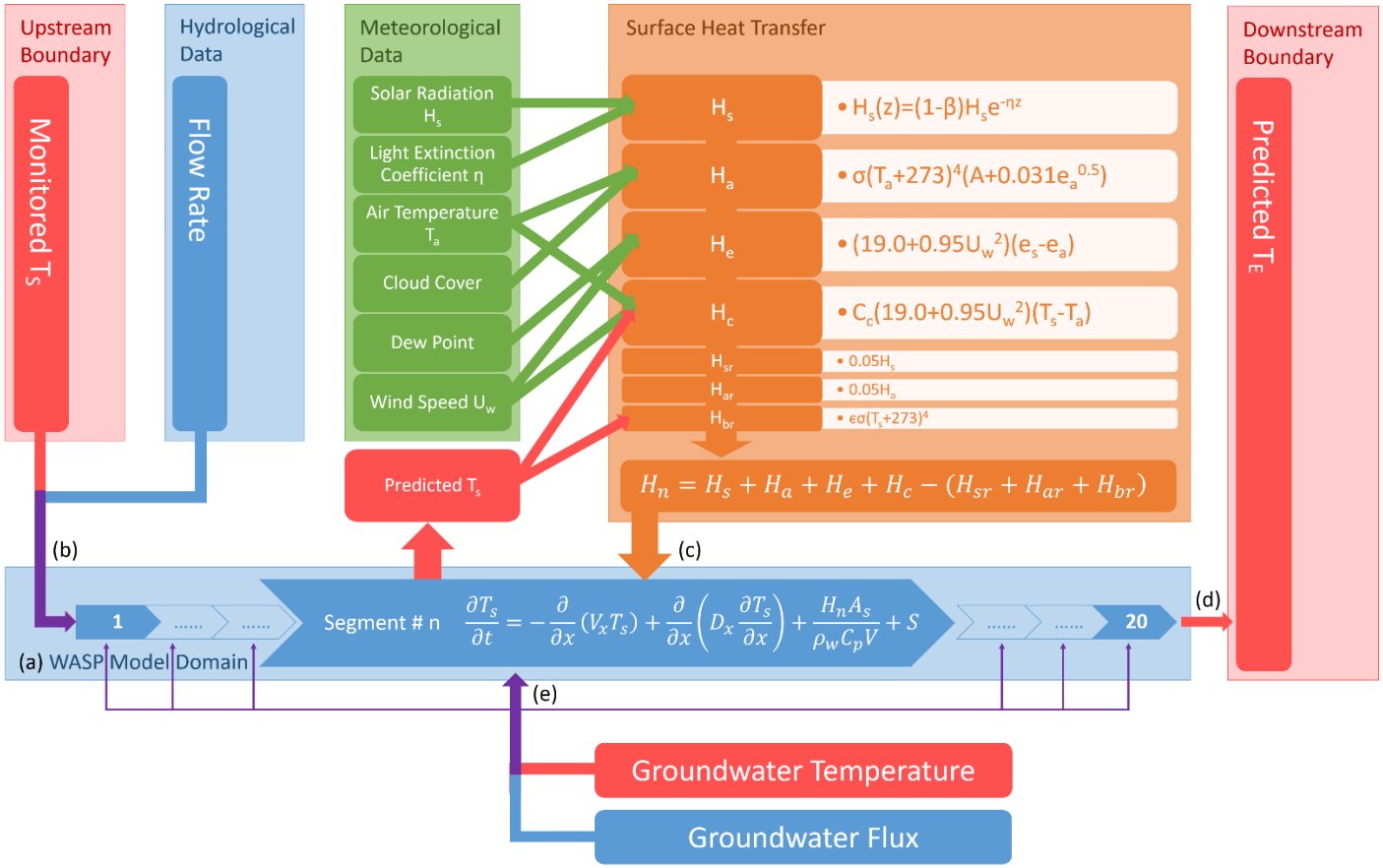

Figure 8. Temperature module of the thermal equilibrium method showing (a) the twenty segment model domain, (b) upstream boundary conditions derived from stream water temperature (T_S) and flow monitoring, (c) atmospheric heat transfer parameters applied to each model segment at each time step, and (d) the predicted equilibrium water temperature (T_E). Various magnitudes of (e) groundwater flux at a given temperature are applied in an iterative manner to segment each as a bottom boundary to minimize the sum of squared errors between the measured and predicted boundaries.

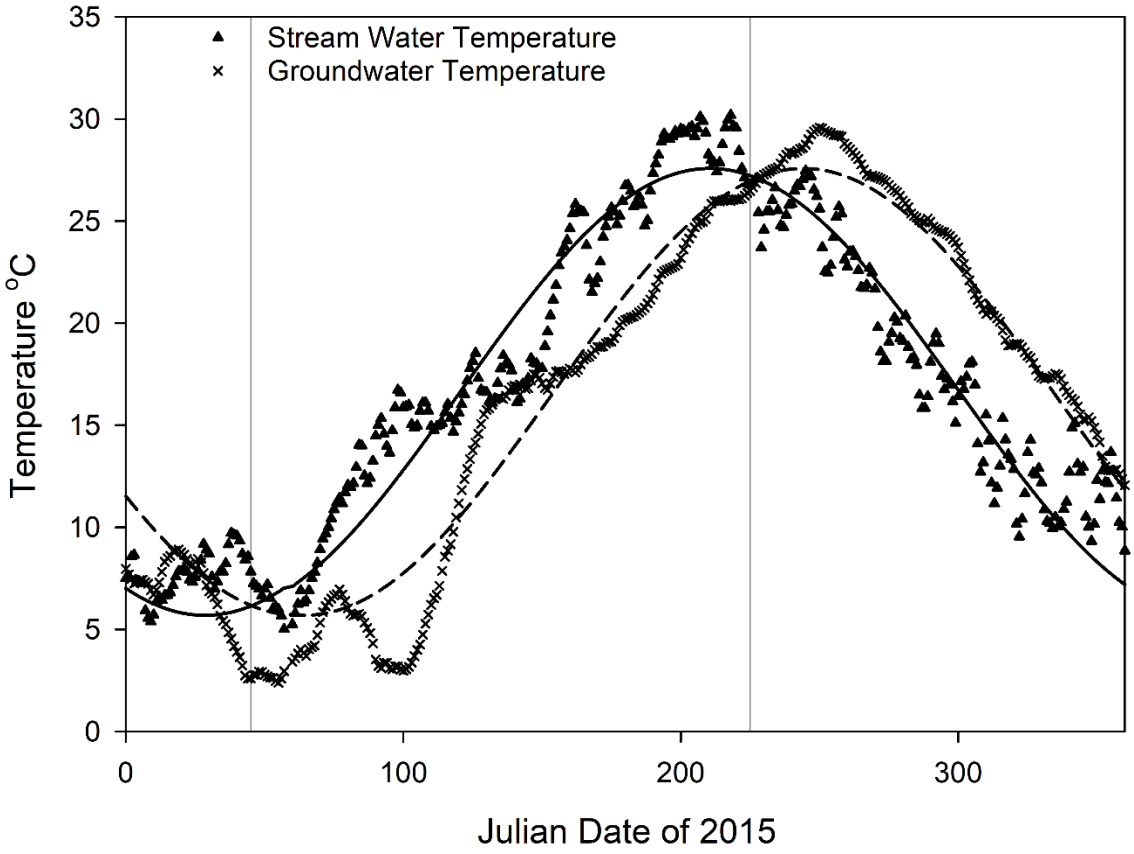

Figure 9. Daily averaged stream water temperatures time series compared to groundwater for 2015. Stream water temperature time series were monitored on Big Cedar USGS gauge, and groundwater temperature time series was estimated using air temperature retrieved from Talihina Mesonet Station 15 miles away with 1.5-month time lag as recommended by Pluhowski (1970). Solid and dotted line represent sine fittings curve for stream water and groundwater, respectively. The vertical lines indicate intersections of the fitting curves where there is no estimated difference between the measured stream water and the estimated groundwater temperatures, and the thermal equilibrium method cannot estimate groundwater flux.

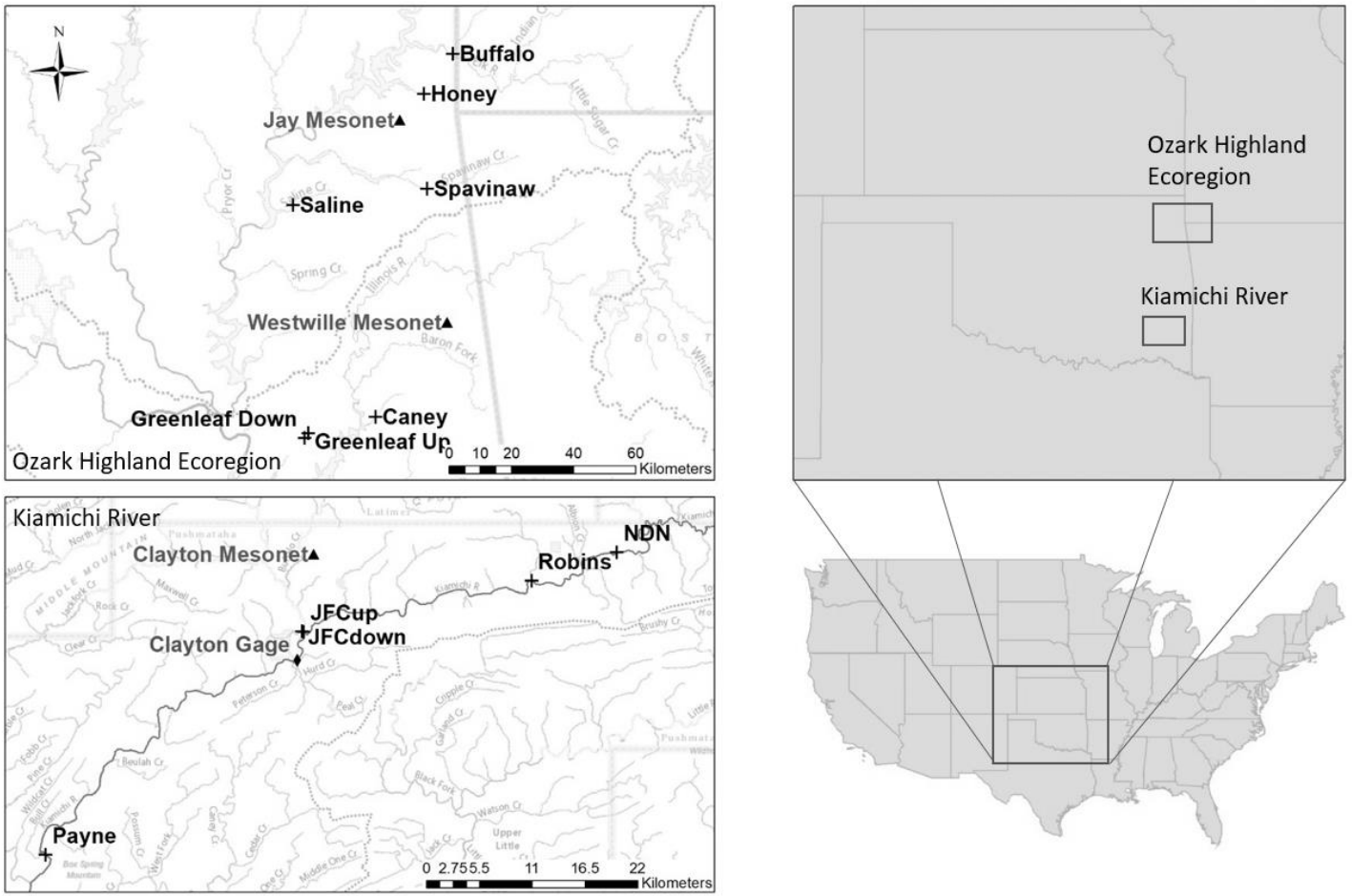

Figure 10. Study sites on the Kiamichi River (bottom left) and Ozark Highland ecoregion (top left). Mesonet station and USGS gage are represented by triangle and diamond markers, respectively. Cross markers indicate monitoring sites where stream water temperature data were collected and seepage runs were performed.

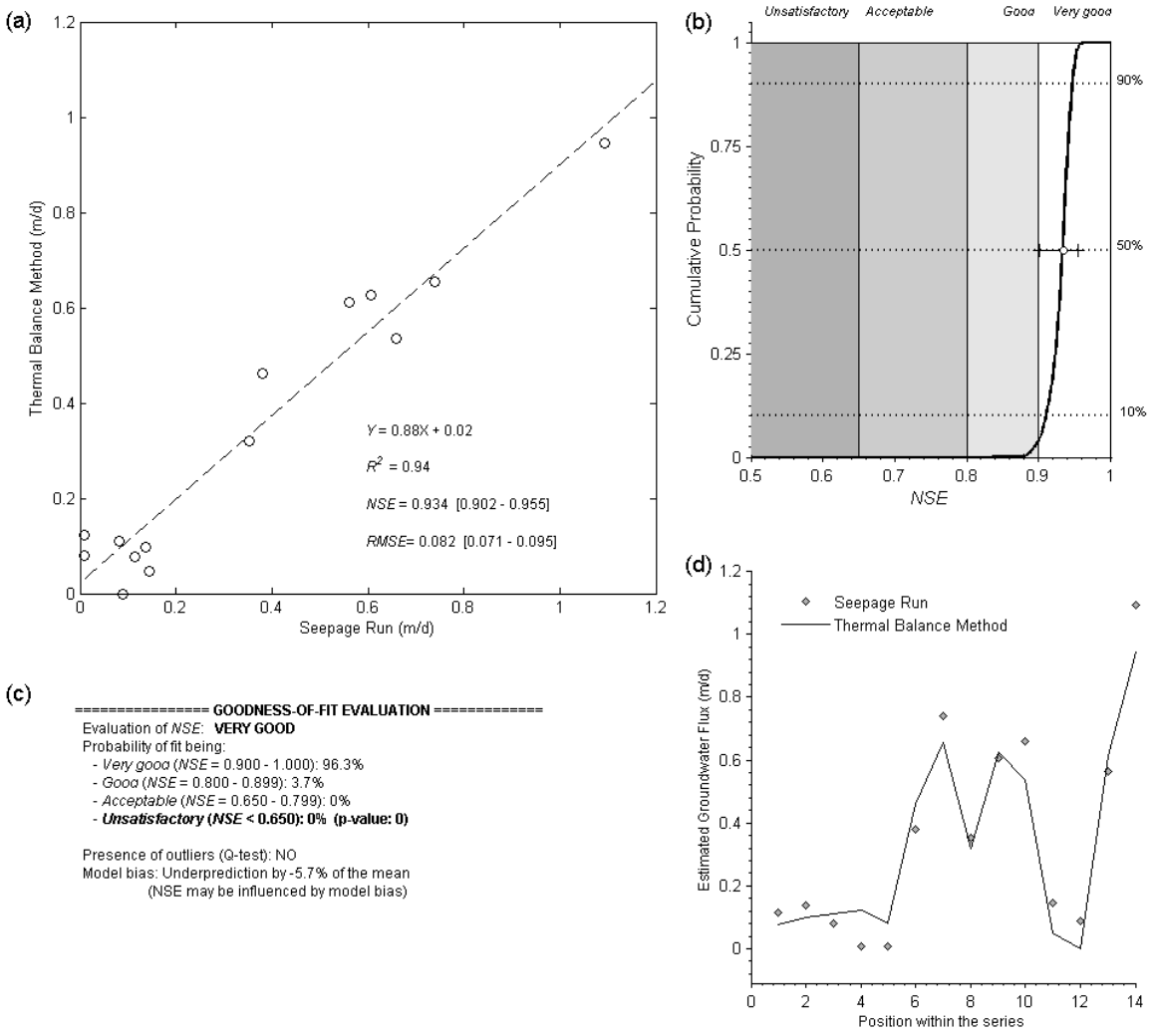

Figure 11. Model validation using FITEVAL to evaluate the regression results between groundwater fluxes estimated by seepage run and thermal equilibrium method indicated a very good fit with bias of under-prediction by -5.7%. Plots showing (a) regression of seepage run and thermal equilibrium method groundwater flux estimates, (b) FITEVAL plot of cumulative probability of Nash-Sutcliffe Efficiency (NSE), with the median value indicating the reported NSE, (c) FITEVAL model diagnostic report including hypothesis test results, outliers, and the sensitivity of the indicators to model bias, and (d) scatter plot showing fit between seepage run and thermal equilibrium method groundwater flux estimates in order of the series. Actual values are shown in Table 2.

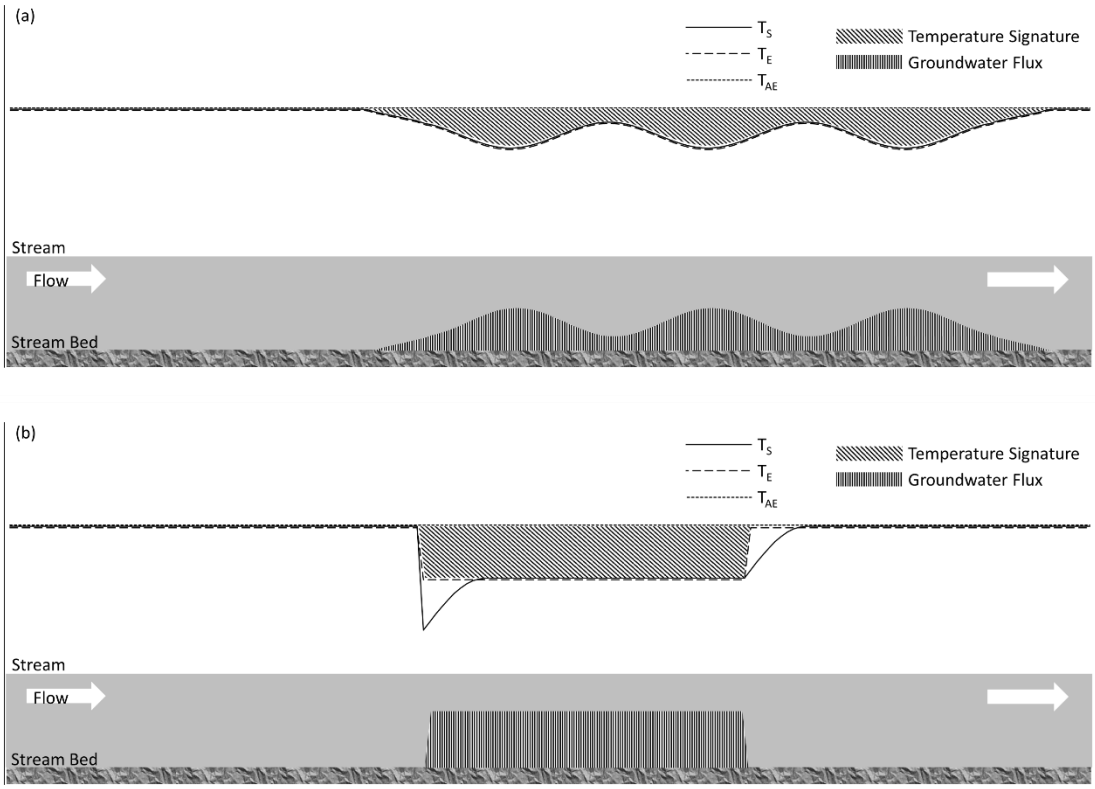

Figure 12. Temperature profile of a hypothetical stream in the presence of cooler groundwater flux. Plots showing (a) stream water temperatures (T_S) remains at equilibrium at the presence of gradual changing groundwater flux, and (b) loss of thermal equilibrium due to drastically changing groundwater flux. The thermal equilibrium method provides an accurate estimate of the groundwater flux for any point at thermal equilibrium. Estimates made with the thermal equilibrium method where $T_S \neq T_E$ will not represent an accurate flux.

CHAPTER IV

EXAMINING FLOW SCENARIOS TO IMPROVE THERMAL CONDITIONS FOR FISHES DOWNSTREAM OF A DAM

Introduction

Human activities on the landscape greatly affect riverine ecosystem through changes of vegetation, climate, and especially hydrology. Many human-induced landscape changes affect riverine ecosystems including land-use change to urban (Nelson and Palmer, 2007) and agricultural landscapes (Poole and Berman, 2001), the construction of dams (Bunn and Arthington, 2002), groundwater withdrawals (e.g., Arkansas Darter *Etheostoma cragini*, Eberle and Stark, 2000; Arkansas River Shiner *Notropis giardi*, Perkin et al., 2010), and warm-water effluents (Coulter et al., 2014). To exacerbate conditions, climate change is expected to increase the drought frequency in some regions of North America (Seager and Vecchi, 2010). More than 50% of the world's large rivers are already fragmented by dams (Nilsson et al., 2005) affecting the persistence of downriver organisms (Olden and Naiman, 2010). To maximizing flood protection, maintain and expand water supplies, and generate power, aquatic systems have been channelized, dammed, dredged, leveed, and pumped (Wootton, 1990). Despite knowledge of the effects of flow patterns on biota (Poff, 1997), water management reservoirs have been developed aggressively with little attention on the downriver ecosystem until relatively recently.

Globally, efforts have increased in recent years to improve conditions in rivers regulated by impoundments (Tharme, 2003). In fact, more than 30 environmental approached have been developed to provide supporting information or frameworks to make flow decisions (Annear et al., 2002), some very useful to implementation in regulated river systems (see review by McManamay et al., 2016). However, the flow-biota relationship observed in many regulated rivers reflect water-quality conditions of the discharging reservoir (Olden and Naiman, 2010). Thus, the resulting flow recommended based on water quantity may improve hydrologic conditions, but do little to improve or even worsen downriver water quality (Krause et al., 2005).

More recent efforts have focused on how to better define and determine environmental flows in a managerial context (Acreman and Dunbar, 2004; Arthington et al., 2006; Richter et al., 2006; Poff et al., 2010). Without proper regulation, water releases from dams and diversions often negatively affect the downstream water quality and biota. The thermal gradients can be altered for an extensive distance downstream (Ellis and Jones, 2013), altering species' phenology (e.g., Sockeye Salmon *Oncorhynchus nerka*, Quinn et al., 1997), decreasing growth (e.g., Brown Trout *Salmo trutta*, Saltveit, 1990), reducing reproduction (e.g., Rainbow Trout *Oncorhynchus mykiss*, Pankhurst, 1997), and even leading to extirpations (Olden and Naiman, 2010). Although the significance of water quality, especially temperature, in riverine ecosystems is widely acknowledged (Magnuson et al., 1979; Poole and Berman, 2001; Caissie, 2006), research efforts have focused primarily on hydrologic alteration (Bunn and Arthington, 2002) often without the explicit consideration of excessive nutrients, dissolved oxygen, sediments and water temperature (Olden and Naiman, 2010). Given the interactions between water quality and quantity, it will be critical to identify solutions that balance both water use and ecological needs (Brewer et al., 2016).

The objective of this research was to evaluate the effects of different reservoir operations on fishes of the Kiamichi River during summer, baseflow conditions. Specifically, I developed

potential reservoir-operation scenarios using the Water Quality Analysis Simulation Program (WASP). The WASP model was used to simulate reservoir releases from different locations to evaluate physicochemical changes downriver as deemed suitable by riverine fishes. The thermal tolerances of several stream fishes were provided by Alexander (2017). This study was timely because hydrological and atmospheric conditions represented both a recent drought (2013) and wet period (2017). This research presents a successful attempt to investigate the interactions between water quantity and temperature and provides an evaluation approach to quantify the effect of reservoir releases on downstream thermal regimes. Identifying and evaluating the relationship between reservoir operations and fish ecology will also provide decision support information for achieving compatibility between growing demands of human water use with options for meeting thermal regimes through environmental flows.

Method

Study Area

The Kiamichi River is located in southeast Oklahoma. A tributary of the Red River, its headwaters originate in Pine Mountain of the Ouachita Mountains near the Arkansas border. From its source in LeFlore County, Oklahoma, it flows approximately 177 miles (285 km) to its confluence with the Red River south of Hugo, Oklahoma.

The entirety of the Kiamichi Basin has an area of about 4800 km^2; elevation ranges between 270 to 810 m (Pyron et al., 1998). The basin serves as drainage for an area of steep east-west trending ridges separated by a broad and flat-bottomed stream valley (Sanford II and Boyd, 2012). The substrate and alluvial areas of the Kiamichi River comprise a mixture of gravel, sand, silt and clay (Sanford II and Boyd, 2012). Within the upland areas, the dominant formations are terrace deposits comprising gravel, sand, silt, clay and volcanic ash. The Kiamichi Basin receives an annual average precipitation of 122 to over 142 cm, but this region of the United States is prone

to drought in recent years (Seager and Vecchi, 2010). The land use of Kiamichi Basin is fragmented, with forested lands accounting for 66% and pasturelands for 25% (Sanford II and Boyd, 2012). Primary vegetation of the Kiamichi Basin is dominated by secondary growth (50 to 70 years old) oak, hickory, and pine vegetation types. Major tributaries of the Kiamichi River include Jackfork, Cedar, Buck and Tenmile creeks (Pigg, 1974).

Between 1977 and 1982, the U.S. Army Corps of Engineers constructed the dam on Sardis Lake as an impoundment of Jackfork Creek under a contract with the State of Oklahoma for municipalities and industrial water demand in Oklahoma. The impoundment of Jackfork Creek by Sardis Lake dam affected the downstream hydrology of the Kiamichi River, resulting in increased median and variation of flows, as well as more frequent high flow pulses and flow reversals. The median flows during July, August and September were reduced from 1.50 m^3/s, 0.76 m^3/s and 1.13 m^3/s to 1.30 m^3/s, 0.34 m^3/s and 1.02 m^3/s, respectively (Fisher et al., 2012).

Data Collection

Time series of stream water temperature, atmospheric and hydrologic data were collected between 7/22 to 9/1 in four years: 2013, 2014 (via the Oklahoma Department of Wildlife Conservation, hereafter ODWC), 2015, and 2017 (the current study). Hourly averaged stream water temperatures were monitored using temperature loggers (HOBO Water Temp Pro v2) at four locations on the Kiamichi River designated as NDN, Robins, Pine Spur and Payne at a depth of 0.5 to 1.5 m (Figure 13). An hourly-averaged time series of air temperature, wind speed, solar radiation, and dew point was obtained from three nearby Oklahoma Mesonet sites (Talihina, Clayton and Antlers). Discharge of the Kiamichi River were retrieved from a U.S. Geological Survey gage near Clayton (gage number 07335790). A time series representing water releases from Sardis Lake was retrieved from the management records of the U.S. Army Corps of Engineers (http://www.swt-wc.usace.army.mil/). Transects at 10 different locations on the

Kiamichi River were surveyed using the SonTek RiverSurveyor M9 ADCP (Acoustic Doppler Current Profiler) for average flow velocity, width and depth of the channel.

Dissolved Oxygen (DO) concentrations were also collected between 9/23/2015 to 10/23/2015 and 7/22/2017 to 9/1/2017 to investigate the effect of reservoir releases on downstream DO. Hourly averaged DO concentrations were monitored using DO loggers (HOBO Dissolved Oxygen Logger U26-001) at the four aforementioned sites with the addition of Jackfork confluence at a depth of 0.5 to 1.5 m. The DO measurements were calibrated based on DO meter reading at the start and end of each monitoring period. The membrane of the DO loggers was protected by antifouling cap, and was also cleaned at least three time per month in case of fouling.

Biochemical oxygen demand (BOD) was determined at each site where I collected DO data. BOD samples were collected on two occasions: 8/30/2017 (only upstream sites as the downstream sites were affected by release) and 9/27/2017. The BOD samples were collected according to standards provided by the Oklahoma Department of Environmental Quality (ODEQ). Samples were placed on ice after collection and were delivered to the ODEQ after all sites were completed. Environmental Laboratory Services Division in ODEQ analyzed the samples the following week.

Critical Thermal Maximum

Thermal tolerances of ten stream fishes were obtained from Alexander (2017) and used as the biological endpoint for the WASP model. Critical thermal maximum (CTMax) is the temperature at which loss of equilibrium or death occurs after exposed to rapid heating. Briefly, fishes were acclimated to 20 ^{o}C, exposed to a 2 ^{o}C per h temperature increase, and observed for loss of equilibrium (Becker and Genoway, 1979). Each species was assigned to a habitat guild based on published descriptions (Pflieger, 1997; Miller and Robison, 2004; Cashner et al., 2010). The benthic guild comprised species that typically use habitat on the stream bottom. The mid-column

guild comprised pelagic species. The surface guild included one species, and was classified based on its occupancy of the surface of slackwater habitats. Guild CTMax were obtained by averaging values for all individuals belonging to each guild (Table 8) because the CTMax of fishes in each guild were not statistically different. CTMax ranged 34.0-38.3 ^{o}C (Table 8). To simplify the thermal exposure responses, guild tolerances were used to evaluate the effects of reservoir releases on downriver fishes. The benthic guild was the most thermally sensitive followed by the mid-column and surface guild, respectively (Table 8).

Kiamichi River Temperature Model

In this study, WASP was used to predict stream water temperature for a 74-km reach of the Kiamichi River starting at its intersection with Indian Highway (designated as site NDN, Figure 13). WASP is a dynamic compartment-modeling program for aquatic systems. The time-varying processes of advection, dispersion, loading, and boundary exchange are represented in the basic program (Wool et al., 2006). The WASP temperature module predicts water column temperatures based on comprehensive surface heat exchange processes including radiation, conduction and latent heat as well as heat exchange between subsurface and benthic layers of the water body.

In the WASP temperature module, the stream water temperature is computed based on the following 1D advection-diffusion equation:

$$\frac{\partial T_s}{\partial t} = -\frac{\partial}{\partial x}(V_x T_s) + \frac{\partial}{\partial x}\left(D_x \frac{\partial T_s}{\partial t}\right) + \frac{H_n A_s}{\rho_w C_p V} + S \tag{19}$$

where T_s is the stream water temperature (^{o}C), V_x is the advective velocities (m/s), D_x is the diffusion coefficients (m^2/s), V is the segment volume (m^3), A_s is the segment surface area (m^2), ρ_w is the density of water (997 kg/m^3), C_p is the specific heat of water (4179 J/kg ^{o}C), H_n is the net surface heat flux (W/m^2), S is the loading rate include boundary, direct and diffuse loading (^{o}C/s).

The net surface heat flux includes the effects of a number of processes computed as (Cole and Wells, 2002):

$$H_n = H_s + H_a + H_e + H_c - (H_{sr} + H_{ar} + H_{br}) \quad (20)$$

where H_n is the net heat flux across the water surface (W/m^2), H_s is the incident short wave solar radiation (W/m^2), H_a is the incident long wave atmospheric radiation (W/m^2), H_{sr} is the reflected short wave solar radiation (W/m^2), H_{ar} is the reflected long wave radiation (W/m^2), H_{br} is the back radiation from the water surface (W/m^2), H_e is the evaporative heat loss (W/m^2), H_c is the heat conduction (W/m^2).

The Kiamichi River was represented as a one-dimensional model in WASP containing 74, 1-km model segments (Figure 14). The upstream boundary was represented by the combination of monitored time series of stream water temperatures at NDN and stream flow rates. Surface heat transfer of each compartment was calculated based on atmospheric time series retrieved from the nearest Oklahoma Mesonet stations. The effect of canopy cover was considered negligible due to the high stream order of Kiamichi River. Hydrological routing was computed based on one-dimensional kinematic wave flow routing where flow velocity, depth and width was calculated as an exponential function of flow rate, with their multipliers and exponents specified in this research. These parameters were estimated based on the channel survey results using the ADCP and applied to all the segments uniformly. Groundwater interaction was incorporated into the model as a uniform inflow to each segment, with its boundary represented by the flow rate reported in Chapter III. Groundwater temperature was estimated from air temperature with a 1.5-month time lag as recommended by Pluhowski (1970). Predicted stream water temperature data were reported as time series for each of the 74 segments at a temporal resolution of 1 h.

The WASP model was calibrated using data for three years: 7/22/2013 to 9/1/2013; 7/22/2014 to 9/1/2014; and 7/22/2015 to 9/1/2015 and the calibrated parameters were applied to the same dates

(7/22-9/1) in 2017 for model validation. During calibration, parameters (minimum depth and light extinction coefficient) were adjusted until the R^2 and root mean squared error (RMSE) were optimized between predicted temperature time series and monitored stream water temperature at monitoring sites. The optimal parameters acquired in calibration were validated by predicting stream water temperature for 7/22/2017 to 9/1/2017 with no additional adjustment. The FITEVAL software (aforementioned in chapter III) was used to evaluate the fit between monitored stream water temperature and predicted stream water temperature using WASP temperature module in terms of R^2, RMSE and Nash-Sutcliffe efficiency coefficients (NSE).

Reservoir Releases Scenarios

The validated WASP model was used to predict downstream temperature in response to hypothetical reservoir operations during the validation period: 7/22/2017 to 9/1/2017. I first simulated stream water temperature without a release. This simulation served as a control and evaluated the thermal stress that would have been experienced by fishes in the absence of the water release. Next, multiple realistic release scenarios were simulated to assess their effects on both downstream water temperatures and fish species. Five constant release levels were chosen: (1) 0.34 m^3/s represented the current longer-term release that was previously used by the U.S. Army Corps of Engineers and the Oklahoma Water Resources Board (OWRB) to provide limited relief to sensitive freshwater mussels during a drought (note, this release does not provide connectivity from Sardis to Hugo); (2) 0.59 m^3/s represented the release that was expected to adequately restore primary mussel habitats (i.e., provide connectivity and coverage of primary beds) at Clayton; (3) 0.76 m^3/s, 1.13 m^3/s and 1.50 m^3/s were chosen to represent the pre-dam median flows of August, September and July, respectively (Fisher et al. 2012). Three water temperatures, 27.64 ^oC, 26.00 ^oC and 24.07 ^oC, were applied in simulations as lateral boundary condition to represent release from three gates at different depth of the reservoir (5, 10 and 20m). These temperatures were calculated as an average of multiple-year samples taken at the Sardis

Lake near the dam during the same period of the year (based on an existing lake profile from 2005, ODWC Unpublished data).

Predicted temperature time series were contrasted against critical thermal maxima to identify the time when stream fishes in each guild experienced severe thermal stress. A cumulative time when stream fish experienced severe thermal stress (hereafter cumulative time above CTMax) was calculated for each guild in every 1-km segments simulated in the Kiamichi River WASP temperature model. The results were visualized based on downstream distance from reservoir confluence and cumulative time above CTMax. The areas bounded by the curve of cumulative time above CTMax (km•h) were calculated to quantify thermal stress experienced by different guilds downstream of the release. The reduction rates of thermal stress against that of the control were calculated to quantify the cooling effect of each release scenario. The distance where the cumulative time above CTMax was reduced by half was calculated as the effective distance indicating the dissipation of the cooling effect.

Results and Discussion

Data used to develop the WASP model

The research periods covered a range of hydrologic and atmospheric conditions. According to long-term averages for the research period reported by U. S. Climate data, 2013 represented a warm summer with an average air temperature of 26.5 ^{o}C (Table 9), during which there were two limited precipitation events (7/28/2013 and 8/15/2013) and no release (Figure 15). The year of 2014 represented a typical summer with a concentrated precipitation event that created a discharge peak over 180 m^3/s (7/30/2014), which significantly decreased both upstream and downstream water temperature by more than 10 ^{o}C (Figure 16). The year of 2015 also represented a warm summer with the highest average air temperature (27.6 ^{o}C) and average solar radiation of (268.9 W/m^2, Table 9). However, there was a continuous release of water from the dam

(7/26/2015 to 8/25/2015) that significantly reduced downstream water temperature by more than 10 ^{o}C (Figure 17). The year of 2017 represented a cool summer with continuous precipitations and multiple significant release events over most of the time that reduced both upstream and downstream water temperatures significantly (Figure 18). The reservoir was likely to have released water from the top gate that represented the surface water temperature.

The ADCP transect survey results indicated that the channel geometry was not significantly different between upstream and downstream locations. While not significant, the channel tended to become slightly wider and shallower with increased flow velocity as discharge increased downstream, (Table 10). Generally, these are the changes in channel dimensions that we would expect to see as we move downriver (Allan and Castillo, 2007).

Dissolved Oxygen and Biochemical Oxygen Demand

The DO time series observed in 2015 represented summer conditions of a relatively warm year with few water releases (Figure 19). The DO concentrations observed at the confluence were above 5 mg/L uniformly more than 95% time. The DO concentrations observed at the sites located downstream of the dam influence were above 5 mg/L during releases, except for the most downriver site. At Payne, DO had a major shift where variances increased substantially during a low-flow period starting 10/13/2017. Because there were no dam releases during that period, and the site immediately upstream (Pine Spur) showed suitable DO conditions, it seems the low DO (near 2 mg/L) at night were likely related to an algae bloom (Jacobsen and Marín, 2008). Algae blooms are relatively common from May through October and negatively affect the DO conditions at night when the plants experience high rates of respiration (i.e., use oxygen). Another possible explanation is that the loggers fouled at that location, which is a common limitation of polarographic membrane-type sensors (Wagner et al., 2000).

The DO concentration time series observed in 2017 represented DO patterns during a higher-flow period because of considerable water releases from Sardis Reservoir due to repeated storm events (Figure 20). The DO concentrations observed at the Jack Fork-Kiamichi rivers confluence were above 5 mg/L during these release scenarios, but dropped significantly following releases. This was likely to result from disturbed aquatic ecosystems by high flows with reduced capacity of photosynthesis and influx or resuspension of oxygen demanding materials as a result of the storm water input (Graczyk and Sonzogni 1991). This pattern was also observed on upstream sites, but dissipated downstream and was not observed at the downstream sites.

The BOD sampling also supported my findings that DO was only low immediately following discharge events. BOD samples reflected low values (less than 2 mg/L, Table 11) during the decreasing of discharge (while discharge was above 1.0 m^3/s) and higher values (2.9 mg/L and 3.8 mg/L observed at most upstream and downstream sites, respectively) immediately following the return to low-flow conditions (when discharge dropped below detectable limit).

Based on the DO conditions observed in 2015 and 2017 and BOD sampling results, reservoir releases did not directly reduce DO concentrations in the Kiamichi River. However, the magnitude and duration of the release, and the conditions within the reservoir in a given year or season, can affect downstream DO concentrations via interactions with aquatic ecosystems. Note that the reservoir was releasing water from the upper gate which would also be expected to have the highest DO. The DO concentration associated with the hypolimnetic layer of a reservoir would be expected to differ (Townsend, 1999), and is supported by existing lake profile data (Oklahoma Department of Wildlife Conservation, Unpublished data).

Kiamichi River Temperature Model

Model calibration indicated that a minimum depth of 0.85 m and light extinction coefficient of 3.3 m^{-1} yielded the optimal fit between predicted and monitored stream water temperatures. The

calibrated model accounted for an average of 64% of the temperature variation across sites (Table 12). The RMSEs between the observed and predicted stream water temperature time series were lower than 2 ^{o}C at 8 of 11 sites. The NSEs ranged from -0.28 to 0.62 (Figure 15, 16, and 17, Table 12).

Model validation yielded a good match between predicted and monitored stream water temperature at monitoring sites with an average R^2 of 0.61 and RMSEs all below 2 ^{o}C. The NSEs ranged from -0.84 to 0.56 (Figure 18, Table 12).

The model performance was considered acceptable. Although 2 ^{o}C could be problematic for fishes during extremely hot periods, it represented average channel conditions. The error was expected to be less than the spatial variance created by fine-scale thermal heterogeneity (Kanno et al., 2014) that provides thermal refugia for fishes. For example, the model is one dimensional, but the actual conditions within the stream would offer some patches of warmer or cooler water (Ebersole et al., 2001); thereby, offsetting the error associated with the 1-D scenario. The RMSEs were also close to other successful research using a similar deterministic model approach (e.g., Caissie et al., 2007). However, according to FITEVAL outputs, the fitting results were categorized as unsatisfactory based on NSEs. This was related to the fact that my predicted stream water temperature time series illustrated larger diurnal variance compared to the observed temperatures. This discrepancy may be due to the bias associated with the stream water temperature being monitored at the bottom of the river while the WASP model predicted average stream water temperature across a transect based on a one-dimensional simplification. The model tended to predict higher temperature than the monitored data with greater fluctuations following flow releases, likely due to the limitation of the model in considering the thermal buffer provided by shallow groundwater interactions. However, for the scenarios I was interested in modeling, the error rate is acceptable. Evaluating the effects of dam releases was completed to examine how

thermal conditions could be improved under different release scenarios. The absolute accuracy of the temperatures is less critical than the relative differences across the scenarios.

Reservoir Releases Scenarios

In the absence of a reservoir release (i.e., the control scenario), downstream fishes were expected to experience an approximately uniform thermal stress throughout the simulated reach of Kiamichi River (Figure 21). The control scenario indicated the benthic guild was expected to experience 130 h of thermal stress, while mid-column guild was expected to experience 73 h thermal stress. The surface guild never experienced temperatures exceeding their CTMax; thus, temperatures were expected to be tolerated by that fish guild so that guild was not investigated further. It is not surprising that fishes occupying the top portion of the water column would be more tolerant of higher temperatures given their regular exposure to solar radiation (Webb and Zhang, 1999; Caissie, 2006).

As expected, the thermal relief increased as indicated by thermal stress (Table 13), reduction rate of thermal stress (Table 14) and effective distance (Table 15) with the increase of the release magnitude and the depth of the release location (i.e., the lower release locations had cooler water, Figure 22). In recent years, the only time a release has been provided for ecological purposes, only 0.34 m^3/s was released from the top gate (Gates et al., 2015). This release scenario only reduced thermal stress by 11% for mid-column fishes and 8% for benthic fishes. The effective distance (i.e., distance where cumulative time above CTMax was reduced by half) of the release was only 1 km for both guilds. The proposed release (0.59 m^3/s released from the top gate), hypothesized to provide relief for downstream mussel habitat (Spooner et al., 2005) reduced thermal stress by 18% for mid-column fishes and 12% for benthic fishes. The effective distance increased to 4 and 2 km for mid-column fishes and benthic fishes, respectively. Three releases that represented pre-dam flow magnitudes (0.76, 1.13 and 1.50 m^3/s released from top gate) reduced thermal stress up to 33% for mid-column fishes and 29% for benthic fishes. The effective

distance increased to approximately 10 km for both fish guilds. In comparison, 0.34 m^3/s release was expected to cause an increase in thermal stress of up to 20% for both guilds.

The WASP model was applied as a one-dimensional model, but if improved resolution of thermal responses were desired, a two-dimensional model could be used. The 1-D WASP model predicts water temperature as an average over the transect. From the perspective of fish habitat, there may still be cooler-water patches available that provide refuge during thermally-stressful conditions. However, to provide decision-making tools to evaluate dam releases over a 74-km stream segment, a one-dimensional model is probably the preferred option. For example, the model predictions are likely conservative as the thermal conditions predicted do not account for the patchy stream environment. This is probably beneficial given CTMax represents morbid conditions for fishes that does not allow fishes to acclimate and, of course, all models have some inherent error. It is important to recognize that even when CTMax values are not exceeded, fish may still experience reduced growth and survival due to exposure to suboptimal temperatures (Coutant, 1976). Use of a 2-D model would likely be most beneficial if identifying greater resolution of thermal conditions at freshwater mussel beds, for example. This would be particularly interesting for freshwater mussels given their sessile life style. A two-dimensional model would also be useful if there was interest in, examining thermal refugia related to other land-use practices (i.e., maintaining riparian corridors, fencing cattle to prevent DO decreases). Lastly, increased thermal resolution of some stream segments might be useful to agencies developing monitoring strategies to target areas during severe drought or other thermally-stressful periods.

Summary and Conclusion

In this research, I evaluated the duration of thermal exposure experienced by downstream fishes in the Kiamichi River to different reservoir operations. The thermal exposure was based on

CTMax of fishes from three habitat-use guilds (Alexander, 2017). I calibrated and validated a stream water temperature model for predicting downstream water temperature on the Kiamichi River. The validated model was used to simulate five dam release magnitudes combined with three different release options based on gate height (i.e., where the water from the reservoir would be released). Based on CTMax of fishes from three habitat-use guilds, the thermal stress, reduction rate and the effective distance were quantified to evaluate downstream thermal stress on fishes. The impoundment of Sardis Lake significantly altered the downstream thermal regime of the Kiamichi River and increased the thermal stress by up to 20% for benthic and mid-column fish species. However, the only ecological flow used in recent years to maintain some river flow (0.34 m^3/s) was insufficient to recover the downstream thermal regime to pre-dam conditions, and that flow does not connect the entire length of river between Sardis Reservoir and Lake Hugo. In addition to providing little improvement to thermal conditions, this scenario also prevents fish movement via lack of connectivity across the riverscape.

To reduce the thermal stress experienced by downstream fishes to pre-dam condition, the study results show that water releases from the dam could be increased (i.e., 0.76 m^3/s). Alternatively, cooler hypolimnetic water could be released to achieve the same level of cooling effect with lower release magnitudes when limited water supplies occur (Marshall et al., 2006; Olden and Naiman, 2010). For example, releasing water at a rate of 0.59 m^3/s from the depth of 10 m results in a similar cooling effect as 0.76 m^3/s release from the top gate in terms of both reduction rate and effective distance. However, hypolimnetic water is usually limited in DO, which may degrade fish habitat near the dam (Hoback and Barnhart, 1996; Marshall et al., 2006) especially when releases are made continuously during extremely hot years. Monitoring efforts should be used to ensure suboptimal conditions are not created if hypolimnetic releases are used as a management option.

Table 8. Critical thermal maxima (CTMax) was obtained from Alexander (2017). CTMax was determined by increasing temperature 2 ºC per h above acclimated temperature (20 ºC) for 10 fish species that occupied the Ouachita Mountain Ecoregion. The average value of species within each of three habitat guilds was used to determine a habitat guild CTMax. Species were assigned to each habitat guild using existing ecological information (references provided). In this study, CTMax for each guild was used to determine when fish will experience thermal stress.

Habitat Guild	Guild CTMax (ºC)	Common Name	Scientific Name	CTMax (ºC)	Typical Habitat	Reference
Surface	38.30	Blackspotted Topminnow	*Fundulus olivaceus*	38.30	Surface water, backwaters, edgewaters	Pflieger, 1997
Mid-column	34.72	Bigeye Shiner	*Notropis boops*	34.42	Mid-column, run, pool	Pflieger, 1997
		Bluntnose Minnow	*Pimephales notatus*	35.26	Mid-column, backwaters, pools	Miller and Robison, 2004
		Highland Stoneroller	*Campostoma spadiceum*	34.78	Mid-column, riffle, run, pool	Cashner et al., 2010
		Steelcolor Shiner	*Cyprinella whipplei*	34.42	Mid-column, riffle, run, pool	Pflieger, 1997
Benthic	34.34	Channel Darter	*Percina copelandi*	34.09	Benthic, riffle, run, pool	Miller and Robison, 2004
		Common Logperch	*Percina caprodes*	35.00	Benthic, riffle, run, pool	Miller and Robison, 2004
		Dusky Darter	*Percina sciera*	34.30	Benthic, riffle, run, pool	Miller and Robison, 2004
		Orangebelly Darter*	*Etheostoma radiosum*	33.97	Benthic, riffle, run, pool	Miller and Robison, 2004
		Slenderhead Darter	*Percina phoxocephala*	34.32	Benthic, riffle, run, pool	Miller and Robison, 2004

*Oklahoma Species of Greatest Conservation Concern

Table 9. Summary of the atmospheric data retrieved from Oklahoma Mesonet stations: Talihina, Clayton and Antlers. Averages were reported for summer 2013, 2014, 2015 and 2017. Data were obtained from 7/22 to 9/1.

	Air Temperature (°C)	Dew Point (°C)	Wind Speed (m/s)	Solar Radiation (W/m^2)
2013	26.5	19.3	3.7	254.8
2014	25.3	19.1	3.3	251.4
2015	27.6	18.2	3.7	268.9
2017	25.6	21.8	3.4	237.7

Table 10. Summary of the transect survey results on Kiamichi River. Site locations are provided with Indian Highway (see figure 13) referenced at 0.00 km. Depth and velocities were averaged across the channel.

Downstream Distance (km)	Latitude (degree)	Longitude (degree)	Width (m)	Flow Velocity (m/s)	Depth (m)	Discharge (m^3/s)
0.00	34.657720	-95.042020	20.52	0.02	0.61	0.24
9.69	34.636131	-95.122021	18.70	0.03	0.56	0.19
21.98	34.621897	-95.233682	44.95	0.01	0.78	0.35
22.29	34.621149	-95.237053	16.40	0.04	0.44	0.26
27.63	34.611820	-95.277660	38.24	0.01	1.15	0.35
34.28	34.597058	-95.335114	27.66	0.10	0.37	0.97
34.28	34.597445	-95.336491	28.91	0.03	1.02	0.81
34.28	34.596635	-95.337009	37.68	0.02	0.67	0.47
39.49	34.572698	-95.359536	20.99	0.14	0.36	1.03
59.88	34.505968	-95.510055	16.34	0.28	0.46	1.08
73.34	34.426470	-95.577740	48.64	0.04	0.73	1.34
		Mean	29.00	0.06	0.65	0.64
		Standard Deviation	11.68	0.08	0.26	0.41

Table 11. Summary of biochemical oxygen demand (BOD) samples. BOD was determined at each site where I collected DO data. BOD samples were collected on two occasions: 8/30/2017 (only upstream sites as the downstream sites were affected by release) and 9/27/2017. BOD samples were analyzed by the Oklahoma Department of Environmental Quality.

Sites Name	Sample Time	BOD (mg/L)	Discharge (m^3/s)
NDN	2017/8/30 9:00 AM	< 2.00*	1.04
	2017/8/30 10:10 AM	< 2.00*	1.04
	2017/9/27 10:17 AM	2.85	**
Robins	2017/8/30 9:35 AM	< 2.00*	1.04
	2017/8/30 11:35 AM	2.15	1.04
	2017/9/27 9:50 AM	2.89	**
Confluence	2017/9/27 9:09 AM	< 2.00*	**
Pine Spur	2017/9/27 8:18 AM	< 2.00*	**
Payne	2017/9/27 7:53 AM	3.76	**

*Below biochemical oxygen demand (BOD) detectable limit

** Below discharge detectable limit

Table 12. Model calibration (2013, 2014 and 2015) and validation (2017) statistical results for 7/22 to 9/1. Predicted stream water temperature time series at NDN, Robins, Pine Spur and Payne were contrasted against monitored data. Three measures, R^2, root mean squared error (RMSE), and NSE, were calculated to determine model fit at each site and in each year. Each site location is shown in Figure 13.

Parameter	Method	Year	NDN	Robins	Pine Spur	Payne
R^2	Calibration	2013	0.75	0.68	0.81	0.66
	Calibration	2014	0.80	0.77	0.48	0.45
	Calibration	2015	0.72	0.68	0.32	*
	Validation	2017	0.77	0.66	0.57	0.45
RMSE (°C)	Calibration	2013	1.45	1.84	1.13	1.56
	Calibration	2014	1.19	1.34	2.23	2.21
	Calibration	2015	1.40	1.89	2.43	*
	Validation	2017	1.07	1.69	1.65	1.90
NSE	Calibration	2013	0.31	-0.06	0.59	-0.04
	Calibration	2014	0.62	0.61	-0.28	-0.06
	Calibration	2015	0.47	-0.11	-0.10	*
	Validation	2017	0.56	0.25	-0.23	-0.84

*Observed data were not available for comparison.

Table 13. Thermal stress of fishes was evaluated by calculating the area under the curve of cumulative time above CTMax downstream of the release (km•h) in Figure 22. The CTMax used to represent the thermal tolerances of a mid-column fish habitat guild was 34.72 ºC and the value used to represent the thermal tolerances of the benthic guild was 34.34 ºC. The thermal tolerances of fishes included in each guild are provided in Table 8. Release scenarios were simulated based on the combination of five different release magnitude (0.34, 0.59, 0.76, 1.13 and 1.50 m^3/s) and three gate levels (5, 10 and 20 m deep representing release water temperature of 27.64 ºC, 26.00 ºC and 24.07 ºC, respectively).

	Mid-column Guild				Benthic Guild			
Depth of water release from dam (m)	Control	5	10	20	Control	5	10	20
Discharge (m^3/s)	2914				5206			
0.34		2607	2516	2401		4808	4679	4557
0.59		2392	2290	2197		4579	4360	4153
0.76		2309	2214	2118		4401	4162	3949
1.13		2119	1980	1831		4027	3776	3534
1.50		1953	1785	1583		3698	3409	3077

Table 14. The reduction rate of thermal stress compared to the control with no release (calculated as the ratio of thermal stress reduction to the thermal stress of the control). The CTMax used to represent the thermal tolerances of a mid-column fish habitat guild was 34.72 ºC and the value used to represent the thermal tolerances of the benthic guild was 34.34 ºC. The thermal tolerances of fishes included in each guild are provided in Table 8. Release scenarios were simulated based on the combination of five different release magnitude (0.34, 0.59, 0.76, 1.13 and 1.50 m^3/s) and three gate levels (5, 10 and 20 m deep representing release water temperature of 27.64 ºC, 26.00 ºC and 24.07 ºC, respectively).

	Mid-column Guild			Benthic Guild		
Depth of water release from dam (m)	5	10	20	5	10	20
Discharge (m^3/s)						
0.34	11%	14%	18%	8%	10%	12%
0.59	18%	21%	25%	12%	16%	20%
0.76	21%	24%	27%	15%	20%	24%
1.13	27%	32%	37%	23%	27%	32%
1.50	33%	39%	46%	29%	35%	41%

Table 15. The distance downstream of the Jack Fork Creek and Kiamichi River where the cumulative time above CTMax was reduced by half (provided in km). The CTMax used to represent the thermal tolerances of a mid-column fish habitat guild was 34.72 ºC and the value used to represent the thermal tolerances of the benthic guild was 34.34 ºC. The thermal tolerances of fishes included in each guild are provided in Table 8. Release scenarios were simulated based on the combination of five different release magnitude (0.34, 0.59, 0.76, 1.13 and 1.50 m^3/s) and three gate levels (5, 10 and 20 m deep representing release water temperature of 27.64 ºC, 26.00 ºC and 24.07 ºC, respectively).

	Mid-column Guild			Benthic Guild		
Depth of water release from dam (m)	5	10	20	5	10	20
Discharge (m^3/s)						
0.34	1	1	2	1	1	2
0.59	4	6	8	2	5	7
0.76	5	7	8	5	7	7
1.13	9	11	12	8	9	10
1.50	10	13	16	10	11	13

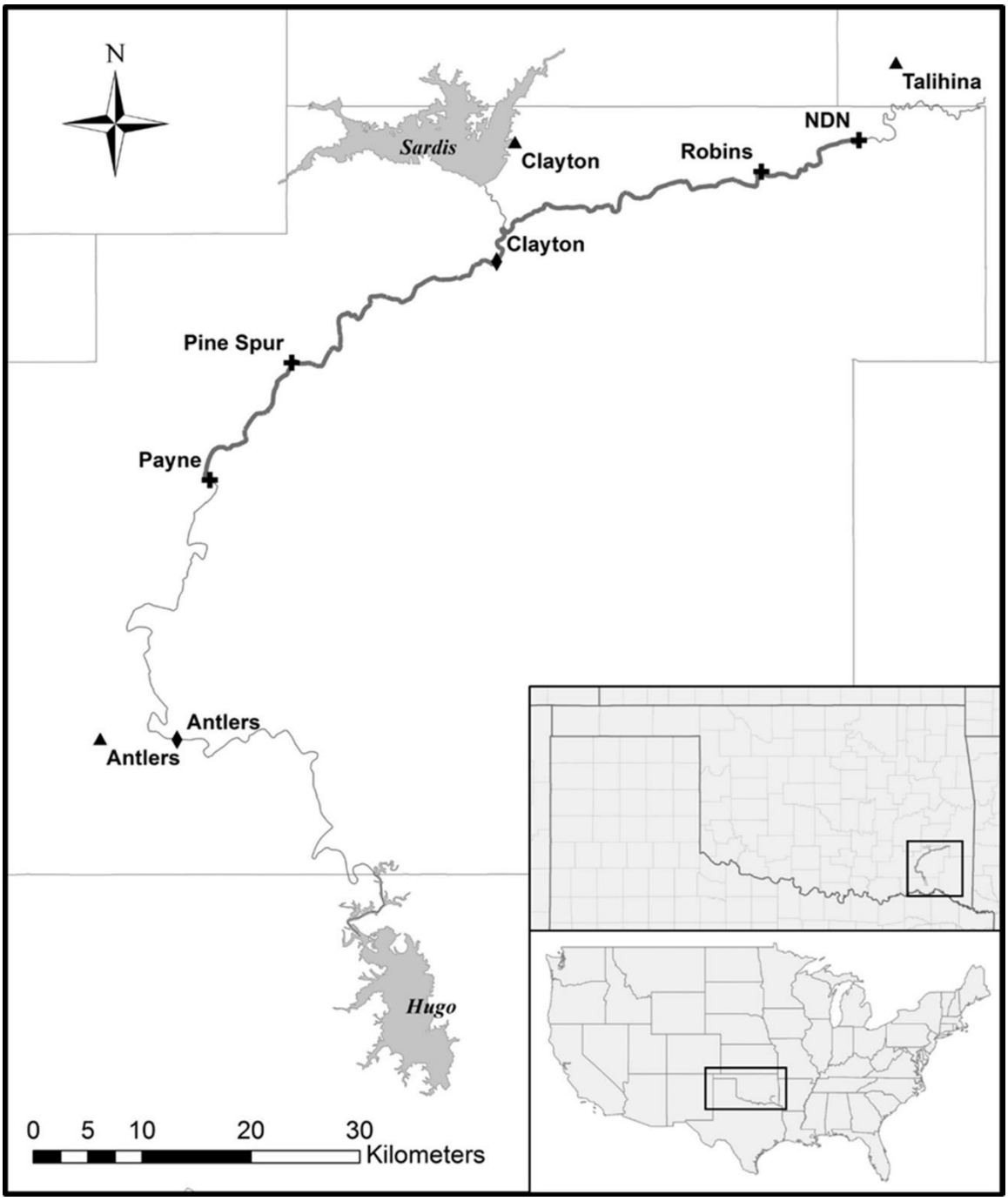

Figure 13. Map of Kiamichi River where the solid line indicates the study reach where water temperature was modeled using the Water Quality Analysis Simulation Program (WASP). Mesonet stations and USGS gages are represented by triangle and diamond markers, respectively. Cross markers indicate monitoring sites where stream water temperature and DO data were collected.

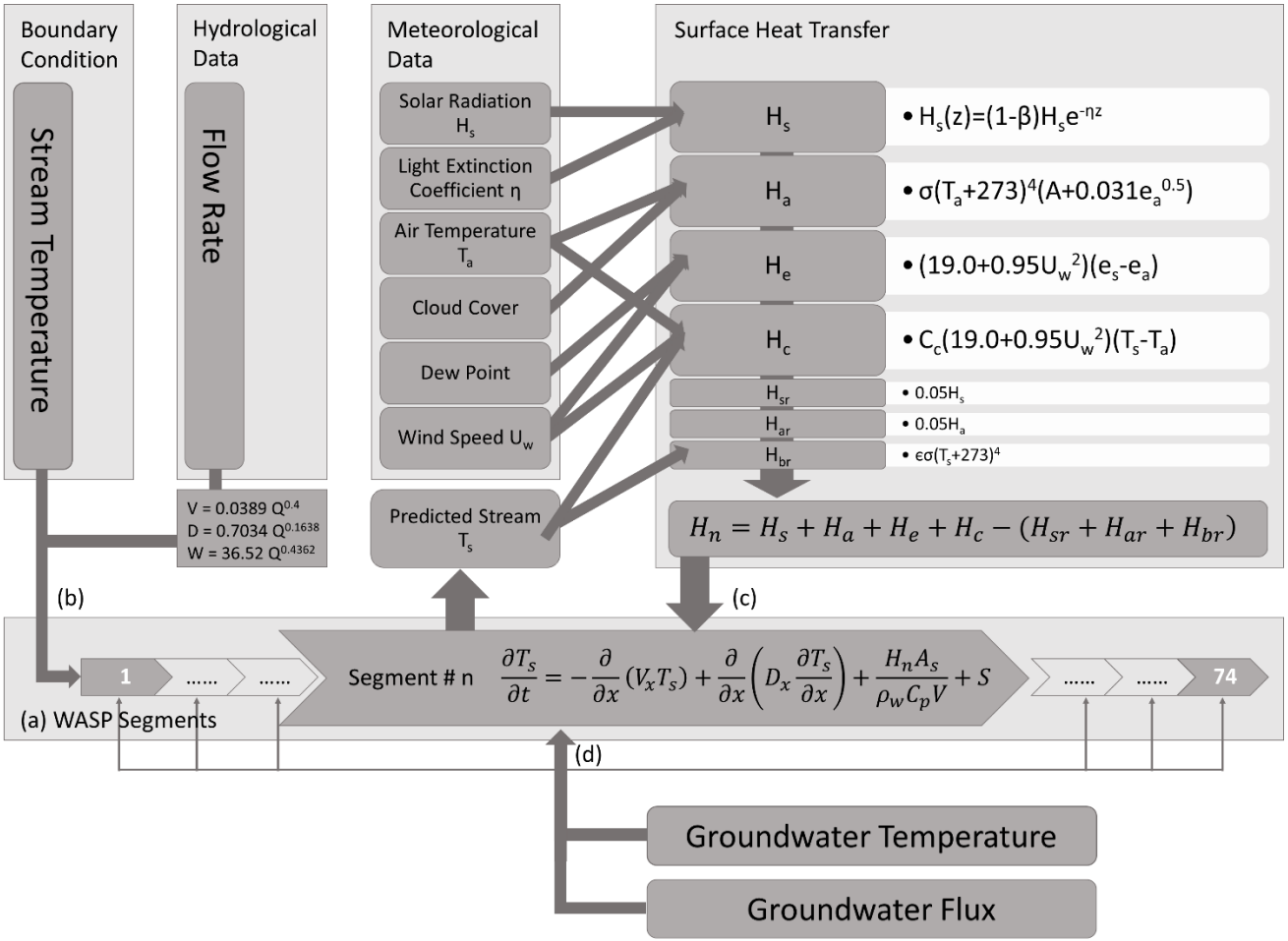

Figure 14. Temperature module of the Water Quality Analysis Simulation Program (WASP) showing (a) temperatures were predicted for each model segment representing stream channel, (b) upstream boundary conditions derived from stream water temperature and discharge, (c) atmospheric heat transfer parameters applied to each model segment at each time step, and (d) groundwater flux represented as a lateral boundary.

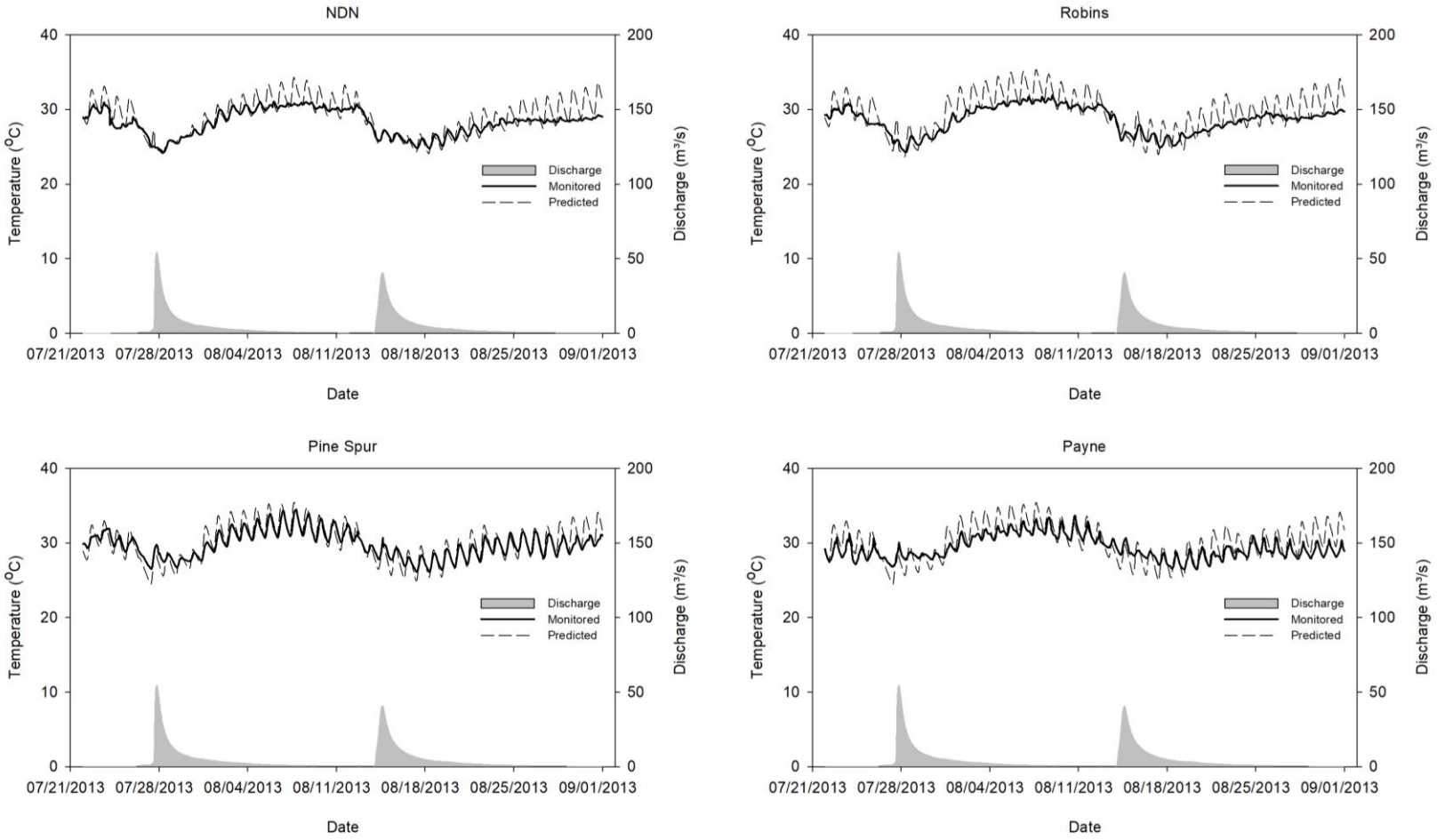

Figure 15. The WASP model was calibrated for 7/21/2013 to 9/1/2013. Predicted temperature time series were contrasted against monitored stream water temperature at four downstream sites: NDN, Robins, Pine Spur and Payne. The four sites are shown on Figure 13. The observed data are shown by solid lines, and the WASP-predicted stream temperatures are shown using dashed lines.

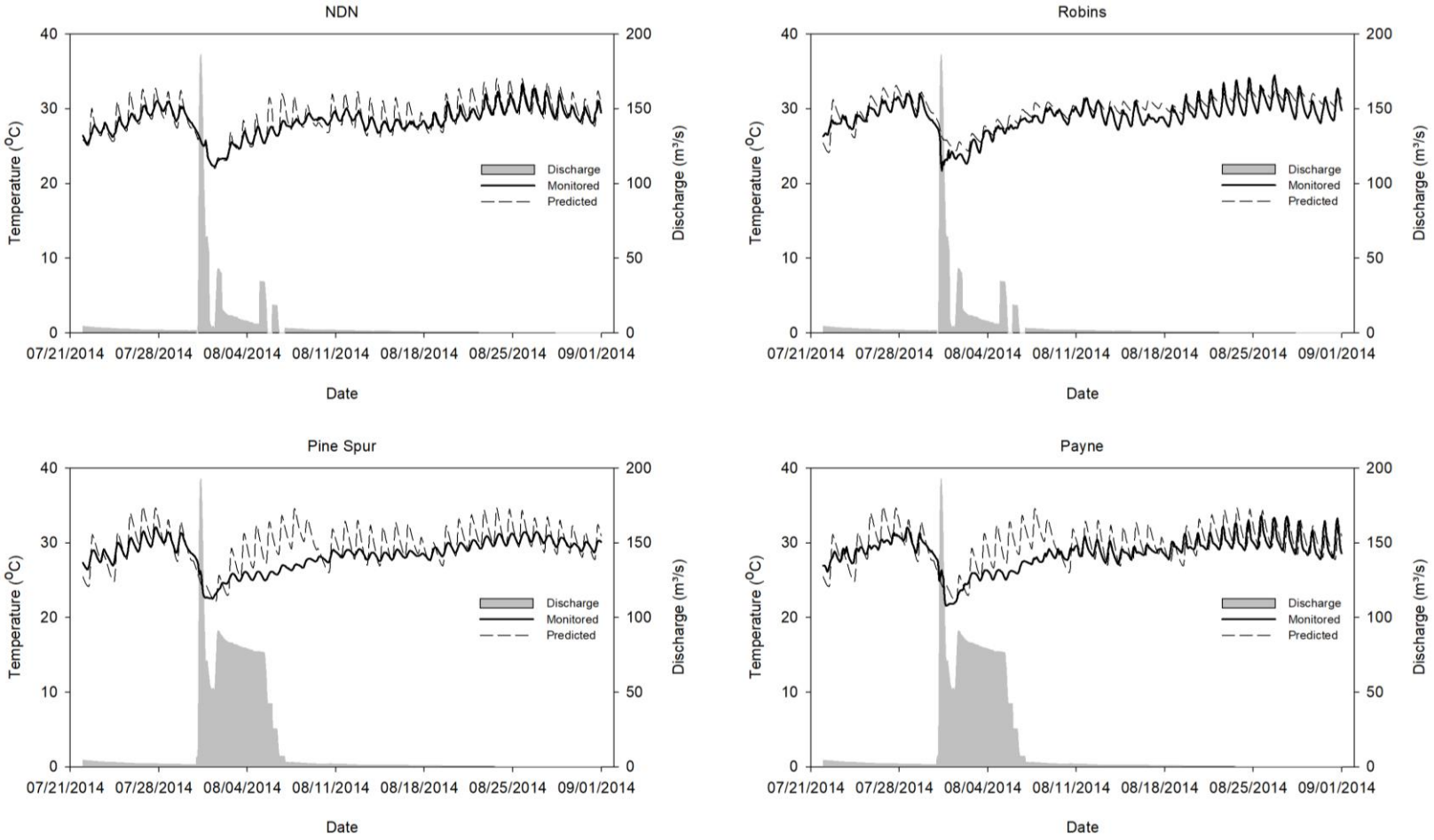

Figure 16. The WASP model was calibrated for 7/21/2014 to 9/1/2014. Predicted temperature time series were contrasted against monitored stream water temperature at four downstream sites: NDN, Robins, Pine Spur and Payne. The four sites are shown on Figure 13. The observed data are shown by solid lines, and the WASP-predicted stream temperatures are shown using dashed lines.

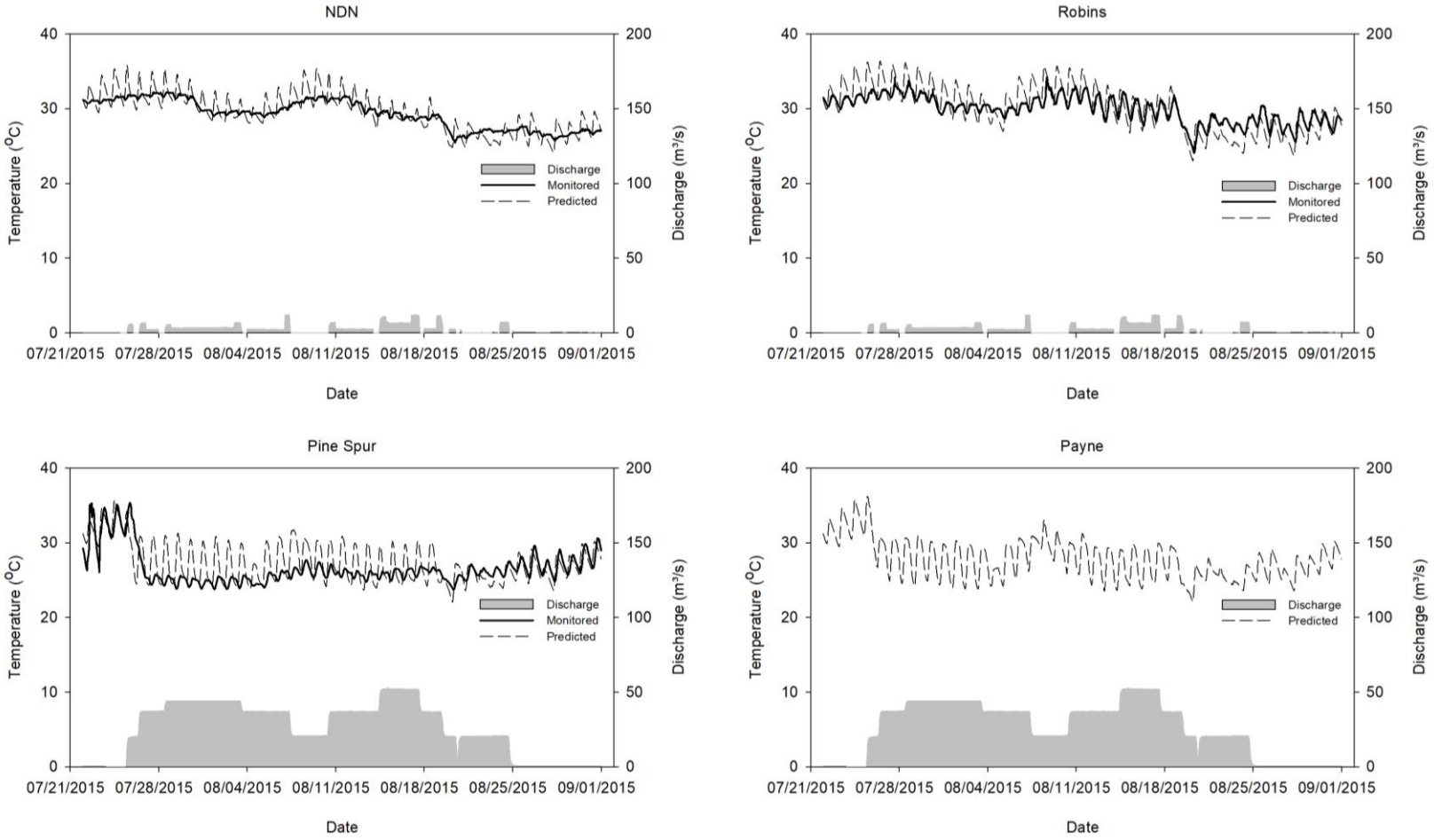

Figure 17. The WASP model was calibrated for 7/21/2015 to 9/1/2015. Predicted temperature time series were contrasted against monitored stream water temperature at four downstream sites: NDN, Robins, Pine Spur and Payne. The four sites are shown on Figure 13. The observed data are shown by solid lines, and the WASP-predicted stream temperatures are shown using dashed lines. Monitored stream water temperature data for Payne were not available during 2015 and were not shown.

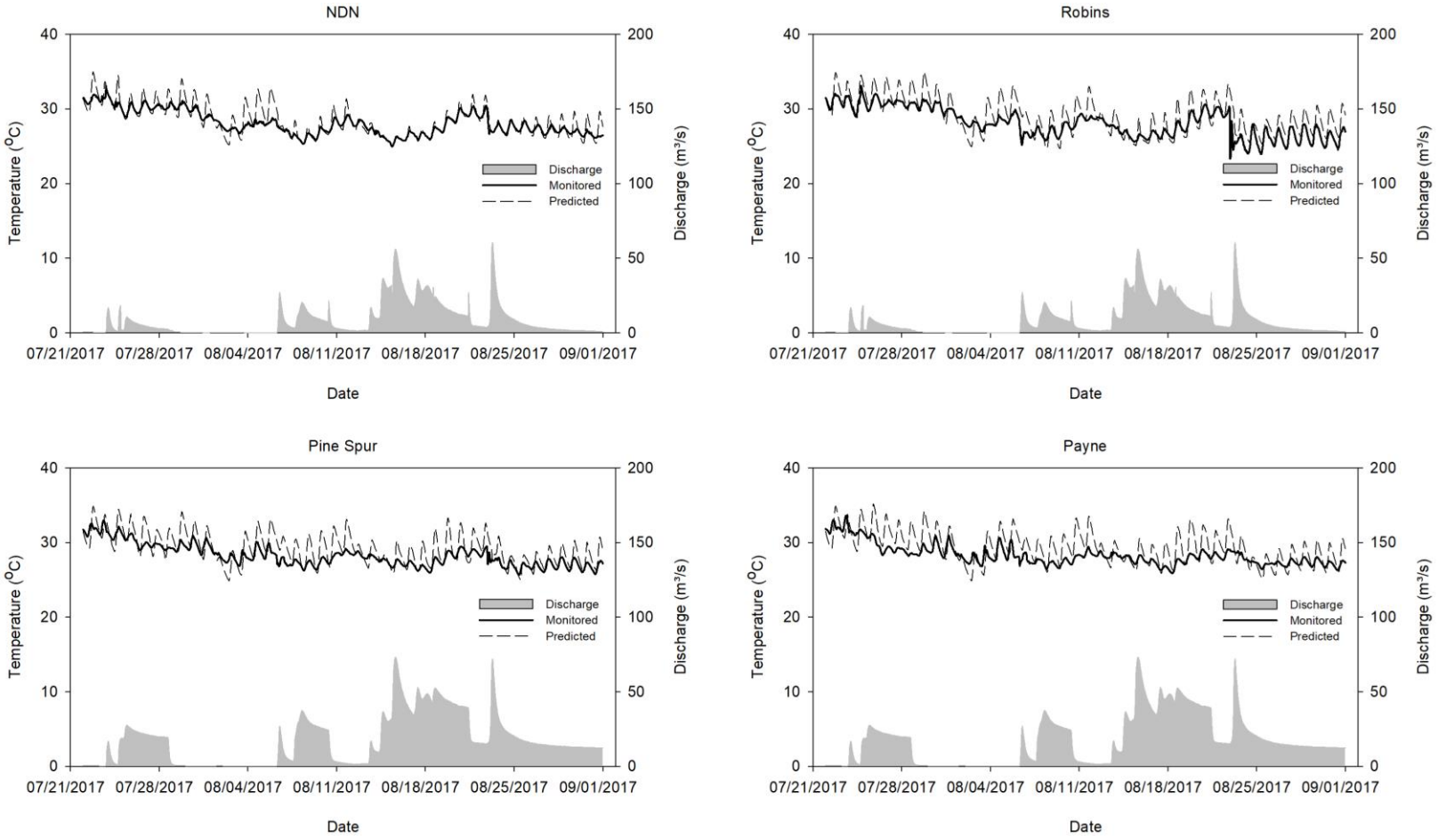

Figure 18. The WASP model was validated during the period of 7/21/2017 to 9/1/2017 using parameters from the calibrated model. The WASP model was calibrated over a 3-year summer, baseflow period. Predicted temperature time series were contrasted against monitored stream water temperature at four downstream locations: NDN, Robins, Pine Spur and Payne. Observation data are represented by solid lines while predicted stream temperature is illustrated in dashes.

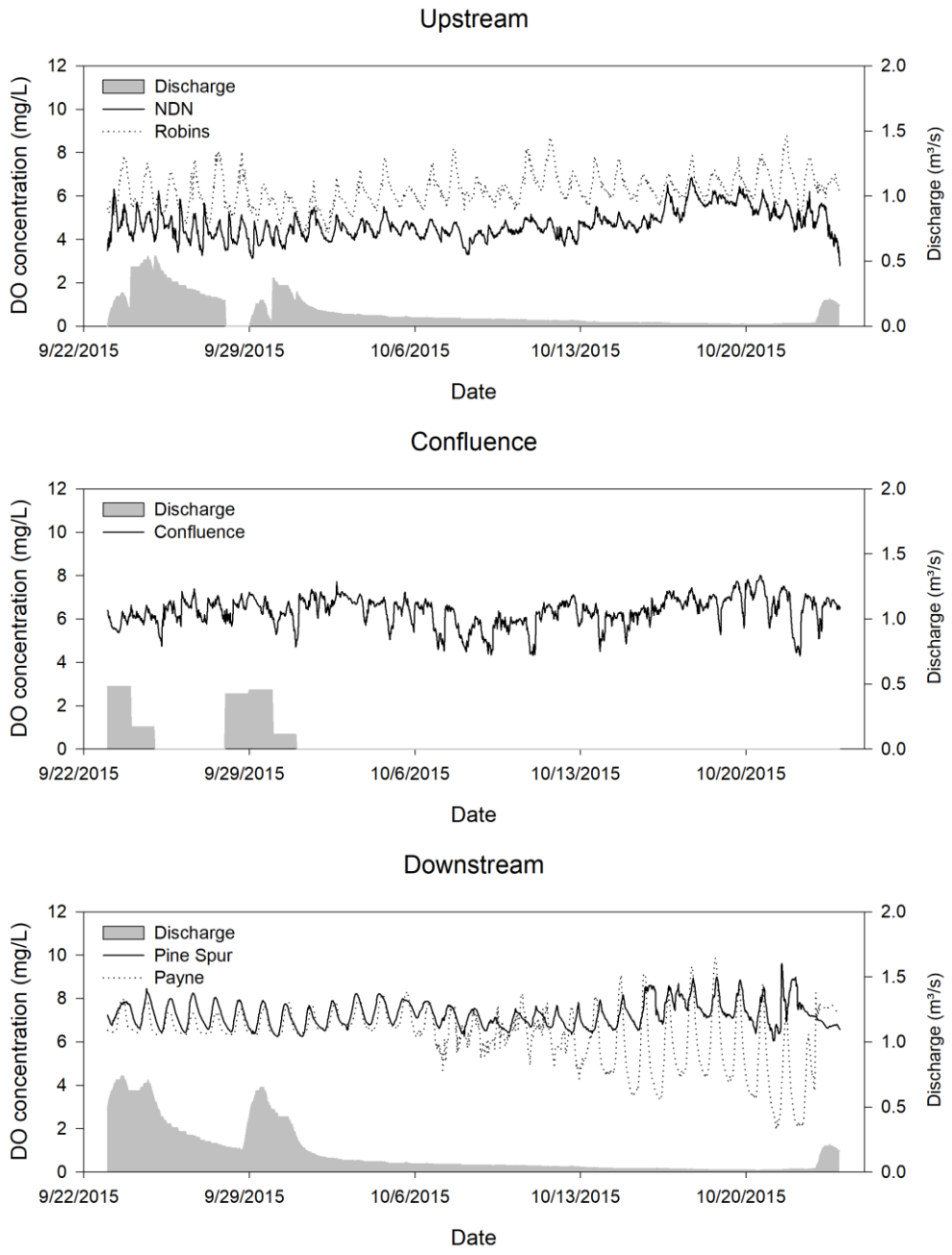

Figure 19. Monitored dissolved oxygen (DO) concentrations at sites upstream of the confluence (Kiamichi River and Jack Fork Creek), at the confluence, and downstream of the confluence. Data were collected during summer 2015 representing DO conditions during a baseflow period with minimal water released from Sardis Dam.

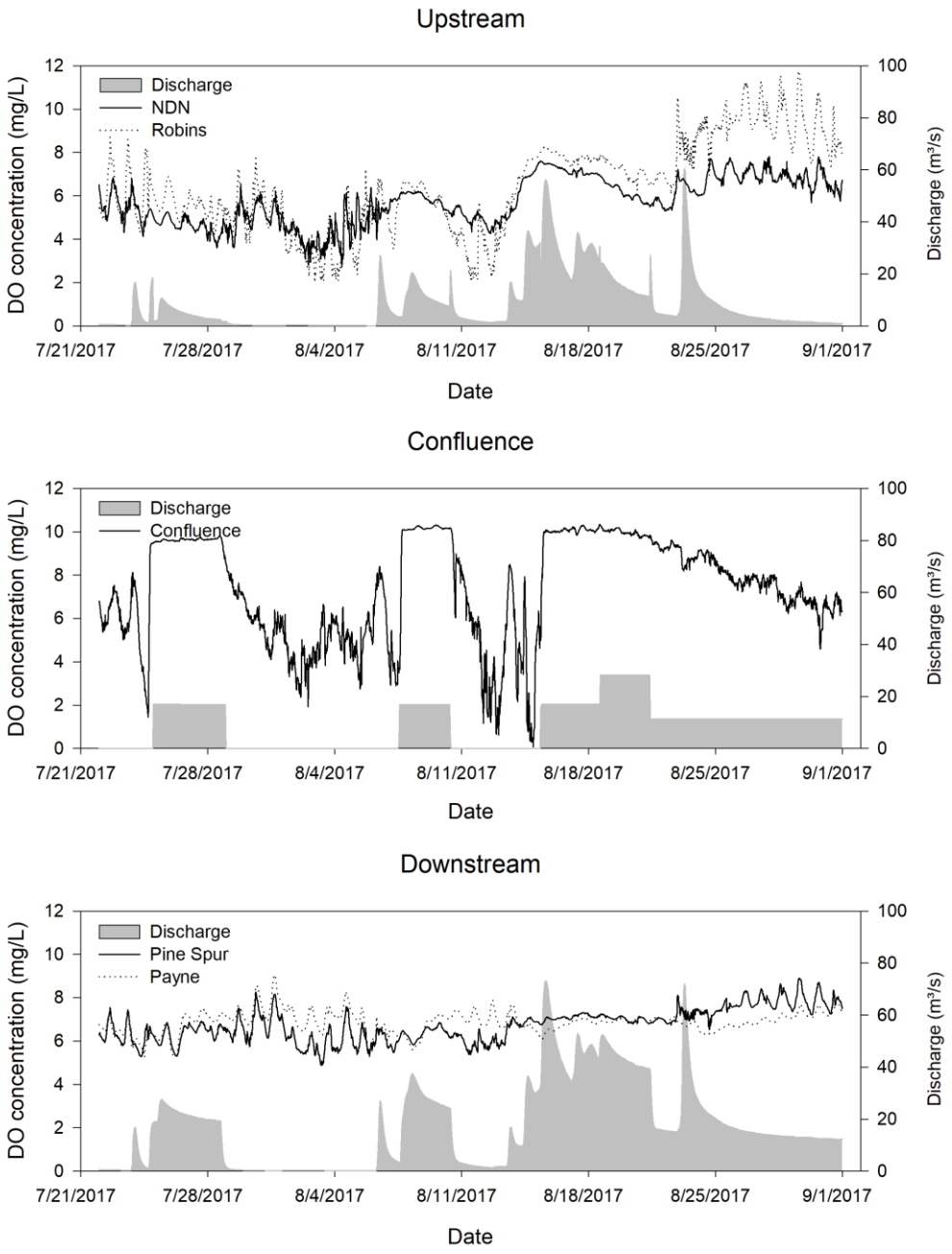

Figure 20. Monitored dissolved oxygen (DO) concentrations at sites upstream of the confluence (Kiamichi River and Jack Fork Creek), at the confluence, and downstream of the confluence. Data were collected during summer 2017 representing DO conditions during a higher flow period with considerable released water from Sardis Dam.

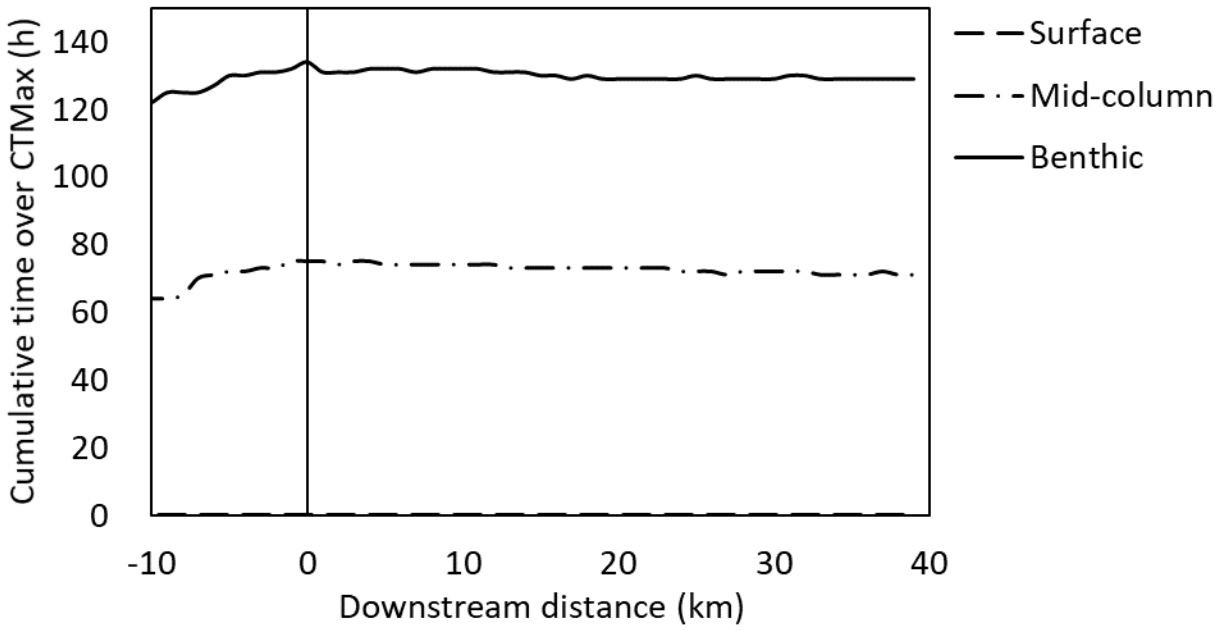

Figure 21. The cumulative time above thermal critical maxima (CTMax) of three fish guilds verses downstream distance from the reservoir confluence calculated with the occurred release removed from the model. This simulation served as a control and evaluated the thermal stress that would have been experienced by fishes in the absence of the water release. The surface guild never experienced temperatures exceeding their CTMax (showing as y = 0 h that overlays with x-axis).

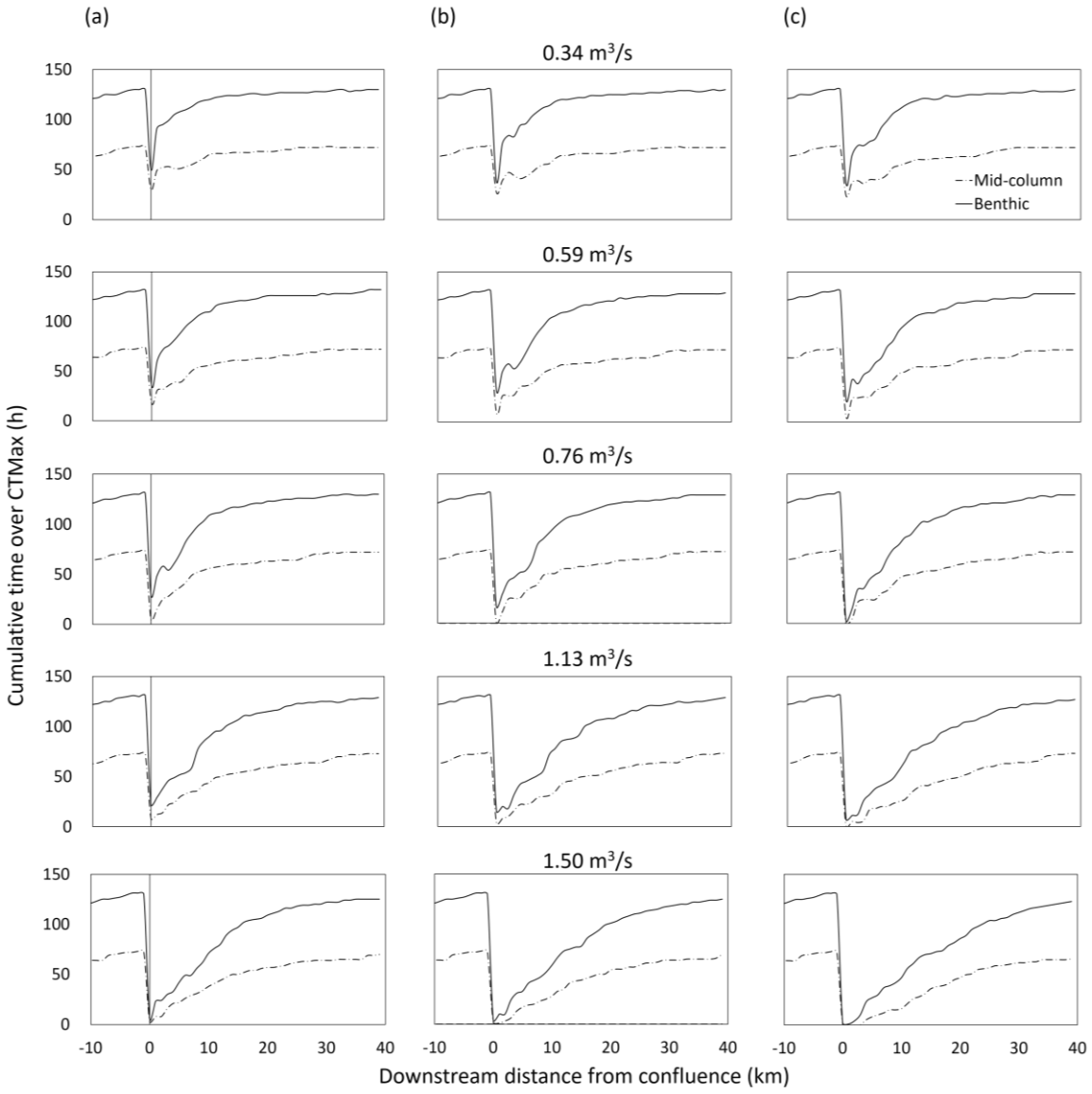

Figure 22. The cumulative time above critical thermal maxima (CTMax) for two fish guilds: mid-column and benthic guilds. The cumulative time about CTMax is shown 10-km upstream of the Jack Fork Creek and Kiamichi River confluence (indicated as 0 on the X axis). Each water-release scenario (second Y axis) is simulated showing the cumulative time above CTMax from the confluence downriver for 40 km. Each water-release scenario was simulated using three different upstream thermal boundary conditions (i.e., water temperature from the dam) that reflect the gate locations where releases could occur from the dam (5, 10 and 20 m), represented by a, b and c, respectively. The temperatures represented by each gate location were: 27.64 ºC, 26.00 ºC and 24.07 ºC, respectively.

CHAPTER V

CONCLUSIONS

Quantifying groundwater-surface water interactions in streams remains a research topic that requires considerable attention. Because of the complex nature of stream-groundwater hydrological connectivity, scientists have attempted to attack this problem from many theoretical backgrounds. However, finding a simpler and more economic approach is still of great research interest due to the high cost and the difficulty in parameterizing watershed properties. Because of the ease of monitoring stream temperatures, thermal methods overcome some of these limitations and have gained increasing popularity in recent decades. The traditional vertical thermal gradient method quantifies vertical water movement across the streambed by simulating coupled heat and water transport through both advection and conduction by monitoring temperature at multiple depths within the streambed. The emerging stream thermal modeling approach uses a process-based model to simulate the heat budget of stream water using known hydrologic and atmospheric variables, and quantifies groundwater flux based on the residual of the known stream water heat budget. In this research, the thermal equilibrium method was developed based on the assumption that streams were at thermal equilibrium with the combination of atmospheric conditions and groundwater interactions. The temperature signatures were used to quantify

groundwater flux at a point scale, which significantly reduced the cost and need of additional data collection while maintaining the sensitivity and independence of a point measurement.

This research comprises three associated components: understanding transient storage mechanisms as a type of groundwater interactions, developing a new approach of quantifying groundwater flux, and applying the groundwater flux estimations to evaluate stream water temperature in a managerial context. In the first project, I successfully applied a transient storage zone model to simulate solute transport in soil pipe systems based on data collected in four tracer injection tests. This project furthered knowledge on groundwater interactions in preferential flow systems and their implications on solute transport in comparison with stream flow systems. In the second project, the thermal equilibrium method, as a type of thermal tracer method, was developed to quantify groundwater flux on a point scale using monitored stream water temperature and existing atmospheric and hydrological data. This project provided a new way of quantifying groundwater flux. Based on the knowledge and groundwater interactions parameters predicted in the Kiamichi River, the third project focused on the application of a stream water temperature model to evaluate the effects of different reservoir operations in the Kiamichi River as related to stream fish thermal tolerance during summer, baseflow conditions. The project demonstrated a successful example of groundwater interactions incorporated into a stream water temperature model that provide a decision support tool for balancing the increasing human demand for water with options for meeting water quality standards that can support environmental flow efforts.

The following conclusions were drawn from the dissertation:

1. The OTIS (One-Dimensional Transport with Inflow and Storage) designed for stream systems was proven applicable to soil pipe systems to quantify hydraulic and solute transport parameters within the soil pipes.

2. Similar to stream systems, transient storage in soil pipes acts to reduce the peak concentrations downstream of the source, delay the breakthrough curve, and enhance the tailing effect.

3. Transport parameters in soil pipes showed considerable variability especially in terms of the transient storage area and first-order exchange coefficient, likely due to pipe irregularities throughout the pipe network.

4. Dimensionless transport metrics of the transient storage model indicated velocities in the soil pipes were generally lower, whereas the storage zone area and exchange coefficients were generally higher than stream systems, likely due to the higher wetted perimeter to flow area (soil-fluid contact) and lower flow velocities.

5. The thermal equilibrium method was proven a suitable technique for quantifying groundwater flux by comparison with an incremental flow method (seepage run) with a R^2 of 0.94, a root mean squared error (RMSE) of 0.08 (m/d) and a Nash–Sutcliffe efficiency (NSE) of 0.93.

6. A model domain design of 2-km segment comprising 20 segments was recommended for balance between accuracy and model efficiency.

7. Streams in Ozark Highland ecoregion showed higher groundwater fluxes compare to Kiamichi River.

8. The thermal equilibrium method performed best at locations of gradual varying groundwater discharge and at weekly scale or coarser.

9. Dissolved oxygen in the Kiamichi River was not directly affected by releases from the top gate of the Sardis Lake. However, the magnitude of release can affect downstream DO concentrations via interactions with aquatic ecosystems.

10. Without water release, the benthic guild was expected to experience 130 hr of thermal stress, mid-column guild was expected to experience 73 hr thermal stress, while the surface guild never experienced temperatures exceeding their CTMax.

11. The only ecological flow used in recent years to maintain river flow (0.34 m^3/s) was insufficient to recover the downstream thermal regime to pre-dam conditions.

12. The only ecological flow used in recent years to maintain river flow (0.34 m^3/s) reduced thermal stress by 11% for mid-column fishes and 8% for benthic fishes, while releases that represented a pre-dam flow magnitude (0.76, 1.13 and 1.50 m^3/s released from top gate) reduced the thermal stress up to 33%.

13. The impoundment of Sardis Lake significantly altered the downstream thermal regime of the Kiamichi River and increased the thermal stress by up to 20% for benthic and mid-column fish species.

During this study, a number of limitations could benefit from future research. In the first project, the large variability observed in the estimated A_s and α_s, suggested differences in potential sinuosity of the pipe networks or pooling of water before continuing through the network. Advances in methodologies to map soil pipes, their sinuosity, network connectivity, and flow characteristics could improve this. To advance the knowledge of the soil pipes development, there is also a need for longer-term studies that continue to monitor pipe geomorphology and hydrometrics to document the development of the pipe network and develop a database of the hydrodynamics. Additional tracer studies are also needed to quantify changes in flow/transport characteristics, presence of transient storage over time, and dilution from other soil pipe and macropore networks feeding the main soil pipe channel as a function of soil wetness or soil pipe hydrograph. For the second project, there is a need for more comprehensive thermal model that adequately quantify the effect of local scale groundwater interactions such as hyporheic flow and

surface exchange. The third project could be further improved by local scale thermal mapping that identify the discrepancy between instream temperature profile and prediction from the one-dimensional temperature model. There is also an urgent need for efforts that focus on quantifying the response of stream fish populations to stream water temperature changes at a finer temporal and spatial scale. To better understanding the effect of hypolimnetic release, future research is needed that quantify the downstream dissolve oxygen concentrations related to release at different depth of the reservoir under various atmospheric and hydrological conditions.

REFERENCES

Acreman, M., Dunbar, M.J., 2004. Defining environmental river flow requirements? A review. *Hydrology and Earth System Sciences Discussions*, **8**(5): 861-876.

Adamski, J.C., Petersen, J.C., Freiwald, D.A., Davis, J.V., 1995. Environmental and hydrologic setting of the Ozark Plateaus study unit, Arkansas, Kansas, Missouri, and Oklahoma. *US Geological Survey Water-Resources Investigations Report*, **94**(4022): 69.

Alexander, J.R., 2017. Determining the effects of thermal increases on stream fishes of the Ouachita Mountain ecoregion, Oklahoma State University, *Stillwater, OK*.

Allan, J.D., Castillo, M.M., 2007. Stream ecology: structure and function of running waters. *Springer Science & Business Media*.

Allison, G., Hughes, M., 1975. The use of environmental tritium to estimate recharge to a South-Australian aquifer. *Journal of Hydrology*, **26**(3): 245-254.

Anderson, M.P., 2005. Heat as a ground water tracer. *Groundwater*, **43**(6): 951-968.

Annear, T. et al., 2002. Instream flows for riverine resource stewardship. *Instream Flow Council, Cheyenne, WY*.

Arnold, J., Allen, P., Muttiah, R., Bernhardt, G., 1995. Automated base flow separation and recession analysis techniques. *Groundwater*, **33**(6): 1010-1018.

Arnott, S., Hilton, J., Webb, B., 2009. The impact of geological control on flow accretion in lowland permeable catchments. *Hydrology Research*, **40**(6): 533-543.

Arthington, A.H., Bunn, S.E., Poff, N.L., Naiman, R.J., 2006. The challenge of providing environmental flow rules to sustain river ecosystems. *Ecological Applications*, **16**(4): 1311-1318.

Barlocher, F., Murdoch, J.H., 1989. Hyporheic biofilms—a potential food source for interstitial animals. *Hydrobiologia*, **184**(1-2): 61-67.

Becker, C.D., Genoway, R.G., 1979. Evaluation of the critical thermal maximum for determining thermal tolerance of freshwater fish. *Environmental Biology of Fishes*, **4**(3): 245-256.

Becker, M., Georgian, T., Ambrose, H., Siniscalchi, J., Fredrick, K., 2004. Estimating flow and flux of ground water discharge using water temperature and velocity. *Journal of Hydrology*, **296**(1): 221-233.

Berry, L., Mutiti, S., Hazzard, S., 2011. Determining the Hydraulic Conductivity of the Subsurface in Wetland Environments, AGU Fall Meeting Abstracts.

Blasch, K.W., Constantz, J., Stonestrom, D.A., 2007. Thermal methods for investigating ground-water recharge. 2330-7102, Geological Survey (US).

Bloomfield, J., Allen, D., Griffiths, K., 2009. Examining geological controls on baseflow index (BFI) using regression analysis: An illustration from the Thames Basin, UK. *Journal of Hydrology*, **373**(1): 164-176.

Bogan, T., Mohseni, O., Stefan, H.G., 2003. Stream temperature-equilibrium temperature relationship. *Water Resources Research*, **39**(9).

Bogan, T., Stefan, H.G., Mohseni, O., 2004. Imprints of secondary heat sources on the stream temperature/equilibrium temperature relationship. *Water Resources Research*, **40**(12).

Bredehoeft, J., Papaopulos, I., 1965. Rates of vertical groundwater movement estimated from the Earth's thermal profile. *Water Resources Research*, **1**(2): 325-328.

Brewer, S.K. et al., 2016. Advancing Environmental Flow Science: Developing Frameworks for Altered Landscapes and Integrating Efforts Across Disciplines. *Environmental management*, **58**(2): 175-192.

Briggs, M. et al., 2016. Strong seepage of shallow groundwater shifts the timing of the annual thermal signals in stream water, AGU Fall Meeting Abstracts.

Brodie, R., Sundaram, B., Tottenham, R., Hostetler, S., Ransley, T., 2007. An overview of tools for assessing groundwater-surface water connectivity. *Bureau of Rural Sciences, Canberra, Australia*: 131.

Brusseau, M., 1998. Multiprocess nonequilibrium and nonideal transport of solutes in porous media. *Physical nonequilibrium in soils: modeling and application*: 63-82.

Brusseau, M.L., Larsen, T., Christensen, T., 1991. Rate-limited sorption and nonequilibrium transport of organic chemicals in low organic carbon aquifer materials. *Water Resources Research*, **27**(6): 1137-1145.

Bunn, S.E., Arthington, A.H., 2002. Basic principles and ecological consequences of altered flow regimes for aquatic biodiversity. *Environmental management*, **30**(4): 492-507.

Caissie, D., 2006. The thermal regime of rivers: a review. *Freshwater Biology*, **51**(8): 1389-1406.

Caissie, D., Satish, M.G., El-Jabi, N., 2007. Predicting water temperatures using a deterministic model: Application on Miramichi River catchments (New Brunswick, Canada). *Journal of Hydrology*, **336**(3): 303-315.

Cashner, R., Matthews, W., Marsh-Matthews, E., Unmack, P., Cashner, F., 2010. Recognition and redescription of a distinctive stoneroller from the Southern Interior Highlands. *Copeia*, **2010**(2): 300-311.

Cole, T., Buchak, E., 1995. A two-dimensional, laterally averaged, hydrodynamic and water quality model, Version 2.0 User Manual. Instruction Report EL-95. *US Army Engineer Waterways Experiment Station, Vicksburg, MS, USA*.

Cole, T., Wells, S., 2002. CE_QUALW2: a two-dimensional, laterally averaged hydrodynamic and water quality model, version 3.1. User manual. *US Army Corps of Engineers, Instruction Report EL-02–1, Washington, DC*.

Constantz, J., 1998. Interaction between stream temperature, streamflow, and groundwater exchanges in alpine streams. *Water Resources Research*, **34**(7): 1609-1615.

Constantz, J., 2008. Heat as a tracer to determine streambed water exchanges. *Water Resources Research*, **44**(4).

Cook, P., Solomon, D.K., 1997. Recent advances in dating young groundwater: chlorofluorocarbons, 3H3He and 85 Kr. *Journal of Hydrology*, **191**(1): 245-265.

Coulter, D., Sepúlveda, M., Troy, C., Höök, T., 2014. Thermal habitat quality of aquatic organisms near power plant discharges: potential exacerbating effects of climate warming. *Fisheries management and ecology*, **21**(3): 196-210.

Coutant, C.C., 1976. Thermal effects on fish ecology.

Delinom, R.M., 2009. Structural geology controls on groundwater flow: Lembang Fault case study, West Java, Indonesia. *Hydrogeology Journal*, **17**(4): 1011-1023.

Dodd, M., Lauenroth, W., 1997. The influence of soil texture on the soil water dynamics and vegetation structure of a shortgrass steppe ecosystem. *Plant Ecology*, **133**(1): 13-28.

Eberle, M.E., Stark, W.J., 2000. Status of the Arkansas darter in south-central Kansas and adjacent Oklahoma. *Prairie Naturalist*, **32**(2): 103-114.

Ebersole, J., Liss, W., Frissell, C., 2001. Relationship between stream temperature, thermal refugia and rainbow trout Oncorhynchus mykiss abundance in arid-land streams in the northwestern United States. *Ecology of freshwater fish*, **10**(1): 1-10.

Ellis, L.E., Jones, N.E., 2013. Longitudinal trends in regulated rivers: a review and synthesis within the context of the serial discontinuity concept. *Environmental Reviews*, **21**(3): 136-148.

Eriksson, E., Khunakasem, V., 1969. Chloride concentration in groundwater, recharge rate and rate of deposition of chloride in the Israel Coastal Plain. *Journal of Hydrology*, **7**(2): 178-197.

Farvolden, R., 1963. Geologic controls on ground-water storage and base flow. *Journal of Hydrology*, **1**(3): 219-249.

Fisher, W.L., Seilheimer, T.S., Taylor, J.M., 2012. Biological assessment of environmental flows for Oklahoma. 2331-1258, US Geological Survey.

Foster, M., Fell, R., Spannagle, M., 2000. The statistics of embankment dam failures and accidents. *Canadian Geotechnical Journal*, **37**(5): 1000-1024.

Fox, G.A. et al., 2007. Measuring streambank erosion due to ground water seepage: correlation to bank pore water pressure, precipitation and stream stage. *Earth Surface Processes and Landforms*, **32**(10): 1558-1573.

Fox, G.A., Heeren, D.M., Miller, R.B., Mittelstet, A.R., Storm, D.E., 2011. Flow and transport experiments for a streambank seep originating from a preferential flow pathway. *Journal of Hydrology*, **403**(3): 360-366.

Fox, G.A., Malone, R., Sabbagh, G.J., Rojas, K., 2004. Interrelationship of macropores and subsurface drainage for conservative tracer and pesticide transport. *Journal of environmental quality*, **33**(6): 2281-2289.

Freeze, R., Cherry, J., 1979. Groundwater Prentice Hall Englewood Cliffs. *New Jersey*, **603**.

Freeze, R.A., 1972. Role of subsurface flow in generating surface runoff: 1. Base flow contributions to channel flow. *Water Resources Research*, **8**(3): 609-623.

Gates, K.K., Vaughn, C.C., Julian, J.P., 2015. Developing environmental flow recommendations for freshwater mussels using the biological traits of species guilds. *Freshwater Biology*, **60**(4): 620-635.

Graczyk, D.J., Sonzogni, W.C., 1991. Reduction of dissolved oxygen concentration in Wisconsin streams during summer runoff. *Journal of environmental quality*, **20**(2): 445-451.

Gregory, J.H., Dukes, M.D., Jones, P.H., Miller, G.L., 2006. Effect of urban soil compaction on infiltration rate. *Journal of soil and water conservation*, **61**(3): 117-124.

Harr, R.D., Levno, A., Mersereau, R., 1982. Streamflow changes after logging 130-year-old Douglas fir in two small watersheds. *Water Resources Research*, **18**(3): 637-644.

Harvey, J.W., Bencala, K.E., 1993. The effect of streambed topography on surface-subsurface water exchange in mountain catchments. *Water Resources Research*, **29**(1): 89-98.

Hawkins, C.P., Hogue, J.N., Decker, L.M., Feminella, J.W., 1997. Channel morphology, water temperature, and assemblage structure of stream insects. *Journal of the North American benthological society*, **16**(4): 728-749.

Hicks, B.J., Beschta, R.L., Harr, R.D., 1991. LONG-TERM CHANGES IN STREAMFLOW FOLLOWING LOGGING IN WESTERN OREGON AND

ASSOCIATED FISHERIES IMPLICATIONS1. *JAWRA Journal of the American Water Resources Association*, **27**(2): 217-226.

Hoback, W.W., Barnhart, M.C., 1996. Lethal limits and sublethal effects of hypoxia on the amphipod Gammarus pseudolimnaeus. *Journal of the North American Benthological Society*, **15**(1): 117-126.

Hutchinson, D.G., Moore, R., 2000. Throughflow variability on a forested hillslope underlain by compacted glacial till. *Hydrological processes*, **14**(10): 1751-1766.

Jacobsen, D., Marín, R., 2008. Bolivian Altiplano streams with low richness of macroinvertebrates and large diel fluctuations in temperature and dissolved oxygen. *Aquatic Ecology*, **42**(4): 643-656.

Johnson, Z.C., Warwick, J.J., Schumer, R., 2014. Factors affecting hyporheic and surface transient storage in a western US river. *Journal of Hydrology*, **510**: 325-339.

Jones, J., 2010. Soil piping and catchment response. *Hydrological Processes*, **24**(12): 1548-1566.

Kalbus, E., Reinstorf, F., Schirmer, M., 2006. Measuring methods for groundwater, surface water and their interactions: a review. *Hydrology and Earth System Sciences Discussions*, **3**(4): 1809-1850.

Kanno, Y., Vokoun, J., Letcher, B., 2014. Paired stream–air temperature measurements reveal fine-scale thermal heterogeneity within headwater brook trout stream networks. *River research and applications*, **30**(6): 745-755.

Keppeler, E.T., Ziemer, R.R., 1990. Logging effects on streamflow: water yield and summer low flows at Caspar Creek in northwestern California. *Water Resources Research*, **26**(7): 1669-1679.

Konrad, C., 2006. Longitudinal hydraulic analysis of river-aquifer exchanges. *Water resources research*, **42**(8).

Krause, P., Boyle, D., Bäse, F., 2005. Comparison of different efficiency criteria for hydrological model assessment. *Advances in geosciences*, **5**: 89-97.

Kurylyk, B., Bourque, C.-A., MacQuarrie, K., 2013. Potential surface temperature and shallow groundwater temperature response to climate change: an example from a small forested catchment in east-central New Brunswick (Canada). *Hydrology and Earth System Sciences*, **17**(7): 2701-2716.

Kurylyk, B.L., Moore, R.D., MacQuarrie, K.T., 2016. Scientific briefing: quantifying streambed heat advection associated with groundwater–surface water interactions. *Hydrological Processes*, **30**(6): 987-992.

Lapham, W.W., 1989. Use of temperature profiles beneath streams to determine rates of vertical ground-water flow and vertical hydraulic conductivity, Dept. of the Interior, US Geological Survey; USGPO; Books and Open-File Reports Section, US Geological Survey.

Laursen, A., Seitzinger, S., 2005. Limitations to measuring riverine denitrification at the whole reach scale: effects of channel geometry, wind velocity, sampling interval,

and temperature inputs of N 2-enriched groundwater. *Hydrobiologia*, **545**(1): 225-236.

Lee, D.R., 1985. Method for locating sediment anomalies in lakebeds that can be caused by groundwater flow. *Journal of Hydrology*, **79**(1): 187-193.

Loheide, S.P., Gorelick, S.M., 2006. Quantifying stream− aquifer interactions through the analysis of remotely sensed thermographic profiles and in situ temperature histories. *Environmental Science & Technology*, **40**(10): 3336-3341.

Magnuson, J.J., Crowder, L.B., Medvick, P.A., 1979. Temperature as an ecological resource. *American Zoologist*, **19**(1): 331-343.

Malard, F., Hervant, F., 1999. Oxygen supply and the adaptations of animals in groundwater. *Freshwater Biology*, **41**(1): 1-30.

Marshall, D.W. et al., 2006. Effects of hypolimnetic releases on two impoundments and their receiving streams in southwest Wisconsin. *Lake and Reservoir Management*, **22**(3): 223-232.

McManamay, R.A., Brewer, S.K., Jager, H.I., Troia, M.J., 2016. Organizing environmental flow frameworks to meet hydropower mitigation needs. *Environmental management*, **58**(3): 365-385.

Midgley, T.L., Fox, G.A., Wilson, G.V., Felice, R., Heeren, D., 2013. In situ soil pipeflow experiments on contrasting streambank soils. *Transactions of the ASABE*, **56**(2): 479-488.

Miller, J.A., Appel, C., 1997. Ground water atlas of the United States: Kansas, Missouri and Nebraska. HA 730-D. *US Geological Survey. USGS Information Services, Denver, CO*.

Miller, R.J., Robison, H.W., 2004. Fishes of Oklahoma. *University of Oklahoma Press*.

Morrice, J.A., Valett, H., Dahm, C.N., Campana, M.E., 1997. Alluvial characteristics, groundwater–surface water exchange and hydrological retention in headwater streams. *Hydrological Processes*, **11**(3): 253-267.

Mulholland, P., Steinman, A., Marzolf, E., Hart, D., DeAngelis, D., 1994. Effect of periphyton biomass on hydraulic characteristics and nutrient cycling in streams. *Oecologia*, **98**(1): 40-47.

Mwakalila, S., Feyen, J., Wyseure, G., 2002. The influence of physical catchment properties on baseflow in semi-arid environments. *Journal of Arid Environments*, **52**(2): 245-258.

Nash, J.E., Sutcliffe, J.V., 1970. River flow forecasting through conceptual models part I—A discussion of principles. *Journal of hydrology*, **10**(3): 282-290.

Nathan, R., McMahon, T., 1990. Evaluation of automated techniques for base flow and recession analyses. *Water Resources Research*, **26**(7): 1465-1473.

Neff, B., Day, S., Piggott, A., Fuller, L., 2005. Base flow in the Great Lakes basin. 2328-0328.

Nelson, K.C., Palmer, M.A., 2007. Stream temperature surges under urbanization and climate change: data, models, and responses. *JAWRA Journal of the American Water Resources Association*, **43**(2): 440-452.

Nieber, J.L., Sidle, R.C., 2010. How do disconnected macropores in sloping soils facilitate preferential flow? *Hydrological Processes*, **24**(12): 1582-1594.

Nigh, T.A., Schroeder, W.A., 2002. Atlas of Missouri ecoregions. *Missouri Department of Conservation*.

Nilsson, C., Reidy, C.A., Dynesius, M., Revenga, C., 2005. Fragmentation and flow regulation of the world's large river systems. *Science*, **308**(5720): 405-408.

Ohnuki, Y. et al., 2008. Seasonal change in thick regolith hardness and water content in a dry evergreen forest in Kampong Thom Province, Cambodia. *Geoderma*, **146**(1): 94-101.

Olden, J.D., Naiman, R.J., 2010. Incorporating thermal regimes into environmental flows assessments: modifying dam operations to restore freshwater ecosystem integrity. *Freshwater Biology*, **55**(1): 86-107.

Pankhurst, N., 1997. Temperature effects on the reproductive performance of fish. *Global warming: implications for freshwater and marine fish*, **61**: 159.

Parker, J., Van Genuchten, M.T., 1984. Determining transport parameters from laboratory and field tracer experiments.

Perkin, J.S., Gido, K.B., Johnson, E., Tabor, V.M., 2010. Consequences of stream fragmentation and climate change for rare Great Plains fishes. *Final Report to USFWS Great Plains Landscape Conservation Cooperative Program*.

Pflieger, W., 1997. The fishes of Missouri, rev. ed. *Missouri Department of Conservation, Jefferson City, MO*.

Pigg, J., 1974. Fishes in the Kiamichi River, Oklahoma, Proceedings of the Oklahoma Academy of Science, pp. 121-130.

Pluhowski, E.J., 1970. Urbanization and its effect on the temperature of the streams on Long Island, New York. 627D.

Poff, N.L. et al., 2010. The ecological limits of hydrologic alteration (ELOHA): a new framework for developing regional environmental flow standards. *Freshwater Biology*, **55**(1): 147-170.

Poff, N.L., 1997. Landscape filters and species traits: towards mechanistic understanding and prediction in stream ecology. *Journal of the north american Benthological society*, **16**(2): 391-409.

Poole, G.C., Berman, C.H., 2001. An ecological perspective on in-stream temperature: natural heat dynamics and mechanisms of human-causedthermal degradation. *Environmental management*, **27**(6): 787-802.

Price, K., 2011. Effects of watershed topography, soils, land use, and climate on baseflow hydrology in humid regions: A review. *Progress in physical geography*, **35**(4): 465-492.

Price, K., Jackson, C.R., Parker, A.J., 2010. Variation of surficial soil hydraulic properties across land uses in the southern Blue Ridge Mountains, North Carolina, USA. *Journal of Hydrology*, **383**(3): 256-268.

Pyron, M., Vaughn, C.C., Winston, M.R., Pigg, J., 1998. Fish assemblage structure from 20 years of collections in the Kiamichi River, Oklahoma. *The Southwestern Naturalist*: 336-343.

Quinn, T.P., Hodgson, S., Peven, C., 1997. Temperature, flow, and the migration of adult sockeye salmon (Oncorhynchus nerka) in the Columbia River. *Canadian Journal of Fisheries and Aquatic Sciences*, **54**(6): 1349-1360.

Richter, B.D., Warner, A.T., Meyer, J.L., Lutz, K., 2006. A collaborative and adaptive process for developing environmental flow recommendations. *River Research and Applications*, **22**(3): 297-318.

Ritter, A., Muñoz-Carpena, R., 2013. Performance evaluation of hydrological models: Statistical significance for reducing subjectivity in goodness-of-fit assessments. *Journal of Hydrology*, **480**: 33-45.

Rosenberry, D.O., LaBaugh, J.W., 2008. Field techniques for estimating water fluxes between surface water and ground water. 2328-7055, Geological Survey (US).

Runkel, R.L., 1998. One-dimensional transport with inflow and storage (OTIS): A solute transport model for streams and rivers. *US Department of the Interior, US Geological Survey*.

Runkel, R.L., 2002. A new metric for determining the importance of transient storage. *Journal of the North American Benthological Society*, **21**(4): 529-543.

Rutledge, A., 1998. Computer programs for describing the recession of ground-water discharge and for estimating mean ground-water recharge and discharge from streamflow records: Update. *US Department of the Interior, US Geological Survey*.

Saltveit, S.J., 1990. Effect of decreased temperature on growth and smoltification of juvenile Atlantic salmon (Salmo salar) and brown trout (Salmo trutta) in a Norwegian regulated river. *River Research and Applications*, **5**(4): 295-303.

Sanford II, D.R., Boyd, S., 2012. Watershed Assessment for the Kiamichi Basin of Oklahoma.

Scanlon, B.R., Healy, R.W., Cook, P.G., 2002. Choosing appropriate techniques for quantifying groundwater recharge. *Hydrogeology Journal*, **10**(1): 18-39.

Schmidt, C., Conant, B., Bayer-Raich, M., Schirmer, M., 2007. Evaluation and field-scale application of an analytical method to quantify groundwater discharge using mapped streambed temperatures. *Journal of Hydrology*, **347**(3): 292-307.

Seager, R., Vecchi, G.A., 2010. Greenhouse warming and the 21st century hydroclimate of southwestern North America. *Proceedings of the National Academy of Sciences*, **107**(50): 21277-21282.

Sharma, R.H., Konietzky, H., Kosugi, K.i., 2010. Numerical analysis of soil pipe effects on hillslope water dynamics. *Acta Geotechnica*, **5**(1): 33-42.

Silliman, S.E., Booth, D.F., 1993. Analysis of time-series measurements of sediment temperature for identification of gaining vs. losing portions of Juday Creek, Indiana. *Journal of Hydrology*, **146**: 131-148.

Smakhtin, V., 2001. Low flow hydrology: a review. *Journal of hydrology*, **240**(3): 147-186.

Smith, K., 1981. The prediction of river water temperatures/prédiction des températures des eaux de rivière. *Hydrological Sciences Journal*, **26**(1): 19-32.

Smith, R., 1991. Effect of clearfelling pines on water field in a small eastern transvaal catchment, South Africa. *Water S. A.*, **17**(3): 217-224.

Sophocleous, M., Perkins, S.P., 2000. Methodology and application of combined watershed and ground-water models in Kansas. *Journal of Hydrology*, **236**(3): 185-201.

Spooner, D.E., Vaughn, C.C., Galbraith, H.S., 2005. Physiological determination of mussel sensitivity to water management practices in the Kiamichi River and review and summarization of literature pertaining to mussels of the Kiamichi and Little River watersheds, Oklahoma. *Oklahoma Department of Wildlife Conservation*.

Stallman, R., 1965. Steady one-dimensional fluid flow in a semi-infinite porous medium with sinusoidal surface temperature. *Journal of Geophysical Research*, **70**(12): 2821-2827.

Stofleth, J.M., Shields Jr, F.D., Fox, G.A., 2008. Hyporheic and total transient storage in small, sand-bed streams. *Hydrological Processes*, **22**(12): 1885-1894.

Suzuki, S., 1960. Percolation measurements based on heat flow through soil with special reference to paddy fields. *Journal of Geophysical Research*, **65**(9): 2883-2885.

Tague, C., Grant, G.E., 2004. A geological framework for interpreting the low-flow regimes of Cascade streams, Willamette River Basin, Oregon. *Water Resources Research*, **40**(4).

Taniguchi, M., Fukuo, Y., 1993. Continuous measurements of ground-water seepage using an automatic seepage meter. *Groundwater*, **31**(4): 675-679.

Tetzlaff, D. et al., 2009. How does landscape structure influence catchment transit time across different geomorphic provinces? *Hydrological Processes*, **23**(6): 945-953.

Thackston, E.L., Schnelle, K., 1970. Predicting effects of dead zones on stream mixing. *Journal of the Sanitary Engineering Division*, **96**(2): 319-331.

Tharme, R.E., 2003. A global perspective on environmental flow assessment: emerging trends in the development and application of environmental flow methodologies for rivers. *River research and applications*, **19**(5 - 6): 397-441.

Toride, N., Leij, F., Van Genuchten, M.T., 1995. The CXTFIT code for estimating transport parameters from laboratory or filed tracer experiments. *US Salinity Laboratory Riverside*.

Townsend, S.A., 1999. The seasonal pattern of dissolved oxygen, and hypolimnetic deoxygenation, in two tropical Australian reservoirs. *Lakes & Reservoirs: Research & Management*, **4**(1-2): 41-53.

Turner, J.V., 2009. Estimation and prediction of the exchange of groundwater and surface water: field methodologies, eWater Technical Report. eWater Cooperative Research Centre, Canberra.

Uchida, T., Kosugi, K., Mizuyama, T., 1999. Runoff characteristics of pipeflow and effects of pipeflow on rainfall-runoff phenomena in a mountainous watershed. *Journal of Hydrology*, **222**(1): 18-36.

Uchida, T., Kosugi, K.i., Mizuyama, T., 2001. Effects of pipeflow on hydrological process and its relation to landslide: a review of pipeflow studies in forested headwater catchments. *Hydrological Processes*, **15**(11): 2151-2174.

USGS. Comparison of Selected Methods for Estimating Groundwater Recharge In Humid Regions. Retrieved from https://water.usgs.gov/ogw/gwrp/methods/compare/. Last accessed on 16 Oct. 2017.

Vineyard, J.D., Feder, G.L., 1974. Springs of Missouri. *Missouri Geological Survey and Water Resources*.

Vivoni, E., Entekhabi, D., Bras, R., Ivanov, V., 2007. Controls on runoff generation and scale-dependence in a distributed hydrologic model. *Hydrology and Earth System Sciences Discussions*, **11**(5): 1683-1701.

Wagner, R.J., Mattraw, H.C., Ritz, G.F., Smith, B.A., 2000. Guidelines and standard procedures for continuous water-quality monitors: Site selection, field operation, calibration, record computation, and reporting. *US Geological Survey Water-Resources Investigations Report 00-4252*, **53**.

Webb, B.W., Hannah, D.M., Moore, R.D., Brown, L.E., Nobilis, F., 2008. Recent advances in stream and river temperature research. *Hydrological Processes*, **22**(7): 902-918.

Webb, B.W., Zhang, Y., 1999. Water temperatures and heat budgets in Dorset chalk water courses. *Hydrological Processes*, **13**(3): 309-321.

Weiler, M., McDonnell, J., 2007. Conceptualizing lateral preferential flow and flow networks and simulating the effects on gauged and ungauged hillslopes. *Water Resources Research*, **43**(3).

Wilson, G., 2011. Understanding soil-pipe flow and its role in ephemeral gully erosion. *Hydrological Processes*, **25**(15): 2354-2364.

Wilson, G., Gwo, J., Jardine, P., Luxmoore, R., 1998. Hydraulic and physical nonequilibrium effects on multiregion flow and transport. *Physical*

nonequilibrium in soils: Modeling and application. Ann Arbor Press, Chelsea, MI: 37-61.

Wilson, G., Rigby, J., Ursic, M., Dabney, S., 2015. Soil pipe flow tracer experiments: 1. Connectivity and transport characteristics. *Hydrological Processes*.

Wilson, G.V., Nieber, J.L., Sidle, R.C., Fox, G.A., 2013. Internal erosion during soil pipeflow: State of the science for experimental and numerical analysis. *Transactions of the ASABE*, **56**(2): 465-478.

Woods, R.A., Sivapalan, M., Robinson, J.S., 1997. Modeling the spatial variability of subsurface runoff using a topographic index. *Water Resources Research*, **33**(5): 1061-1073.

Wool, T.A., Ambrose, R.B., Martin, J.L., Comer, E.A., Tech, T., 2006. Water quality analysis simulation program (WASP). *User's Manual, Version*, **6**.

Wootton, R., 2012. Ecology of teleost fishes, 1. *Springer Science & Business Media*.

Yeakley, J.A., Swank, W., Swift, L., Hornberger, G., Shugart, H., 1998. Soil moisture gradients and controls on a southern Appalachian hillslope from drought through recharge. *Hydrology and Earth System Sciences Discussions*, **2**(1): 41-49.

Zamora, C., 2008. Estimating water fluxes across the sediment-water interface in the lower Merced River, California. 2328-0328, US Geological Survey.

Zamora, C., 2008. Estimating water fluxes across the sediment-water interface in the lower Merced River, California. 2328-0328, US Geological Survey.

Zhou, Y., Wilson, G., Fox, G., Rigby, J., Dabney, S., 2015. Soil pipe flow tracer experiments: 2. Application of a streamflow transient storage zone model. *Hydrological Processes*.

Zimmermann, B., Elsenbeer, H., De Moraes, J.M., 2006. The influence of land-use changes on soil hydraulic properties: implications for runoff generation. *Forest ecology and management*, **222**(1): 29-38.

VITA

YAN ZHOU

Candidate for the Degree of

Doctor of Philosophy

Thesis: QUANTIFYING GROUNDWATER INTERACTION WITH STREAMS AND THERMAL REGIME IMPLICATIONS

Major Field: Biosystems Engineering

Biographical:

Education:

Completed the requirements for the Bachelor of Engineering in Hydraulics and Hydropower at Northwest Agricultural and Forestry University, Yangling, Shaanxi, P.R.China in 2013.

Experience:

Graduate Research Assistant, Cooperative Units Program of the Biological Resources Division, Oklahoma State University
Research Assistant, Department of Agricultural Sciences and Natural Resources, Oklahoma State University